ANALYSING URBAN AIR POLLUTION USING LOW-COST METHODS AND COMMUNITY SCIENCE:

Asrah Heintzelman

Submitted to the faculty of the University Graduate School
in partial fulfillment of the requirements
for the degree
Doctor of Philosophy
in the Department of Earth Sciences,
Indiana University

December 2022

Accepted by the Graduate Faculty of Indiana University, in partial fulfillment of the requirements for the degree of Doctor of Philosophy.

Doctoral Committee

_____
Gabriel Filippelli, PhD, Chair

_____
Max J. Moreno-Madriñan, PhD

August 26, 2022

_____
Jeffrey S. Wilson, PhD

_____
Lixin Wang, PhD

_____
Gregory K. Druschel, PhD

© 2022

Asrah Heintzelman

DEDICATION

I have been fortunate to have had people in my life who loved, patiently supported, and encouraged me to push my boundaries to explore and learn outside of my comfort zone. From my parents, family members, to my teachers, mentors, friends, and finally my husband and children, who played a crucial role in supporting and cheering me on; I dedicate this work to you. Thank you.

ACKNOWLEDGEMENT

I thank all the individuals including the staff of the Department of Earth Sciences that have assisted, supported, and guided me during my journey to complete this dissertation. I am unable to recognize each person individually, however, I am grateful for the role they have all played in my success. I start by recognizing my advisor, Dr. Gabriel Filippelli, who gave me the opportunity to research air quality and mentored me over the years. I also recognize and thank my committee members: Dr. Jeffrey Wilson, Dr. Max J. Moreno-Madriñan, Dr. Lixin Wang, and Dr. Gregory Druschel for their time, efforts, and comments that pushed me to think more deeply about my research.

My research was enriched by the contribution from Keep Indianapolis Beautiful and in particular Karl Selm and all the citizen scientist volunteers. Additionally, I would not have had enough participants if Melissa Benton from the John Boner Neighborhood Center had not connected me to her extensive list of contacts who agreed to host the sensors. I also thank Adam Khalil with the platform StreetLight who granted me an academic license and guided me in optimizing their platform.

There were colleagues and friends I made along the way that enriched my experience. Dr. Aniruddha Banerjee (Rudy) I thank for encouraging me to pursue a Ph.D. in Earth Sciences. Also, I could not have established the network of sensors without the assistance of my husband Chuck, who was with me during most of the sensor installations. My children Zaki and Noor, along with other students also assisted me from time to time collecting and deploying sensors throughout the process.

I would be remiss if I didn't recognize my father, Hamid Masood Sohail, who pushed me to explore this path, my mother, Nadira Sohail, who encouraged me to stick

with it, and my husband Chuck who supported me and stood by me each step of the way. Last but not least, the support of my family members and friends notably Naveen, Omar, and Masooma, also contributed to my success. I truly appreciate all of you and thank you all for your sincere love and support in standing beside me on this wonderful journey.

Asrah Heintzelman

ANALYSING URBAN AIR POLLUTION USING LOW-COST METHODS AND COMMUNITY SCIENCE

Rise in air pollution resulting in negative health externalities for humans has created an urgent need for cities and communities to monitor it regularly. At present we have insufficient ground passive and active monitoring networks in place which presents a huge challenge. Satellite imagery has been used extensively for such analysis, but its resolution and methodology present other challenges in estimating pollution burden. The objective of this study was to propose three low-cost methods to fill in the gaps that exist currently. First, EPA grade sensors were used in 11 cities across the U.S. to examine NO_2. This is a simplistic way to assess the burden of air pollution in a region. However, this technique cannot be applied to fine scale analysis, which resulted in the next two components of this research study. Second, a citizen science network was established on the east side of Indianapolis, IN who hosted 32 Ogawa passive sensors to examine NO_2 and O_3 at a finer scale. These low-cost passive sensors, not requiring power, and very little maintenance, have historically tracked very closely with Federal Reference Monitors. Third, a low-cost PurpleAir PA-II-SD active sensors measuring $PM_{2.5}$ were housed with the citizen scientists identified above. This data was uploaded via Wi-Fi and available via a crowd sourced site established by PurpleAir. These data sets were analyzed to examine the burden of air pollution. The second and third research studies enabled granular analyses utilizing citizen science, tree canopy data, and traffic data, thus accommodating some of the present limitations. Advancement in low-cost sensor technology, along with ease of use and maintenance, presents an opportunity for not just communities, but cities to take charge of

some of these analyses to help them examine health equity impacts on their citizens because of air pollution.

Gabriel Filippelli, PhD, Chair

Max J. Moreno-Madriñan, PhD

Jeffrey S. Wilson, PhD

Lixin Wang, PhD

Gregory K. Druschel, PhD

TABLE OF CONTENTS

LIST OF TABLES xi
LIST OF FIGURES xii
LIST OF ABBREVIATIONS xiii
CHAPTER 1: INTRODUCTION 1
1.1 Motivation 1
1.2 Rationale 1
1.3 Objectives of dissertation 4
1.4 Organization of dissertation 5
1.5 References 5
CHAPTER 2: SUBSTANTIAL DECREASES IN U.S. CITIES' GROUND-BASED NO_2 CONCENTRATIONS DURING COVID-19 FROM REDUCED TRANSPORTATION 9
2.1 Introduction 9
2.2 Methodology 11
2.2.1 NO_2 and Vehicle Miles Travelled (VMT) data 11
2.2.2 Indianapolis traffic sensor data 13
2.3 Results 14
2.3.1 NO_2 14
2.3.2 VMT and NO_2 19
2.3.3 Indianapolis road sensor data 28
2.4 Discussion 30
2.5 Conclusion 33
2.6 References 34
CHAPTER 3: THE ROLE OF LOCAL VEHICULAR TYPE AND GREEN DENSITY IN CONTROLLING GROUND-LEVEL NO2 IN THE URBAN ENVIRONMENT 41
3.1 Introduction 41
3.2 Methodology 45
3.2.1 Passive sampling of NO_2 and O_3 45
3.2.2 Meteorological data 47
3.2.3 Tree canopy data 48
3.2.4 Land use data 49
3.2.5 American Community Survey 50
3.2.6 GIS based measurements and StreetLight data 50
3.2.7 Statistical analysis 51
3.3 Results 52
3.3.1 Regression 52
3.3.2 Three passive sensors and Washington Park continuous regulatory monitor data 55
3.3.3 NO_2, and O_3 for all passive sensors and Washington Park (WP) continuous regulatory monitor data 57
3.3.4 StreetLight data 58
3.4 Discussion 59
3.4.1 Regression output 60

3.4.2 Trees 60
3.4.3 Health impacts quantified 61
3.4.4 Census data 63
3.4.5 Vehicle and land use data 64
3.4.6 Meteorology 64
3.4.7 Distance to highway and gas stations 65
3.5 Conclusion 65
3.6 References 67
CHAPTER 4: EFFICACY OF LOW-COST SENSOR NETWORKS AT DETECTING FINE-SCALE VARIATIONS IN PARTICULATE MATTER IN URBAN ENVIRONMENTS 83
4.1 Introduction 83
4.2 Methodology 86
4.2.1 Sensor Network 86
4.2.2 Processing $PM_{2.5}$ data 88
4.2.3 Meteorological data 89
4.2.4 Land use and land cover 89
4.2.5 American Community Survey 90
4.3 Results 90
4.3.1 PurpleAir data and portable EPA grade sensor 92
4.3.2 Correlation of PurpleAir data against IDEM monitor data 92
4.3.3 Driving factors impacting daily averages of $PM_{2.5}$ exceeding WHO limits 95
4.3.4 Identify sensors with highest odds ratio of exceeding the WHO daily limit 97
4.3.5 Analysis at the census tract level 97
4.4 Discussion 100
4.5 Conclusion 103
4.6 References 104
CHAPTER 5: DISSERTATION CONCLUSION 114
5.1 Air pollution 114
5.2 Contributions of this dissertation 115
5.3 Study limitations 116
5.4 Future suggestions 117
5.5 References 118
APPENDICES 124
Appendix A 124
Appendix B 127
Appendix C 130
Appendix D 134
CURRICULUM VITAE

LIST OF TABLES

Table 2.1 - 2020 NO_2 averages and percent changes in 2020 14
Table 2.2 - NO_2 averages of January, March, and April from 2015–2019 15
Table 2.3 - NO_2 and VMT changes between January to March and January to April 2020 22
Table 2.4 - Spearman correlations between NO_2 and VMT in March and April of 2020 (alpha = 0.05)....27
Table 2.5 - NO_2 and VMT ratios from January to April 2020 for cities....28
Table 2.6 - Spearman correlation between vehicles and VMT and NO_2 in Indianapolis, March–April 2020....28
Table 2.7 - Indianapolis vehicle count, NO_2, and VMT in 2020....29
Table 2.8 - Percentage and unit change of vehicles, VMT, and NO_2 from January to April of 2020....29
Table 3.1 - Data....51
Table 3.2 - Ogawa and StreetLight platform averages in the study area....52
Table 3.3 - Significant Correlation output of variables with NO_2....53
Table 3.4 - Three regression models including a stepwise regression model output of coefficients and significance for NO_2....54
Table 3.5 - 2019 NO_2 and O_3 data from three closest sensors to Washington Park (WP) continuous regulatory monitor data....56
Table 3.6 - 2019 NO_2 and O_3 descriptive statistics from passive Ogawa samplers....57
Table 3.7 - March and June 2019, NO_2 data comparison across all sensors from passive Ogawa samplers and Washington Park (WP) continuous regulatory monitor data....58
Table 3.8 - March and June, 2019 NO_2 data comparison across all sensors from passive Ogawa samplers and Washington Park (WP) continuous regulatory monitor data....58
Table 4.1 - Correlation of sensor 25,30, and 31 with IDEM monitors and $PM_{2.5}$ data 93
Table 4.2 - Results from applying equation 3 to PurpleAir data....94
Table 4.3 - Logistic regression observation breakdown by month for 25 deployed sensors....95
Table 4.4 - Logistic regression output. Negative values indicate a decrease, and positive values an increase, in the number of days with $PM_{2.5}$ averages above WHO guidelines. 96
Table 4.5 - Odds of the significant coefficients from the regression output....97
Table 4.6 - Odds ratios output from significant sensors....97
Table 4.7 - Correlations of average $PM_{2.5}$ at the census tract level....98
Table 4.8 - stepwise regression output....99

LIST OF FIGURES

Figure 2.1 - January to March and January to April NO_2 changes for 2002, the average of the previous 5-years of non-COVID conditions, and the decrease from the annual averages 16
Figure 2.2 - March and April combined NO_2 averages in parts per billion (ppb) from 2020 versus 5 -year (2015-2019) 18
Figure 2.3 – Tropospheric NO_2 column averages from April in 2019 and 2020....18
Figure 2.4 - NO_2 averages from January, March, and April in 2020....20
Figure 2.5 - Vehicle miles travelled (VMT) for 11 cities from January, March, and April of 2020 21
Figure 2.6 - VMT changes between January to March and January to April in 2020....23
Figure 2.7 - NO_2 and VMT percent changes between January and March in 2020 25
Figure 2.8 - NO_2 and VMT percent changes between January and April 2020 26
Figure 3.1 - The spatial distribution of 32 sensors in the study area 45
Figure 3.2 - Passive sensor contraption designed for this deployment at 32 sites....47
Figure 3.3 - Sensors closest to Indiana Department of Environmental Management monitors 56
Figure 3.4 - StreetLight data from the three deployments for medium truck, and heavy-duty truck index in 2019 59
Figure 4.1 - Locations of 25 PurpleAir sensors in the study area....86
Figure 4.2 - PurpleAir map from the website with daily averages for Sensor 16 and 22, highlighting July 4 and 21, 2021....91
Figure 4.3 - Sensors nearest to Indiana Department of Environmental Management (IDEM) regulatory monitors....92
Figure C.1 - Kriging interpolation in ArcMap for $PM_{2.5}$ data....130
Figure C.2 - Inverse Distance Weighting interpolation in ArcMap for $PM_{2.5}$ data 131

LIST OF ABBREVIATIONS

ACS: American community survey

CDC: Centers for Disease Control

COPD: Chronic obstructive pulmonary disease

EPA: U.S. Environmental Protection Agency

FEM: Federal Equivalent Method

KIB: Keep Indianapolis Beautiful

$\mu g\ m^{-3}$: micrograms per meter cubed

NO_2: Nitrogen dioxide

NO: Nitrogen oxide

NOx: NO + NO_2

O_3: Ozone

PA: PurpleAir sensors

$PM_{2.5}$: Particulate matter 2.5

PPB: parts per billion

PR: Pleasant Run

SL: StreetLight

TC: Tree canopy cover

UHI: Urban heat island

VMT: Vehicle miles travelled

WHO: World Health Organizations

CHAPTER 1: INTRODUCTION

1.1 **Motivation**

Increased anthropogenic activities and urbanization have resulted in increased pollutants emitted into the atmosphere, which has shown to directly tie into negative health impacts (Nowak & Greenfield, 2018; Nowak & Walton, 2005; Szyszkowicz et al., 2022). On June 22, 2022, a search in PubMed in the last 10 years on "urban pollution and health" resulted in 4,785 results, "NO_2 and health" resulted in 1,787 results and "$PM_{2.5}$ and health" resulted in 2,026 results. Nitrogen dioxide, $PM_{2.5}$ and O_3 are among the six commonly known "criteria air pollutants" that are regulated by the Environmental Protection Agency (US EPA, 2014). NO_2, a highly reactive gas, is primarily formed from vehicular emissions (Patil et al., 2015) and can result in respiratory diseases, cardiovascular diseases, and birth defects, among others. This gas has a short lifespan of between 5-10 days and chemically converts to nitric acid before eventually precipitating out of the atmosphere. NO_2 and NOx react to chemicals in the atmosphere to form O_3 and $PM_{2.5}$. Particulate matter with an aerodynamic diameter <= 2.5 microns, termed $PM_{2.5}$, is 30 times smaller than human air. can stay in the air for several days, and is a risk factor for death (US EPA, 2014).

1.2 Rationale

The EPA's current network of Federal Reference Monitors, designed to protect the health of the populace, has many gaps. For example, Marion County, Indiana, which is incorporated as the City of Indianapolis and has a population of almost one million people, has only five Federal Reference Monitors, and only two that record continuous data. The entire state of Indiana has only 24 monitors, many of which do not provide continuous data.

Cost and maintenance alone result in a huge void in the state of Indiana's air pollution examination which presents a significant knowledge gap in the state.

A study in Seoul covering 4,017 days and 80,634 admissions in the emergency room, showed a direct connection with increased admissions due to mental health diseases, which was heightened in warmer seasons. Additionally, a short-term low dose of $PM_{2.5}$ between 0-30 $\mu g/m^3$ resulted in a steep dose-response association, making PM2.5 toxicologically relevant in the environment (Lee et al., 2019). In 2021, WHO agreed that lower concentrations of air pollution can also impact our health. They identify air pollution as the largest threat to the health of humans with increased mortality and morbidity that results from diseases (respiratory disease, cardiovascular disease, and lung cancer) and also negatively impacts other organs (WHO Global Air Quality Guidelines, 2021). Air pollution also poses psychosocial stressors that are present at individual as well as the neighborhood level (Hazlehurst et al., 2018).

The urban built environment is changing rapidly, with an increase in impervious surfaces and reduction in tree cover that have also contributed to a decrease in health benefits (Nowak & Greenfield, 2018, 2020). With 99% of the global population breathing air that has pollutants in excess of WHO guidelines (WHO Urges Accelerated Action to Protect Human Health and Combat the Climate Crisis at a Time of Heightened Conflict and Fragility, 2022), we need to monitor and examine the burden of air pollution regularly in transformative ways spatially and temporally to not just get granular information to inform the citizens but also assist policy makers in enhancing legislation to address the current conditions. We cannot only rely on expensive stationary equipment which are not able to capture the heterogeneity in air quality at the hyperlocal level, which is important

for developing and implementing land use policy decisions. This need has resulted in increase in the usage of low-cost sensors in several studies (Kortoçi et al., 2022).

Some of the low-cost (ranging from $70 - $7,800) air pollution sensors have been evaluated by the South Coast Air Quality Sensor Performance Evaluation Center. When testing PurpleAir PA-II (~$200 at the time of the test) against two Federal Equivalent Method (FEM) devices, the center concluded that the correlation between PurpleAir devices and FEM GRIMM (optical particle counters) and FEM Beta-attenuation monitors BAM had R-square > 0.93 and R-square > 0.86, respectively. These values were higher than some of the costliest low-cost sensors. They did report that chamber testing should be recommended for more extreme weather conditions. (*Evaluations*, 2022). PurpleAir sensors were addressed in an EPA webinar on low-cost sensors in 2019. Most low-cost sensors range between $100 - $2,500 with PM sensors having a lifespan of 1-3 years. Even though there are limitations in low-cost sensors, with data validation being one, with proper handling such data should not be discarded (US EPA, 2019).

Various techniques have been used independently or for calibrating low-cost monitors from adjustments based on mobile monitoring stations or other equipment (Apte et al., 2017; Cui et al., 2021; Zaldei et al., 2017). These methods provide us more spatial temporal data than the FEMs in place currently. However, even though these methods may be cheaper than the cost of maintained a Federal Reference Monitor, they are still cost prohibitive for most communities.

With this growing concern, researchers have been turning to citizen scientists to engage communities and to educate people at the same time (Grootjans et al., 2022). In this study preparation, for example, we were at times met with trepidation by potential participants,

but soon after making a connection the citizen scientists took ownership of the study. We were in constant contact, and they were educating themselves when to not go outside, especially when they saw high air pollution numbers on the PurpleAir crowd sourced data website. Additionally, engaging citizen scientist with low-cost sensors can fill the spatial and temporal void in measuring air pollution variability in the built environments. This can aid in incorporating land use in understanding pollution exposures (Zimmerman et al., 2020).

1.3 Objectives of dissertation

The primary objective of this dissertation was to utilize low-cost methods to examine urban air pollution. Online air pollution data was used for cities and for fine scale analysis low-cost active PurpleAir and low-cost passive Ogawa sensors (the latter capture data on criteria gasses) were utilized. Fine scale analysis objective was accomplished by establishing a citizen science network which was then used as both active and passive air pollution sensor networks. The PurpleAir sensor data required a minor humidity correction in the study, whereas no adjustment was required of the Ogawa sensor data as it has historically tracked well with FEM. In addition to the low-cost sensor data, land use data, tree canopy coverage data, and census data were also incorporated in the fine scale analysis. Additionally, as a novel introduction, accurate traffic data based on active traffic from a platform called StreetLight was incorporated to examine the variation and potential connections in the space.

1.4 Organization of dissertation

This dissertation consists of three manuscripts: Chapter 2) Substantial decreases in U.S. cities' ground-based NO_2 concentrations during COVID-19 from reduced transportation; Chapter 3) Efficacy of low-cost sensor networks at detecting fine-scale variations in particulate matter in urban environments; and Chapter 4) The role of local vehicular type and green density in controlling ground-level NO_2 in the urban environment

Chapter 2 examines changes in NO_2 in 11 cities in the U.S. and explores its connection to vehicular traffic in Indianapolis, Indiana, during the natural experiment with the onset of COVID-19 lockdown in March through April 2020. Chapter 2 provides an air quality assessment during COVID-19 based on data from continuous monitors managed by states hosting the 11 cities. Chapter 3 incorporates low-cost passive NO_2 Ogawa sensors placed on a citizen science network in Indianapolis. It examines 3 cycles of deployment and incorporates tree canopy, land-use, census data, and Streetlight platform, a transportation-based platform that reports real-time traffic data. Chapter 4 explores almost a year of continuous data from 32 active $PM_{2.5}$ PurpleAir PA-II SD sensors placed on the established citizen science network in Indianapolis.

1.5 References

Apte, J. S., Messier, K. P., Gani, S., Brauer, M., Kirchstetter, T. W., Lunden, M. M., Marshall, J. D., Portier, C. J., Vermeulen, R. C. H., & Hamburg, S. P. (2017). High-Resolution Air Pollution Mapping with Google Street View Cars:

Exploiting Big Data. *Environmental Science & Technology*, *51*(12), 6999–7008. https://doi.org/10.1021/acs.est.7b00891

Cui, H., Zhang, L., Li, W., Yuan, Z., Wu, M., Wang, C., Ma, J., & Li, Y. (2021). A new calibration system for low-cost Sensor Network in air pollution monitoring. *Atmospheric Pollution Research*, *12*(5), 101049. https://doi.org/10.1016/j.apr.2021.03.012

Evaluations. (2022, June 23). http://www.aqmd.gov/aq-spec/evaluations

Grootjans, S. J. M., Stijnen, M. M. N., Kroese, M. E. A. L., Ruwaard, D., & Jansen, I. M. W. J. (2022). Citizen science in the community: Gaining insight in community and participant health in four deprived neighbourhoods in the Netherlands. *Health & Place*, *75*, 102798. https://doi.org/10.1016/j.healthplace.2022.102798

Hazlehurst, M., Nurius, P., & Hajat, A. (2018). Individual and Neighborhood Stressors, Air Pollution and Cardiovascular Disease. *International Journal of Environmental Research and Public Health*, *15*(3), 472. https://doi.org/10.3390/ijerph15030472

Kortoçi, P., Motlagh, N. H., Zaidan, M. A., Fung, P. L., Varjonen, S., Rebeiro-Hargrave, A., Niemi, J. V., Nurmi, P., Hussein, T., Petäjä, T., Kulmala, M., & Tarkoma, S. (2022). Air pollution exposure monitoring using portable low-cost air quality sensors. *Smart Health*, *23*, 100241. https://doi.org/10.1016/j.smhl.2021.100241

Lee, S., Lee, W., Kim, D., Kim, E., Myung, W., Kim, S.-Y., & Kim, H. (2019). Short-term PM2.5 exposure and emergency hospital admissions for mental disease. *Environmental Research*, *171*, 313–320. https://doi.org/10.1016/j.envres.2019.01.036

Nowak, D. J., & Greenfield, E. J. (2018). Declining urban and community tree cover in the United States. *Urban Forestry & Urban Greening*, *32*, 32–55. https://doi.org/10.1016/j.ufug.2018.03.006

Nowak, D. J., & Greenfield, E. J. (2020). The increase of impervious cover and decrease of tree cover within urban areas globally (2012–2017). *Urban Forestry & Urban Greening*, *49*, 126638. https://doi.org/10.1016/j.ufug.2020.126638

Nowak, D. J., & Walton, J. T. (2005). Projected Urban Growth (2000 – 2050) and Its Estimated Impact on the US Forest Resource. *Journal of Forestry*, 7.

Patil, R. R., Chetlapally, S. K., & Bagvandas, M. (2015). Application environmental epidemiology to vehicular air pollution and health effects research. *Indian Journal of Occupational and Environmental Medicine*, *19*(1), 8–13. https://doi.org/10.4103/0019-5278.156999

Szyszkowicz, M., Link to external site, this link will open in a new window, Lukina, A., & Dinu, T. (2022). Urban Air Pollution and Emergency Department Visits for Neoplasms and Outcomes of Blood Forming and Metabolic Systems. *International Journal of Environmental Research and Public Health*, *19*(9), 5603. https://doi.org/10.3390/ijerph19095603

US EPA, O. (2014, April 9). *Criteria Air Pollutants* [Other Policies and Guidance]. https://www.epa.gov/criteria-air-pollutants

US EPA, O. (2019, April 17). *Low-Cost Air Quality Sensors Webinar Archive* [Data and Tools]. https://www.epa.gov/research-states/low-cost-air-quality-sensors-webinar-archive

WHO global air quality guidelines. (2021). World Health Organization.

WHO urges accelerated action to protect human health and combat the climate crisis at a time of heightened conflict and fragility. (2022, June 23). https://www.who.int/news/item/06-04-2022-who-urges-accelerated-action-to-protect-human-health-and-combat-the-climate-crisis-at-a-time-of-heightened-conflict-and-fragility

Zaldei, A., Camilli, F., De Filippis, T., Di Gennaro, F., Di Lonardo, S., Dini, F., Gioli, B., Gualtieri, G., Matese, A., Nunziati, W., Rocchi, L., Toscano, P., & Vagnoli, C. (2017). An integrated low-cost road traffic and air pollution monitoring platform for next citizen observatories. *Transportation Research Procedia*, *24*, 531–538. https://doi.org/10.1016/j.trpro.2017.06.002

Zimmerman, N., Li, H. Z., Ellis, A., Hauryliuk, A., Robinson, E. S., Gu, P., Shah, R. U., Ye, Q., Snell, L., Subramanian, R., Robinson, A. L., Apte, J. S., & Presto, A. A. (2020). Improving Correlations between Land Use and Air Pollutant Concentrations Using Wavelet Analysis: Insights from a Low-cost Sensor Network. *Aerosol and Air Quality Research*, *20*(2), 314–328. https://doi.org/10.4209/aaqr.2019.03.0124

CHAPTER 2: SUBSTANTIAL DECREASES IN U.S. CITIES' GROUND-BASED NO_2 CONCENTRATIONS DURING COVID-19 FROM REDUCED TRANSPORTATION

2.1 Introduction

Due to a 13-fold increase in Coronavirus disease 2019 (COVID-19) cases outside of China on 11 March 2020, the World Health Organizations Director General characterized it as a pandemic (WHO Director-General's Opening Remarks at the Media Briefing on COVID-19 - 11 March 2020, 2020). At the time of this writing, on 5 August 2021, the Centers for Disease Control reported that there were over 35 million cases of COVID-19 in the U.S., with the total deaths exceeding 600,000 (CDC COVID Data Tracker, 2020). This pandemic has resulted in stay-at-home orders being instituted around the world, which has many negative externalities associated with it, but one positive one has been a marked decrease in many criteria air pollutants due to decreases in transportation volumes and industrial production (Nakada & Urban, 2020; Sharma et al., 2020), including reduced concentrations of nitrogen dioxide (NO_2) (Baldasano, 2020; Şahin, 2020; Tanzer-Gruener et al., 2020; Wu et al., 2021). This change has also been quantified via satellite imagery, which indicates a substantial drop in NO_2 tropospheric column of over 20% from January to April 2020 versus the same time frame in 2019 over parts of China, Western Europe, and the United States (Bauwens et al., 2020) and similarly in 20 North American cities. Goldberg et al. (2020) calculated decreases in NO_2 during this similar timeframe; when adjusted for seasonality and meteorology in a North American city study, they were between 9% and 43%. It is important to note that satellite data, due to its analysis being

based on the entire tropospheric column and its spatial and temporal coverage limitations, can misreport on the ground-pollutant measurements. Additionally, urban regions versus remote regions can have daily NO_2 retrievals varying up to 40% (Lamsal et al., 2014).

As anthropogenic activities of nitrogen oxide (NOx) far surpass natural emissions (Walters et al., 2015), they have resulted in a three- to six-fold increase in nitrogen oxide ($NOx = NO + NO_2$) emissions since the pre-industrial era (Jaeglé et al., 2005). Anthropogenic sources of NOx include fossil fuel/biofuel combustion, industry, and the transportation sector, and natural sources of NOx include soil nitrification-denitrification processes, wild fires, and lightning (Walters et al., 2015). NO_2 from traffic emissions have profound and measurable health implications, such as heart disease or upper respiratory infections, in populations with increase in nonaccidental mortality (Cesaroni Giulia et al., 2013; Peel et al., 2005). Besides increasing acidification, exacerbating global climate change, decreasing visibility, and increasing ozone and aerosol in the troposphere (Bermejo-Orduna et al., 2014), NOx also induces small-particle formation and has shown to be positively correlated to adverse health conditions as a result of long-term exposure (Galloway et al., 2003; Marco et al., 2002).

High vehicular emissions can result in corridors of heavy air pollution (Redling et al., 2013) in rural and urban regions. NO_2 pollution, a tracer for vehicular emissions, has been linked to adverse health effects for increased asthma events in predominantly urban areas (Achakulwisut et al., 2019). A 20 ppb increase in NO_2 has been found to increase chronic obstructive pulmonary disease (COPD) hospital visits, cardiovascular disease, lung cancer in adults, and respiratory mortality (Cesaroni Giulia et al., 2013; Peel et al., 2005).

Recent COVID-19 research has consistently shown reduction of vehicular travel as the cause of NO_2 decreases; however, the one knowledge gap in this body of research is simply that the vehicle type (cars versus multiple-axled vehicles) is nearly as important as the vehicle number, and this varies substantially between cities. The onset of COVID-19 and the stay-at-home orders in March and April have posed a unique opportunity to examine these changes in vehicular NO_2 emission because of reduction of vehicle volume and type in the U.S. To examine changes in NO_2 in cities and how that relates to vehicular traffic during the COVID-19 lockdown, we examine the impact of stay-at-home orders in March through April 2020 versus a five-year average of calibrated high-quality data from March–April from 2015–2019. We utilize 2020 daily raw data for NO_2 from EPA-grade sensors in 11 large cities around the U.S. Additionally, NO_2 concentrations in Indianapolis, IN, are assessed and compared to vehicle volume broken down by classification with the premise that truck-traffic volumes (with varying axles) are a good metric for vehicular emissions in cities.

2.2 Methodology

2.2.1 NO_2 and Vehicle Miles Travelled (VMT) data

To examine the impact of stay-at-home orders, daily NO_2 data from roadside continuous ground level sensors from 11 major cities in the U.S. were downloaded from the respective state agencies for our study period (Daily Summary Report By Site, 2021; GeoTAM, 2021; New York State Air Quality, 2021; Quality Assurance Air Monitoring Site Information | California Air Resources Board, 2021). These cities were chosen for their population size and the availability of comparable data for air quality. Based on

Federal Audits required by the Environmental Protection Agency (EPA), the uncertainty associated with the measurement (sum of possible deviations due to the different sources of error that may appear) must remain below 15%(*Air Sensor Guidebook*, 2014).

Data for NO_2 over the months of March and April 2020 were used as lockdown reference months, acknowledging that some states were phasing in lockdowns during March and that states and cities often had different shutdown policies. This was compared to January 2020 data from those same sensors to determine in-year changes. The 2020 data are also compared to the mean 5-year sensor data (2015–2019) for March and April to take the meteorological conditions into account. We identified two fixed monitors within most regions (Cakmak et al., 2016); however, due to excessive number of missing days of data for San Antonio and Austin, we utilized data from one sensor each in those locations. Additionally, for Queens (at Queens College) and San Francisco, we were able to identify only one fixed continuous monitor maintained by the state. For the remaining cities, we averaged NO_2 data from two fixed sensors each for 2020 and 2015–2019 (Indianapolis—at Washington Park and I-70 sensor; Los Angeles—at Main Street and VA; San Jose—at Jackson Street an K Avenue; San Diego—Rancho and Kearny; Dallas—Cam 63 and Cam 1067, Fort Worth—Cam 13 and Cam 17; Austin—Cam 1068, San Antonio—Cam 23, Houston—Cam 416 and Cam 403; Dallas—Cam 1067 and Cam 63; San Diego—at Rancho and Kearny) (Daily Summary Report By Site, 2021; GeoTAM, 2021; New York State Air Quality, 2021; Quality Assurance Air Monitoring Site Information | California Air Resources Board, 2021).

Aggregate VMT data, generated at the county level, were accessed from StreetLight Data to examine changes in traffic patterns and emissions to obtain a uniform scale of

vehicle usage (Jia et al., 2020). Streetlight runs over 100 billion location data points gathered from smart phones and navigational devices connected to vehicles (cars and trucks) into an algorithm to aggregate and normalize travel patterns by region. Their metrics are validated not only against public sources or external sources but also using private data in all states except Hawaii and Alaska (StreetLight Volume Methodology & Validation White Paper, 2019). The percentage of population in the study area (versus the full country population) was used to normalize the VMT data.

2.2.2 Indianapolis traffic sensor data

Traffic counts are used in numerous studies to connect urban pollution like NO_2 to examine regions, their health impacts, and the socio-economic disparities that occur as a result of it (Cakmak et al., 2016; Madariaga et al., 2003; Nicolai et al., 2003). For this study, we downloaded daily traffic volume and classification data of vehicles from 5 continuous sensors placed on major roadways in Indianapolis, identification numbers 990362, 950109, 990309, 990311, and 991392, reported by the Indianapolis Department of Transportation (INDOT). These data are publicly available via INDOT's online Traffic Count Database System (TCDS). March and April 2020 daily counts were examined against the count and classification data from January 2020 for the referenced continuous sensors. INDOT has 15 vehicle classifications; however, we focused on total vehicular traffic, total cars, and classification of motorcycle, car, pickup, and bus as a sub-category (1–4) and heavy emitters (excluding sub-category 1–4). Classification 5 and above were primarily trucks with varying axles (Traffic Count Database System (TCDS), 2020)

2.3 Results

2.3.1 NO_2

The percentage drop in NO_2 values when 2020 values are compared to the 5-year aver- ages between January and March range from 11–56% and 4–43%, respectively (Tables 2.1 and 2.2), while January and April reflect a NO_2 drop ranging from 14–65% in 2020 and a drop of 13–51% in the 5-year averages (Tables 2.1 and 2.2). Between January and March, San Antonio was the only location where the 2020 percent change was lower than the 5-year average percent change (Figure 2.1). From January to April (Figure 2.1), the percent changes in 2020 and the 5-year averages of San Antonio and Austin were almost the same, while the other nine locations showed a sharp reduction in NO_2 values in 2020 compared to the same 2-month window from 2015–2019 (Figure 2.1). Excluding the cities of Austin and San Antonio from January to April in 2020, Indianapolis had the smallest reduction of NO_2 at 33%, and San Francisco had the largest reduction of NO_2 values at 65% (Table 2.1).

Table 2.1 - 2020 NO_2 averages and percent changes in 2020.

Location (NO_2 Sensors)	Jan (ppb)	Mar (ppb)	Apr (ppb)	2020 Change (Jan to Mar)	2020 Change (Jan to Apr)
LA	21.40	9.44	8.33	−55.89%	−61.08%
Indianapolis	10.54	9.38	7.08	−11.03%	−32.90%
San Francisco	13.84	7.81	4.85	−43.59%	−64.93%
Ft. Worth	10.15	6.56	5.35	−35.39%	−47.32%
Houston	11.70	7.04	7.11	−39.79%	−39.25%
San Antonio	8.06	4.96	4.04	−38.39%	−49.82%
Austin	12.43	10.26	10.75	−17.42%	−13.51%
Dallas	11.38	6.82	6.07	−40.05%	−46.67%
San Jose	16.74	9.45	6.07	−43.55%	−63.76%
San Diego	14.99	7.83	6.80	−47.76%	−54.62%
Queens, NY	20.55	12.04	9.12	−41.39%	−55.61%

Table 2.2 - NO_2 averages of January, March, and April from 2015–2019.

Location (NO_2 Sensors)	Jan (ppb)	Mar (ppb)	Apr (ppb)	5-yr Change (Jan to Mar)	5-yr Change (Jan to Apr)
LA	22.01	16.60	13.68	−24.57%	−37.85%
Indianapolis	13.79	13.23	11.83	−4.00%	−14.18%
San Francisco	18.21	11.45	8.88	−37.12%	−51.21%
Ft. Worth	10.26	7.69	6.07	−25.09%	−40.88%
Houston	15.00	10.42	10.02	−30.54%	−33.20%
San Antonio	9.64	5.54	4.71	−42.56%	−51.10%
Austin	15.42	13.83	13.35	−10.32%	−13.44%
Dallas	12.57	8.73	7.25	−30.61%	−42.34%
San Jose	18.11	12.98	10.80	−28.31%	−40.38%
San Diego	15.32	12.93	11.41	−15.64%	−25.51%
Queens, NY	20.60	17.68	14.35	−14.14%	−30.31%

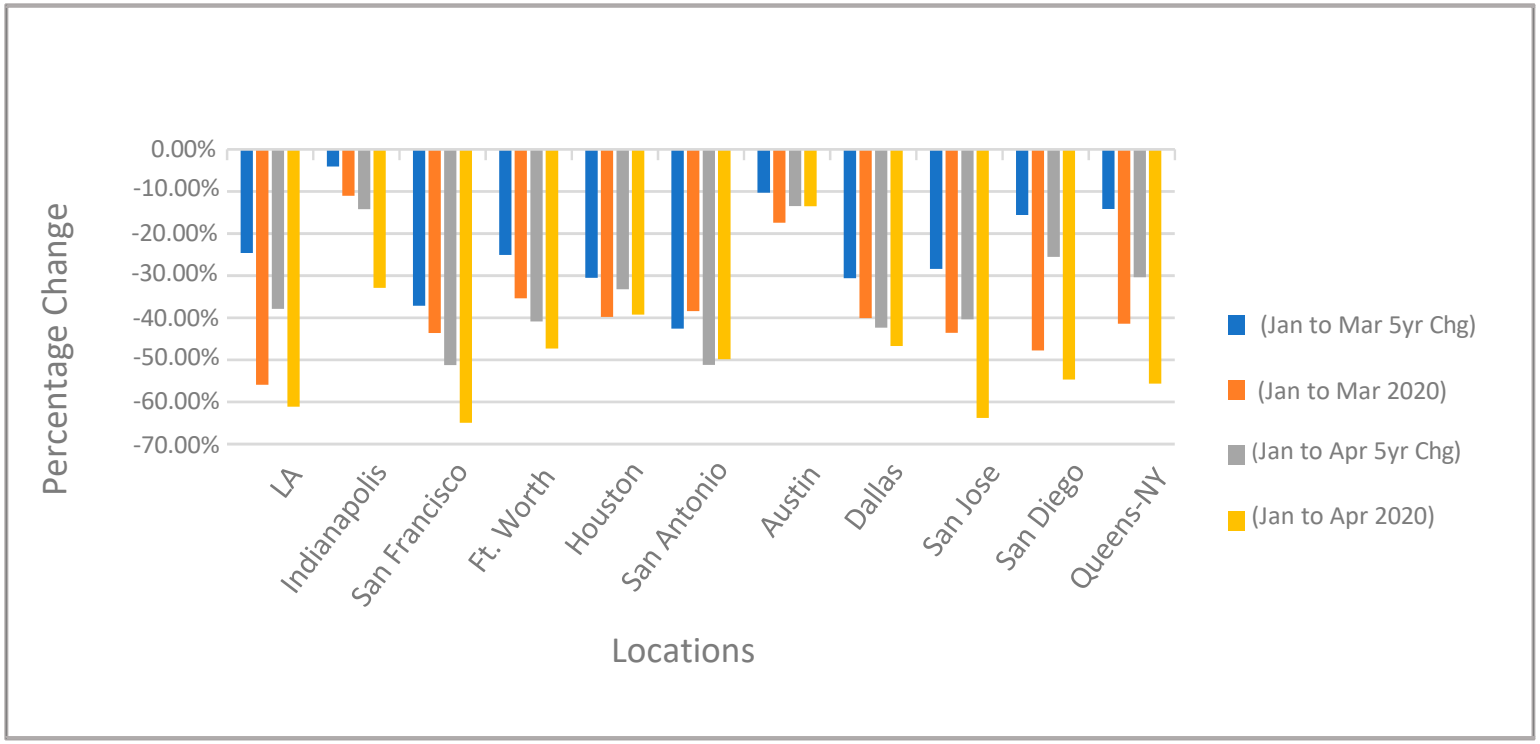

Figure 2.1 - January to March and January to April NO_2 changes for 2020, the average of the previous 5-years of non-COVID conditions, and the decrease from annual averages.

Seasonal changes in NO_2 naturally occur and must be considered. In summer, NOx and other volatile organic compounds from traffic and other sources result in photochemical smog, with December through February having seasonal maximum in the U.S. (A et al., 2008). Oxidation by photochemically produced OH in the summer reduces NOx, while lower concentrations of OH in the winter months results in an increased lifetime of NOx (Shah et al., 2020). Extrapolating further from Table 2.1, we see this in our multi-city data, with an average decrease in 2020 NO_2 values in March and April ranging from −40% to −50% compared to their respective average January values. In April 2020, Austin had the smallest reduction of −13.51%, with San Francisco having the largest reduction of −64.93% (Table 2.1). These decreases constitute seasonal changes plus any change related to COVID lockdown policies in the various cities.

To determine the typical seasonal decrease in NO_2 values and thus remove this from the COVID-related signals, we calculated the 5-year averages for each city to normalize for weather-related variations year-on-year. We found that the typical seasonal decreases were significantly less than the COVID-impacted 2020 decreases (Figure 2.1). Apart from Ft. Worth, San Antonio, and Dallas, rest of the cities had a greater than 20% drop in March–April averages in 2020 versus the 5-year averages (Figure 2.2). On average, between January and March and January and April in 2020, NO_2 values decreased by 14% when compared to their respective 5-year averages from 2015–2019 (Tables 2.1 and 2.2), indicating the significant impact of lockdowns and agreeing with the more regional results obtained by satellite analysis (Goldberg et al., 2020). We can visualize such impacts from the free use of tropospheric NO_2 monthly mean averages from GOME-2 sensor from

www.temis.nl over the U.S. from April 2019 when compared to April 2020 (Figure 2.3) (Boersma et al., 2004).

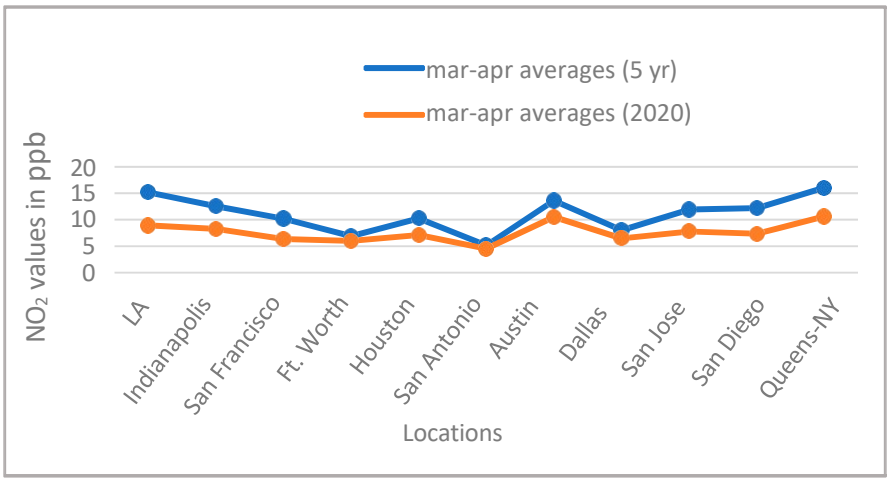

Figure 2.2 - March and April combined NO_2 averages in parts per billion (ppb) from 2020 versus 5 -year (2015-2019).

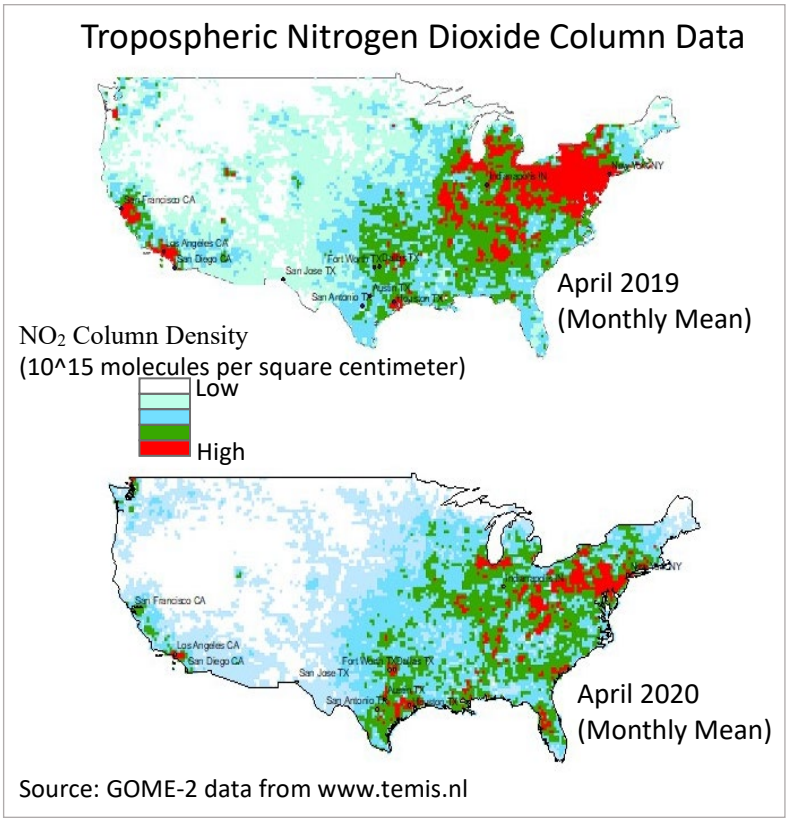

Figure 2.3 - Tropospheric NO_2 column averages from April in 2019 and 2020.

2.3.2 VMT and NO_2

Similar to the NO_2 trends between January, March, and April in 2020 (Figure 2.4), VMT in all the locations significantly dropped with the implementation of stay-at-home orders (Figure 2.5). March showed a significant reduction in VMT between 11–51%, with NO_2 reduction being between 11–56% (Table 2.3). April in comparison to January showed a much higher reduction of VMT between 62–89% (Table 2.3), with NO_2 reduction being between 14–65% (Table 2.3, Figure 2.6)

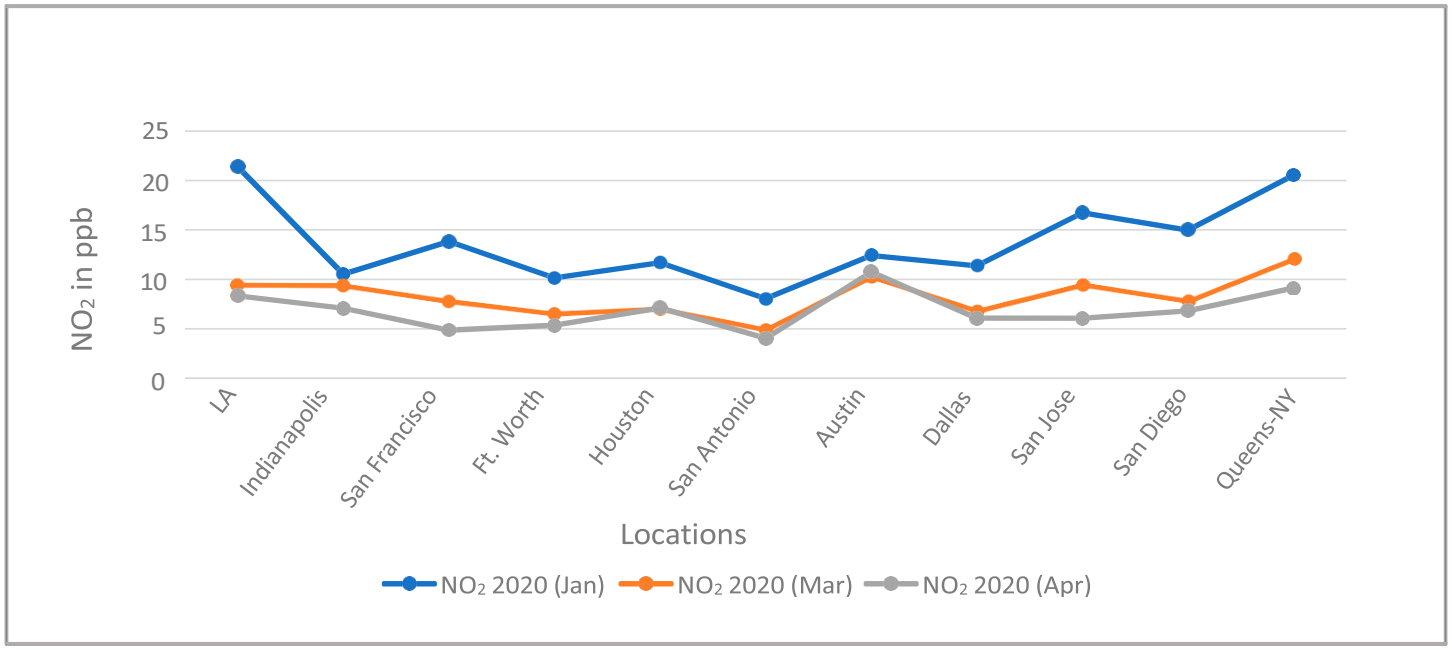

Figure 2.4 - NO_2 averages from January, March, and April in 2020.

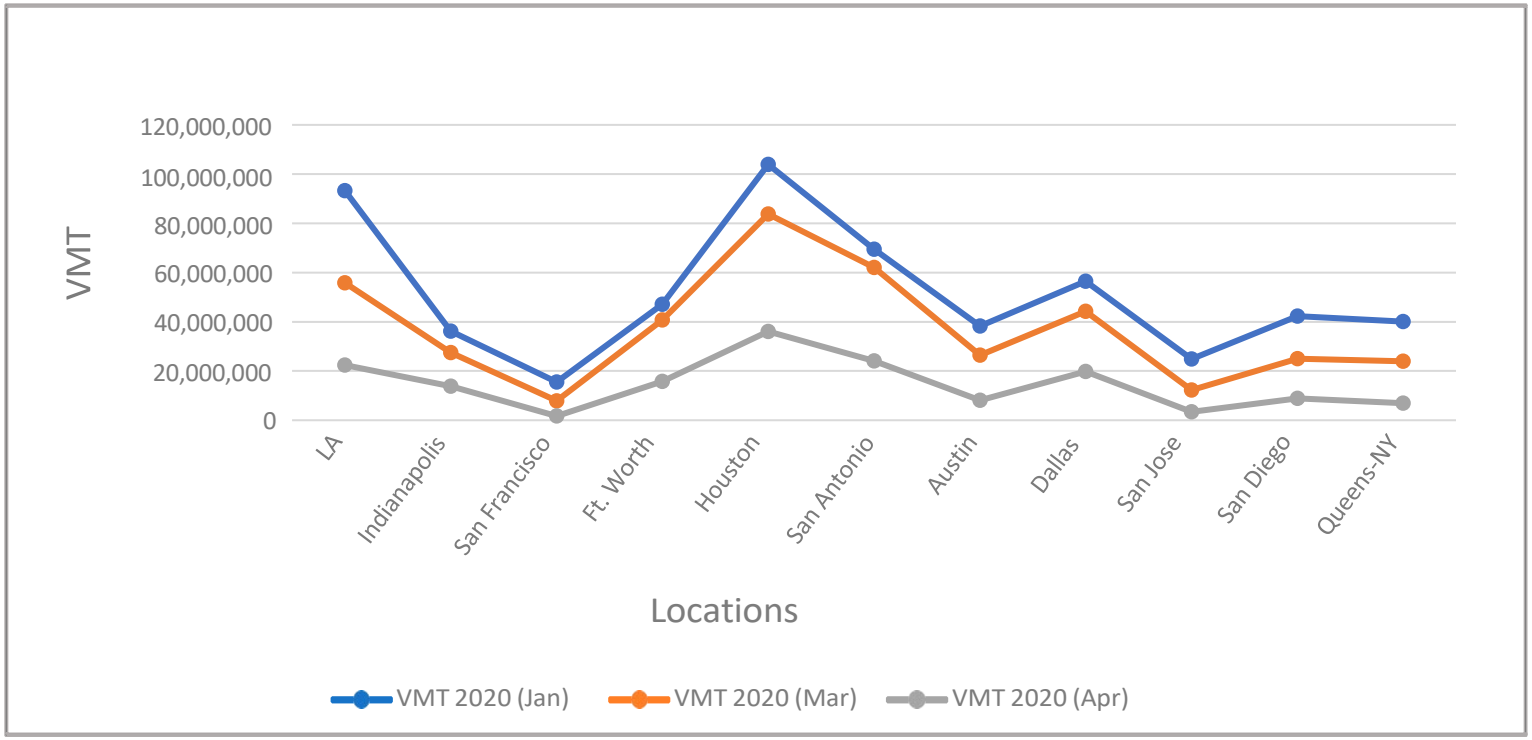

Figure 2.5 - Vehicle miles travelled (VMT) for 11 cities from January, March, and April of 2020.

Table 2.3 - NO_2 and VMT changes between January to March and January to April 2020.

Location	NO_2 Jan to Mar	VMT Jan to Mar	NO_2 Jan to Apr	VMT Jan to Apr
LA	−55.89%	−40.11%	−61.08%	−75.97%
Indianapolis	−11.03%	−23.95%	−32.90%	−61.87%
San Francisco	−43.59%	−49.12%	−64.93%	−89.07%
Ft. Worth	−35.39%	−13.57%	−47.32%	−66.50%
Houston	−39.79%	−19.38%	−39.25%	−65.29%
San Antonio	−38.39%	−10.73%	−49.82%	−65.29%
Austin	−17.42%	−30.97%	−13.51%	−78.88%
Dallas	−40.05%	−21.63%	−46.67%	−64.91%
San Jose	−43.55%	−50.62%	−63.76%	−86.35%
San Diego	−47.76%	−40.69%	−54.62%	−78.99%
Queens, NY	−41.39%	−40.29%	−55.61%	−82.66%

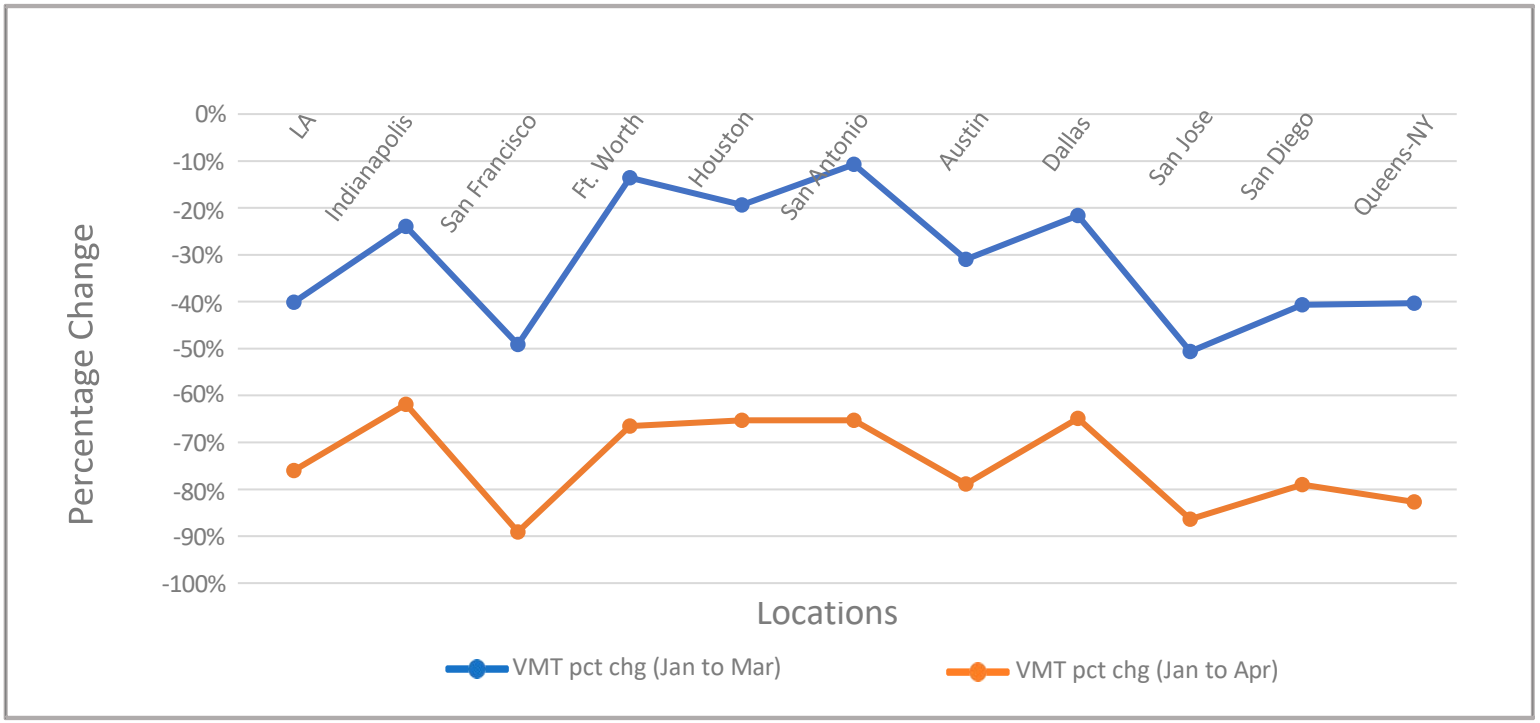

Figure 2.6 - VMT changes between January to March and January to April in 2020.

Comparing the trends of NO_2 and VMT from January to March 2020, the percentage changes of NO_2 of Indianapolis, San Francisco, Austin, and San Jose are higher than the VMT percent changes in the same time frame. For LA, Ft Worth, Houston, San Antonio, Dallas, and San Diego, VMT percent changes, causes of which were not investigated, are lower than the NO_2 percent changes, with Queens being about the same (Figure 2.7). For April, a month into the shutdown period in most states, NO_2 changes are consistently higher than the VMT percent changes in that time (Figure 2.8).

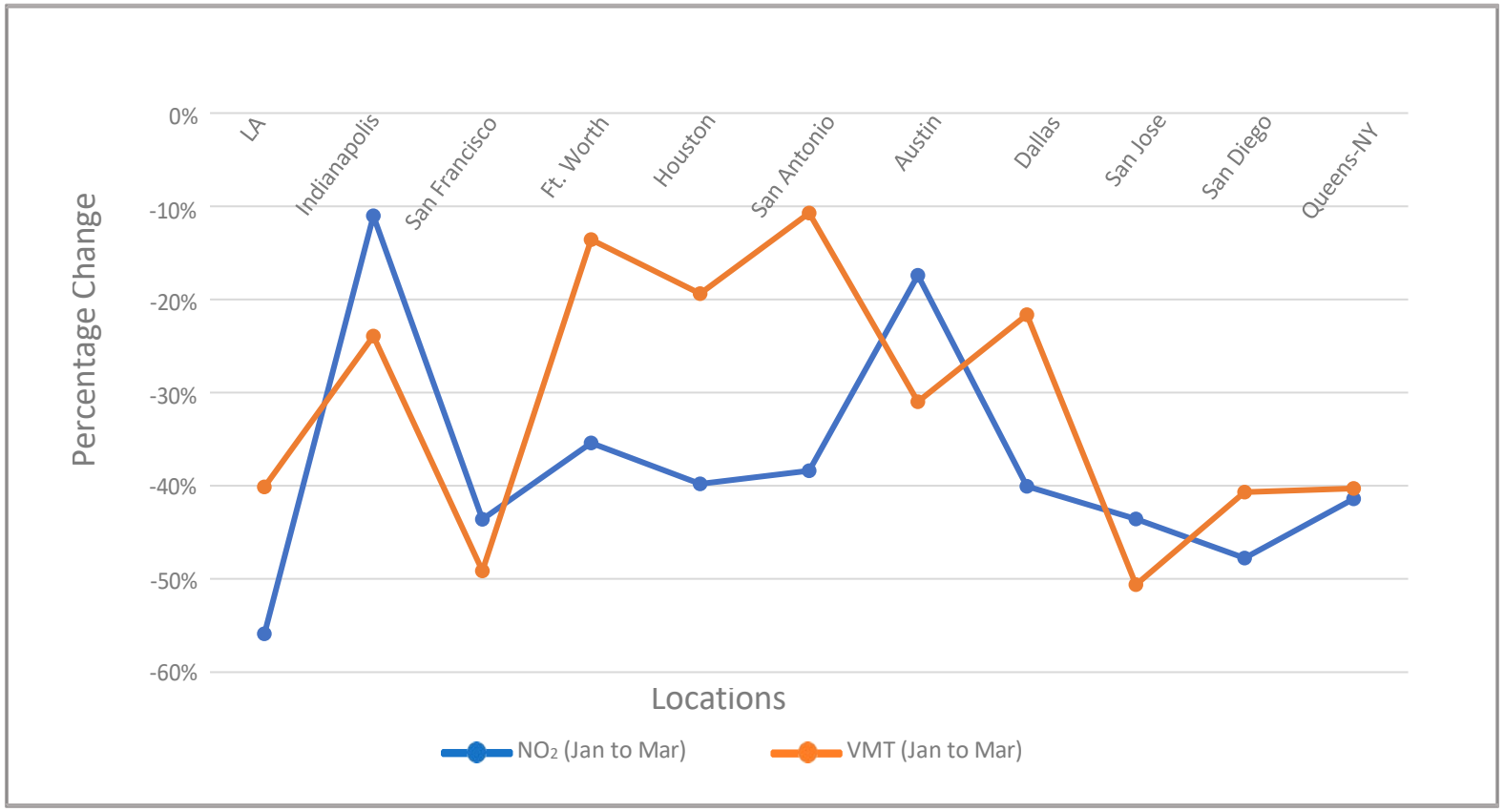

Figure 2.7 - NO_2 and VMT percent changes between January and March in 2020.

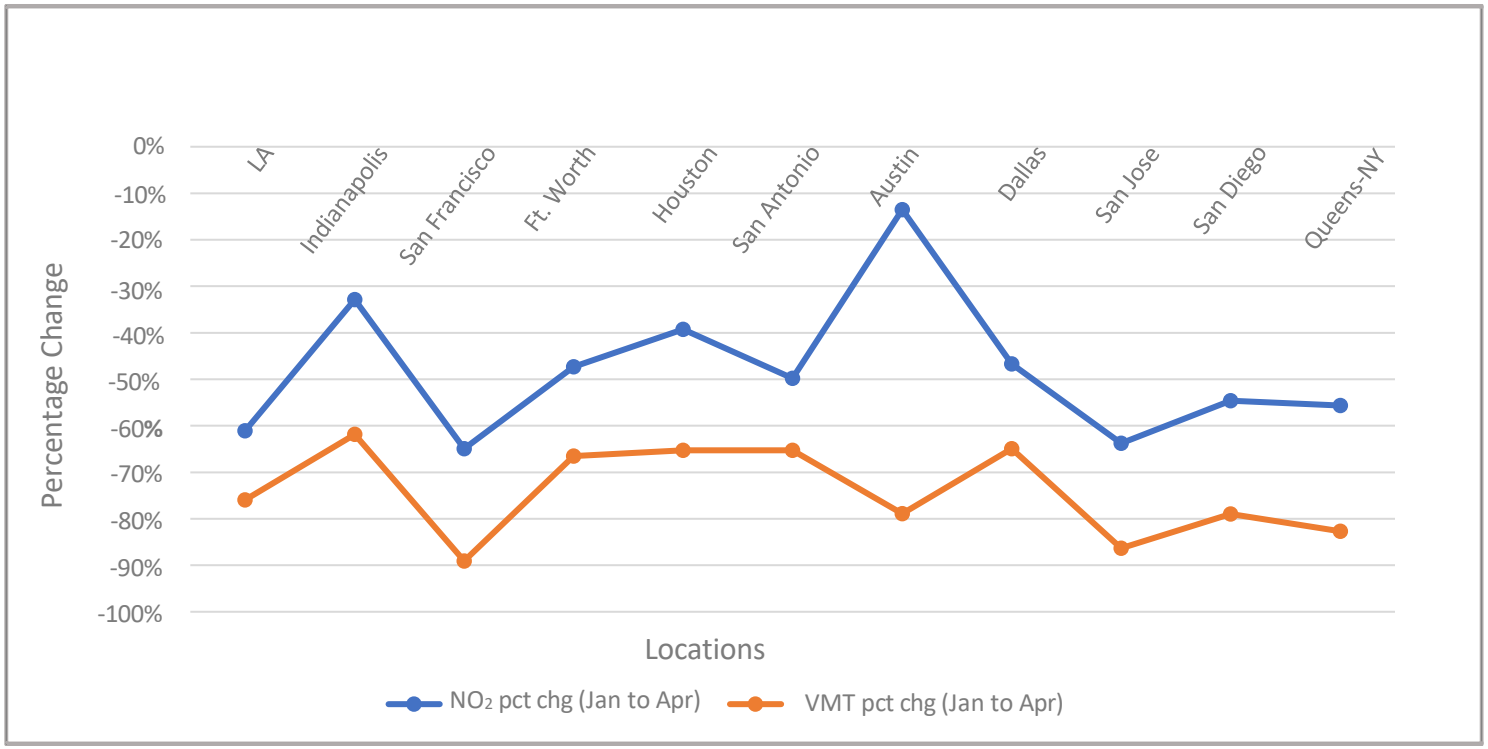

Figure 2.8 - NO_2 and VMT percent changes between January and April 2020

Spearman rank-correlation statistics was calculated between NO_2 and VMT, with alpha level set at 0.05 to examine the strength of their relationship. It ranges between −1 to +1, with zero indicating no association between two variables; −1 indicating a perfectly inverse strength of relationship; and a +1 indicating a perfect strength of association. This analysis revealed that San Diego, San Jose, and Indianapolis have higher significant correlation (r = 0.43–0.53) and LA, Houston, San Francisco, and Queens have lower significant correlations (r = 0.29–0.39) (Table 2.4). High *p*-values for the four cities in Texas (Ft. Worth, San Antonio, Austin, and Dallas) indicate that, in those locations, we do not have strong evidence of a relationship between NO_2 and VMT variations, thus preventing us from understanding the relationship with this dataset. Examining the ratios of NO_2 to VMT for January to April 2020 for all 11 cities, we find that, on average, a 1,000,000 reduction in VMT resulted in a reduction of 0.24 ppb in NO_2 for all cities. Austin was well below that average, at 0.06 ppb, and San Francisco had the highest impact of the decreased VMT (with a reduction of 0.65 ppb) for an average of a 1,000,000 reduction in VMT (Table 2.5).

Table 2.4 - Spearman correlations between NO_2 and VMT in March and April of 2020 (alpha = 0.05).

Location	X	Y	Correlation Coefficient	P-Value	P-Value < 0.05
LA	NO2	VMT	0.3543	0.0051	X
Indianapolis	NO2	VMT	0.4569	0.0002	X
San Francisco	NO2	VMT	0.3230	0.0111	X
Ft Worth	NO2	VMT	0.1329	0.3072	
Houston	NO2	VMT	0.2910	0.0229	X
San Antonio	NO2	VMT	0.2225	0.0848	
Austin	NO2	VMT	0.0454	0.7285	
Dallas	NO2	VMT	0.1173	0.3679	
San Jose	NO2	VMT	0.4295	0.0006	X
San Diego	NO2	VMT	0.5320	0.0000	X
Queens	NO2	VMT	0.3916	0.0028	X

Table 2.5 - NO_2 and VMT ratios from January to April 2020 for cities

Location	VMT Avg Chg (Jan–Apr) = [B]	NO_2 Avg Chg in ppb (Jan–Apr) = [A]	NO_2/VMT = A/B (all Cities)
LA	−70,802,793.41	−13.07	0.18×10^{-6}
Indianapolis	−22,364,196.21	−3.47	0.16×10^{-6}
San Francisco	−13,824,506.67	−8.99	0.65×10^{-6}
Ft. Worth	−31,308,793.60	−4.80	0.15×10^{-6}
Houston	−67,843,483.92	−4.59	0.07×10^{-6}
San Antonio	−45,369,086.33	−4.01	0.09×10^{-6}
Austin	−30,210,481.83	−1.68	0.06×10^{-6}
Dallas	−36,617,918.66	−5.31	0.15×10^{-6}
San Jose	−21,531,553.94	−10.67	0.50×10^{-6}
San Diego	−33,359,270.66	−8.19	0.25×10^{-6}
Queens	−33,089,110.33	−11.43	0.35×10^{-6}
Average			0.24×10^{-6}

2.3.3 Indianapolis road sensor data

Given that the Spearman correlation between NO_2 and VMT in Indianapolis is significant, we examined the city further. An expanded Spearman correlation test indicates that the correlation between VMT, NO_2, and vehicle counts in March and April 2020 are all highly significant, with moderate correlations between VMT and NO_2 and high correlations between total vehicles and VMT, as expected (Table 2.6).

Table 2.6 - Spearman correlation between vehicles and VMT and NO_2 in Indianapolis, March–April 2020.

Location	X	Y	Correlation Coefficient	*p*-Value
Indianapolis	Avg Total Vehicles	VMT	0.90	<0.005
Indianapolis	Avg Total Vehicles	NO2	0.54	<0.005
Indianapolis	VMT	NO2	0.46	<0.006

Average counts of total vehicles, vehicle classification excluding categories 1–4 (excluding motorcycle, car, pickup, and bus-proxy for trucks), NO_2, and VMT show a decline in all categories in March and April when compared to January 2020 (Table 2.7).

VMT percentage reduction in April versus January is almost two times that of the average total vehicles in Indianapolis and of the NO_2 percentage reduction in that time period (Table 2.8), indicating that a percentage reduction in the average total vehicles results in almost an equivalent percentage reduction in NO_2 in the city in that month. Extrapolating from Table 2.8, we can make the following observation regarding the change from January to April.

An average of 1,876 (38,494–36,618)-unit reduction in average total vehicles, excluding motorcycle, car, pickup, and bus, is equivalent to a 32% (Matthes et al., 2007) or an 1.11 ppb (0.32 × 3.46) average burden reduction of NO_2 in Indianapolis.

Table 2.7 - Indianapolis vehicle count, NO_2, and VMT in 2020

Month	Avg Total Vehicles	Avg Total Cars	Avg Vehicles (1 to 4)	Avg Vehicles (Excl 1 to 4)	Avg NO_2 2020 (ppb)	Avg VMT 2020
Jan	336,971	239,289	298,476	38,494	10.54	36,147,631
Mar	310,327	210,699	268,216	42,111	9.38	27,490,875
Apr	220,784	137,125	184,166	36,618	7.08	13,783,435

Table 2.8 - Percentage and unit change of vehicles, VMT, and NO_2 from January to April of 2020.

Variable	January	April	Unit_Chg (Jan–April)	Pct_Chg (Jan–Apr)
Avg_VMT	36,147,631	13,783,435	−22,364,196	−61.87%
Avg_NO_2(ppb) 1	10.54	7.08	−3.46	−32.83%
Avg_tot_veh 2	336,971	220,784	116,187	−34.48%
Avg_tot_cars 3	239,289	137,125	102,164	−42.69%
Avg_veh (1–4) 4	298,476	184,166	114,310	−38.30%
Avg_veh (excl 1–4) 5	38,494	36,618	1876	−4.87%

1 NO_2 averaged from two sensors in Indianapolis. 2 Total count of vehicles averaged over the 5 sensors in Indianapolis. 3 Total count of cars averaged over the 5 sensors in Indianapolis. 4 Total count of vehicle class 1–4 (motorcycle, car, pickup, and bus) averaged over the 5 sensors in Indianapolis. 5 Total count of a proxy for trucks averaged over the 5 sensors in Indianapolis.

2.4 Discussion

The onset of COVID-19 and the stay-at-home orders in March and April have presented an opportunity to examine the changes in NO_2 concentrations and their relationship to VMT in 11 cities in the U.S., with implications for local health outcomes.

Our analysis of the impacts of stay-at-home orders utilized ground-based sensor data from 11 U.S. cities. We found an average reduction of NO_2 of 45% measured in March and April 2020 when compared with their 5-year averages of 29% (2015–2019) (Tables 2.1 and 2.2). January to April 2020 resulted in a NO_2 drop between 14–65% versus its respective 5-year average drop between 13–51%. Four Texas cities had poor correlation between VMT and NO_2 (Ft. Worth, San Antonio, Austin, and Dallas). This offset compared to studies using satellite data is likely due to differences in the air being sampled with each approach (i.e., ground-level versus troposphere scale). San Diego, San Jose, and Indianapolis had the strongest strength of relationship between VMT and NO_2, as is illustrated from the correlation analysis.

The VMT reduction in April 2020 ranged between 62% and 89% (Table 2.3) when compared to January 2020. Average ratios of NO_2/VMT for the 11 locations indicates that for every 1,000,000 less VMT, NO_2 decreases by an average of 0.24 ppb (Table 2.5). A 1,000,000 average VMT drop in San Francisco resulted in the most significant decrease in NO_2 (0.65 ppb), and Houston resulted in the least significant decrease (0.07 ppb). The petrochemical industry in Texas, and particularly in the greater Houston area, probably plays a significant role in NO_2 production (Jobson et al., 2004), and thus the VMT-NO_2 relationship is not likely the only significant factor influencing the scale of observed decreases in NO_2.

The lack of observed significant correlations between NO_2 and VMT for the four Texas cities remains unresolved. We suggest two options: (1) the locations of the fixed AQ sensors' locations in relation to emission sources as related to traffic and non-traffic need to be identified and incorporated with meteorology, as their absence may not be ideal for capturing the more regional emission sources that are better characterized by satellite observations (Goldberg et al., 2020) that might be an issue for more sprawling cities, and/or (2) VMT along with specific traffic volume and classification analysis from platforms like StreetLight may be a more robust metric for extrapolating local impacts of NO_2 emissions from vehicle sources. A much denser array of high-quality, ground-based sensors would likely have to be in place to address option (1) above, but with option (2), we can, at least for one of the cities (Indianapolis), compare NO_2 to actual vehicle count and classification data for several locations to address the issue.

Since VMT may not be the best indicator of pollution impacts, we can use traffic counts and vehicle classifications in addition to VMT to create localized indices that can assist local governments to plan and/or to adjust traffic flows to address the impacts of high NO_2 values. In future studies, placement of NO_2 sensors in relation to the NO_2 sources, which would also impact the sensors readings, should be considered. This NO_2/VMT ratio (Table 2.5) should be tested in other cities in different seasons, which could be then used as a proxy in examining NO_2 production in different regions while gauging the impact of transportation changes. This can assist in classifying the impact of traffic changes in regions from the most sensitive to the least. In addition to sensor placement, meteorological conditions, like temperature, wind speed, relative humidity, and precipitation, also play a role in the transport of atmospheric gases (Tobías et al., 2020), which were also not

considered in this analysis. Such conditions are not uniform spatially and have shown to cause column NO_2 readings to differ by about 15% over monthly timescales (Goldberg et al., 2020); high winds in particular can play a role in dispersing NO_2 pollutant concentrations throughout the year (Arain et al., 2009).

A deeper look into vehicle counts and classification in Indianapolis indicates that the drop in average total vehicles percentage is almost identical to the percentage drop in its NO_2 values (Table 2.8). An 1,876-unit reduction in proxy truck average in Indianapolis results in lowering VMT, which in turn should yield a decrease in average NO_2 values by 1.11 ppb (Table 2.8). Building on this process in time and space, this calculation can be useful in examining regions that should be targeted first and would have the biggest impact of the reduction in NO_2 through traffic manipulation. In places like Houston, where there is a presence of other significant industrial emissions of NO_2, their emission impacts should also be incorporated for a more comprehensive understanding.

In qualitative terms, the observed substantial reductions in NO_2 would, all other things being equal, provide some benefits to human health. With the return to business- as-usual practices, these health benefits will be transitory. Satellite measurements of NO_2 are outstanding for capturing regional trends, but the heterogeneity of NO_2 at the ground level in a given city (Coppalle et al., 2001) is not well-captured and thus pinpointing that emission sources that are proximal to population centers at the fine scale should be a high priority for city planners and transportation design. This latter point is critical in that the highest concentrations of NO_2 and many other criteria air pollutants are disproportionately located in lower-income communities (Cakmak et al., 2016; Miranda et al., 2011). The overlapping issues of poor air quality and particular susceptibility, likely via co-

morbidities, of these same communities to severe COVID disease (Fattorini & Regoli, 2020) speaks to the need to better constrain ground-level air pollution levels with an eye toward applying health equity solutions in cities.

2.5 Conclusion

The pandemic-driven shutdown policies instituted in cities across the U.S. substantially decreased many harmful air pollutants, including NO_2 (Berman & Ebisu, 2020; Goldberg et al., 2020). We found this stable reduction within cities using ground-based monitors, and it is largely tied to reduced traffic volume, with other factors, such as industrial emissions, playing a variable role. Although ground-based monitoring ties the concentration data much more closely to com- munities and local health impacts than does more regionally comprehensive satellite data, the paucity of monitors and likely disconnects between metrics that are meant to capture traffic volume reduces their effectiveness from a public health standpoint.

This observed reduction in urban NO_2 concentrations ranging between 11% and 65%, a rare silver lining of the devastating pandemic, is likely temporary, but it does point to the tight connection between traffic-related pollution sources and local impacts. This connection highlights a two-fold issue: that local air-pollution hotspots may exacerbate diseases like COVID and are currently under-studied, especially when it comes to examining pollutant burden by taking vehicle classifications into account, as we illustrated in Indianapolis, where we accounted for an average of 1.11 ppb reduction in NO_2. Two actions that city planners can take to promote health equity in their communities are to implement environmental-monitoring programs that link data points (i.e., monitors) more

strategically to population density and to implement local transportation and zoning policies that examine and protect community health and build health equity into the system.

2.6 References

A, R. J. van der, Eskes, H. J., Boersma, K. F., Noije, T. P. C. van, Roozendael, M. V., Smedt, I. D., Peters, D. H. M. U., & Meijer, E. W. (2008). Trends, seasonal variability and dominant NOx source derived from a ten year record of NO2 measured from space. *Journal of Geophysical Research: Atmospheres*, *113*(D4), Article D4. https://doi.org/10.1029/2007JD009021

Achakulwisut, P., Brauer, M., Hystad, P., & Anenberg, S. C. (2019). Global, national, and urban burdens of paediatric asthma incidence attributable to ambient NO2 pollution: Estimates from global datasets. *The Lancet Planetary Health*, *3*(4), e166–e178. https://doi.org/10.1016/S2542-5196(19)30046-4

Air Sensor Guidebook. (2014, June). https://cfpub.epa.gov/si/si_public_file_download.cfm?p_download_id=519616

Arain, M. A., Blair, R., Finkelstein, N., Brook, J., & Jerrett, M. (2009). Meteorological influences on the spatial and temporal variability of NO2 in Toronto and Hamilton. *The Canadian Geographer / Le Géographe Canadien*, *53*(2), 165–190. https://doi.org/10.1111/j.1541-0064.2009.00252.x

Baldasano, J. M. (2020). COVID-19 lockdown effects on air quality by NO2 in the cities of Barcelona and Madrid (Spain). *Science of The Total Environment*, *741*, 140353. https://doi.org/10.1016/j.scitotenv.2020.140353

Bauwens, M., Compernolle, S., Stavrakou, T., Müller, J.-F., Gent, J. van, Eskes, H., Levelt, P. F., A, R. van der, Veefkind, J. P., Vlietinck, J., Yu, H., & Zehner, C. (2020). Impact of Coronavirus Outbreak on NO2 Pollution Assessed Using TROPOMI and OMI Observations. *Geophysical Research Letters*, *47*(11), e2020GL087978. https://doi.org/10.1029/2020GL087978

Berman, J. D., & Ebisu, K. (2020). Changes in U.S. air pollution during the COVID-19 pandemic. *The Science of the Total Environment*, *739*, 139864. https://doi.org/10.1016/j.scitotenv.2020.139864

Bermejo-Orduna, R., McBride, J. R., Shiraishi, K., Elustondo, D., Lasheras, E., & Santamaría, J. M. (2014). Biomonitoring of traffic-related nitrogen pollution using Letharia vulpina (L.) Hue in the Sierra Nevada, California. *Science of the Total Environment*, *490*, 205–212.

Boersma, K. F., Eskes, H. J., & Brinksma, E. J. (2004). Error analysis for tropospheric NO2 retrieval from space. *Journal of Geophysical Research: Atmospheres*, *109*(D4), Article D4. https://doi.org/10.1029/2003JD003962

Cakmak, S., Hebbern, C., Cakmak, J. D., & Vanos, J. (2016). The modifying effect of socioeconomic status on the relationship between traffic, air pollution and respiratory health in elementary schoolchildren. *Journal of Environmental Management*, *177*, 1–8. https://doi.org/10.1016/j.jenvman.2016.03.051

CDC COVID Data Tracker. (2020, November 12). https://www.cdc.gov/covid-data-tracker/#cases

Cesaroni Giulia, Badaloni Chiara, Gariazzo Claudio, Stafoggia Massimo, Sozzi Roberto, Davoli Marina, & Forastiere Francesco. (2013). Long-Term Exposure to Urban Air

Pollution and Mortality in a Cohort of More than a Million Adults in Rome. *Environmental Health Perspectives*, *121*(3), 324–331. https://doi.org/10.1289/ehp.1205862

Coppalle, A., Delmas, V., & Bobbia, M. (2001). Variability of Nox and No2 concentrations observed at pedestrian level in the city centre of a medium sized urban area. *Atmospheric Environment*, *35*(31), 5361–5369. https://doi.org/10.1016/S1352-2310(01)00296-5

Daily Summary Report By Site. (2021, July 1). https://idem.meteostar.com/cgi-bin/select_summary.pl

Fattorini, D., & Regoli, F. (2020). Role of the chronic air pollution levels in the Covid-19 outbreak risk in Italy. *Environmental Pollution (Barking, Essex : 1987)*, *264*, 114732. https://doi.org/10.1016/j.envpol.2020.114732

Galloway, J. N., Aber, J. D., Erisman, J. W., Seitzinger, S. P., Howarth, R. W., Cowling, E. B., & Cosby, B. J. (2003). The Nitrogen Cascade. *BioScience*, *53*(4), 341–356. https://doi.org/10.1641/0006-3568(2003)053[0341:TNC]2.0.CO;2

GeoTAM. (2021, July 1). https://tceq.maps.arcgis.com/apps/webappviewer/index.html?id=ab6f85198bda483a997a6956a8486539

Goldberg, D. L., Anenberg, S. C., Griffin, D., McLinden, C. A., Lu, Z., & Streets, D. G. (2020). Disentangling the Impact of the COVID-19 Lockdowns on Urban NO2 From Natural Variability. *Geophysical Research Letters*, *47*(17), e2020GL089269. https://doi.org/10.1029/2020GL089269

Jaeglé, L., Steinberger, L., Martin, R. V., & Chance, K. (2005). Global partitioning of NOx sources using satellite observations: Relative roles of fossil fuel combustion, biomass burning and soil emissions. *Faraday Discussions*, *130*(0), 407–423. https://doi.org/10.1039/B502128F

Jia, C., Fu, X., Bartelli, D., & Smith, L. (2020). Insignificant Impact of the "Stay-At-Home" Order on Ambient Air Quality in the Memphis Metropolitan Area, U.S.A. *Atmosphere*, *11*(6), 630. https://doi.org/10.3390/atmos11060630

Jobson, B. T., Berkowitz, C. M., Kuster, W. C., Goldan, P. D., Williams, E. J., Fesenfeld, F. C., Apel, E. C., Karl, T., Lonneman, W. A., & Riemer, D. (2004). Hydrocarbon source signatures in Houston, Texas: Influence of the petrochemical industry. *Journal of Geophysical Research: Atmospheres*, *109*(D24), Article D24. https://doi.org/10.1029/2004JD004887

Lamsal, L., Krotkov, N., Celarier, E., Swartz, W., Pickering, K., Bucsela, E., Gleason, J., Martin, R., Philip, S., Irie, H., Cede, A., Herman, J., Weinheimer, A., Szykman, J., & Knepp, T. (2014). Evaluation of OMI operational standard NO2 retrievals using in situ and surface-based NO2 observations. *Atmospheric Chemistry and Physics*, *14*, 11587–11609. https://doi.org/10.5194/acp-14-11587-2014

Madariaga, I., Agirre, E., & Uria, J. (2003). *Short-term forecasting of ozone and NO2levels using traffic data in Bilbao (Spain)*. *64*, 8.

Marco, R. D., Poli, A., Ferrari, M., Accordini, S., Giammanco, G., Bugiani, M., Villani, S., Ponzio, M., Bono, R., Carrozzi, L., Cavallini, R., Cazzoletti, L., Dallari, R., Ginesu, F., Lauriola, P., Mandrioli, P., Perfetti, L., Pignato, S., Pirina, P., & Struzzo, P. (2002). The impact of climate and traffic-related NO2 on the prevalence

of asthma and allergic rhinitis in Italy. *Clinical & Experimental Allergy*, *32*(10), 1405–1412. https://doi.org/10.1046/j.1365-2745.2002.01466.x

Matthes, S., Grewe, V., & Sausen, R. (2007). Global impact of road traffic emissions on tropospheric ozone. *Atmos. Chem. Phys.*, *30*, 13.

Miranda, M. L., Edwards, S. E., Keating, M. H., & Paul, C. J. (2011). Making the Environmental Justice Grade: The Relative Burden of Air Pollution Exposure in the United States. *International Journal of Environmental Research and Public Health*, *8*(6), 1755–1771. https://doi.org/10.3390/ijerph8061755

Nakada, L. Y. K., & Urban, R. C. (2020). COVID-19 pandemic: Impacts on the air quality during the partial lockdown in São Paulo state, Brazil. *Science of The Total Environment*, *730*, 139087. https://doi.org/10.1016/j.scitotenv.2020.139087

New York State Air Quality. (2021, July 1). http://www.nyaqinow.net/

Nicolai, T., Carr, D., Weiland, S. K., Duhme, H., von Ehrenstein, O., Wagner, C., & von Mutius, E. (2003). Urban traffic and pollutant exposure related to respiratory outcomes and atopy in a large sample of children. *European Respiratory Journal*, *21*(6), 956–963. https://doi.org/10.1183/09031936.03.00041103a

Peel, J. L., Tolbert, P. E., Klein, M., Metzger, K. B., Flanders, W. D., Todd, K., Mulholland, J. A., Ryan, P. B., & Frumkin, H. (2005). Ambient Air Pollution and Respiratory Emergency Department Visits. *Epidemiology*, *16*(2), 164–174. JSTOR.

Quality Assurance Air Monitoring Site Information | California Air Resources Board. (2021, July 1). https://ww2.arb.ca.gov/applications/quality-assurance-air-monitoring-site-information

Redling, K., Elliott, E., Bain, D., & Sherwell, J. (2013). Highway contributions to reactive nitrogen deposition: Tracing the fate of vehicular NOx using stable isotopes and plant biomonitors. *Biogeochemistry*, *116*(1), 261–274. https://doi.org/10.1007/s10533-013-9857-x

Şahin, Ü. A. (2020). The Effects of COVID-19 Measures on Air Pollutant Concentrations at Urban and Traffic Sites in Istanbul. *Aerosol and Air Quality Research*, *20*(9), 1874–1885. https://doi.org/10.4209/aaqr.2020.05.0239

Shah, V., Jacob, D. J., Li, K., Silvern, R. F., Zhai, S., Liu, M., Lin, J., & Zhang, Q. (2020). Effect of changing NO_x lifetime on the seasonality and long-term trends of satellite-observed tropospheric NO_2 columns over China. *Atmospheric Chemistry and Physics*, *20*(3), 1483–1495. https://doi.org/10.5194/acp-20-1483-2020

Sharma, S., Zhang, M., Anshika, Gao, J., Zhang, H., & Kota, S. H. (2020). Effect of restricted emissions during COVID-19 on air quality in India. *The Science of the Total Environment*, *728*, 138878. https://doi.org/10.1016/j.scitotenv.2020.138878

StreetLight Volume Methodology & Validation White Paper. (2019, August). https://www.streetlightdata.com/

Tanzer-Gruener, R., Li, J., Eilenberg, S. R., Robinson, A. L., & Presto, A. A. (2020). Impacts of Modifiable Factors on Ambient Air Pollution: A Case Study of COVID-19 Shutdowns. *Environmental Science & Technology Letters*, *7*(8), 554–559. https://doi.org/10.1021/acs.estlett.0c00365

Tobías, A., Carnerero, C., Reche, C., Massagué, J., Via, M., Minguillón, M. C., Alastuey, A., & Querol, X. (2020). Changes in air quality during the lockdown in Barcelona

(Spain) one month into the SARS-CoV-2 epidemic. *Science of The Total Environment*, *726*, 138540. https://doi.org/10.1016/j.scitotenv.2020.138540

Traffic Count Database System (TCDS). (2020). https://indot.ms2soft.com/tcds/tsearch.asp?loc=indot

Walters, W. W., Goodwin, S. R., & Michalski, G. (2015). Nitrogen Stable Isotope Composition (δ15N) of Vehicle-Emitted NOx. *Environmental Science & Technology*, *49*(4), 2278–2285. https://doi.org/10.1021/es505580v

WHO Director-General's opening remarks at the media briefing on COVID-19—11 March 2020. (2020, May 21). https://www.who.int/dg/speeches/detail/who-director-general-s-opening-remarks-at-the-media-briefing-on-covid-19---11-march-2020

Wu, C., Wang, H., Cai, W., He, H., Ni, A., & Peng, Z. (2021). Impact of the COVID-19 lockdown on roadside traffic-related air pollution in Shanghai, China. *Building and Environment*, *194*, 107718. https://doi.org/10.1016/j.buildenv.2021.107718

CHAPTER 3: THE ROLE OF LOCAL VEHICULAR TYPE AND CANOPY COVERAGE IN CONTROLLING GROUND-LEVEL NO_2 IN THE URBAN ENVIRONMENT

3.1 Introduction

Nitrogen Oxides (NOx), including nitrogen dioxide (NO_2) and nitrogen oxide (NO), negatively impact biodiversity and human health worldwide (Almaraz et al., 2018). Ground-level nitrogen oxide, a reactive nitrogen specie (Nr) is limited by the amount of available ozone (O_3) as seen in Equations 1-3 (Matthes et al., 2007; Palmgren et al., 1996):

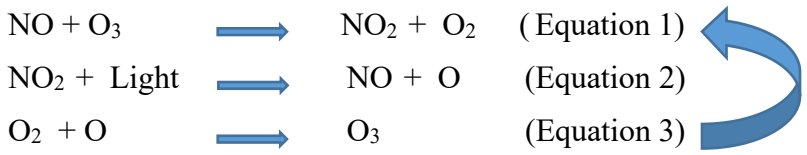

In vehicles, N_2 reacts with O to form NO and N. This is limited by the high amount of energy that is required to break the bond of N_2 (Heaton, 1990). During daytime photolytically produced OH oxidizes NO_2 to nitric acid (HNO_3). While as at night the oxidation of NO_2 by O_3 produces nitrate radical (NO_3^{-1}) which in a couple of further steps forms HNO_3 as well (Elliott et al., 2007).

NO_2 concentrations rise in the cooler months not only due to increase of anthropogenic contribution sources but also due to its longer residence time due to seasonal photochemical and seasonal conditions of the planetary boundary layer. Higher boundary layers in spring and summer contribute to increased dispersion during those months and thus resulting in lower ground-level concentrations (Kendrick et al., 2015; Voiculescu et

al., 2020a). Connection between these pollutants was witnessed globally during COVID lockdown due to decreased anthropogenic activities (e.g., Heintzelman et al., 2021). Data analyzed from over 10,000 ground-based global monitors, during the lockdown, showed that NO_2 and $PM_{2.5}$ had a marked reduction of 45.8% and 16.1% when it was compared to previous five years, whereas O_3 increased by 5.4% which could be attributed to reduced traffic as well as industrial activities (He et al., 2021).

Globally, anthropogenic reactive nitrogen is modeled to increase to approximately 156-270 Tg N/yr from the early 1990s to 2050 (Galloway et al., 2004). In 2020, the global contribution to reactive nitrogen from fossil fuel combustion alone was 34 Tg N/year (Galloway et al., 2021). Anthropogenic emissions have also resulted in significant negative impacts to terrestrial and aquatic ecosystems through wet and dry deposition (Anenberg et al., 2018; Díaz-Álvarez et al., 2018; Galloway et al., 2003).

Nitrogen oxides and ground-level ozone are causing higher incident of asthma, upper respiratory disease, cardiovascular disease, birth defects, and sudden infant death syndrome (Anenberg et al., 2018; Hazlehurst et al., 2018; Hwang et al., 2019; Meng et al., 2021; Padula et al., 2021). As NO_2 increases, formation of ozone and fine particulate matter ($PM_{2.5}$) also increases, raising respiratory mortality and morbidity (Lamsal et al., 2013; Meng et al., 2021; Olaniyan et al., 2020; Rao et al., 2014). An overlap of high atmospheric pollution, high population and poor health quality in the Midwestern region of the U.S results in highest incident of premature mortality in this area (Fann et al., 2011).

In 2015 alone, 9-23 million emergency room visits globally were estimated to be attributed to ozone exposures. While as between 0.4 – 0.5 million could be attributed to exposure to NO_2, which was underestimated as near road exposures were not captured in

the study. NO_2 and $PM_{2.5}$ was found to have the greatest association, in this 2015 data, between it and onset of new asthma cases, with a third of the yearly new pediatric cases resulting from it. $PM_{2.5}$ had limited cases in pediatrics, but NO_2 was consistently reported as a risk factor in all age groups (Anenberg et al., 2018). Ozone exposure not only results in alterations to the central nervous system, but also results in brain responses similar to systemic stress (Gackière et al., 2011).

Due to these serious health impacts and increased risk of mortality, the U.S. Environmental Protection Agency (EPA) has set NO_2 hourly maximum standards at 100 ppb and 8-hour O_3 standards at 0.070 ppm (70 ppb) (US EPA, 2014a), and requires states to monitor these gases. As examined in our previous study, typically, states have very few continuous monitors, and even large cities might only have 1 or 2 continuous monitors (Heintzelman et al., 2021). This spatially-limited dataset is due to the challenging and cost prohibitive nature of conducting such analyses at a finer scale (Jaeglé et al., 2005). Local anthropogenic sources like vehicles are some of the primary contributors to these pollutants, having local as well as regional impacts. Several of these pollutants decrease with decay to background levels on average at 115-300 m (0.12 - 0.3 Km) from road edge (Karner et al., 2010). Because of the relatively short residence time of NO_2 (~1 day; Wallace & Hobbs, 2006), it is typically at its highest concentrations near its source (Lamsal et al., 2013), and thus fine spatial and temporal scale analysis are necessary to examine and predict the burden and outcomes of human exposure to pollutants. Additionally, we know that there are over 45 million individuals in the U.S living in close proximity to busy roadways who are exposed to vehicular emission, a threat to human health(US EPA, 2014b).

These health impacts from air pollution (Meo et al., 2022; Olaniyan et al., 2020; Roberts et al., 2019) and the nature of the pollutants presents a need to locally monitor them in a cost effective way. To fill this gap, there has been a rise in interest and use of low cost sensors in air quality studies (English et al., 2017; Knibbs et al., 2016; Mavko et al., 2008; Pope et al., 2018; Sather et al., 2001; Tanzer-Gruener et al., 2020). In conjunction with pollution sources, meteorologic factors are critical for modulating air pollutant concentrations at the ground level. For example, seasonal meteorological parameters play a role in reducing or increasing air pollution, with lower solar radiation (resulting in lower temperatures) and humidity in winter resulting in typically higher levels of NO_2 in the winter and lower levels in the more intense solar radiation (higher temperature) months during summer (Çel, 2007; Cichowicz et al., 2017; Voiculescu et al., 2020a). Additionally, the impacts of vehicles on NO_2 levels (Harper et al., 2021; Heintzelman et al., 2021) as well as vegetations (Harper et al., 2021) role in altering NO_2 levels as we move towards more urbanization has also been recognized (Nowak et al., 2006; Nowak & Greenfield, 2018b).

This study aims to gain insight into spatio-temporal variability of ground-level urban air pollution by analyzing data from 32 low-cost Ogawa & Co passive samplers in an eastern portion of Marion County, Indianapolis, Indiana. Ogawa samplers have been evaluated in several studies of various timespans, ranging from hours to a year, with over 90% of resulting values consistent with Federal Reference Methods Monitors (FRM) data. Not only are these samplers designed to perform like an equivalent method, but they are also low-maintenance, convenient to load and transport, don't require a power source, and are cost effective. This prevents loss of data due to any breakdown of equipment making it

a very valuable tool in air pollution studies (Korf et al., 2020; Mukerjee et al., 2004; Sather et al., 2006, 2007). We used air quality data from Ogawa sensor network along with various meteorological, land use, traffic, and census variables (APPENDIX A) in the Pleasant Run (PR) airshed to examine the impact of: (1) vehicle count, and medium and heavy truck indices on local NO_2 concentrations, (2) tree canopy coverage on NO_2 concentrations.

3.2 Methodology

3.2.1 Passive Sampling of NO_2 and O_3

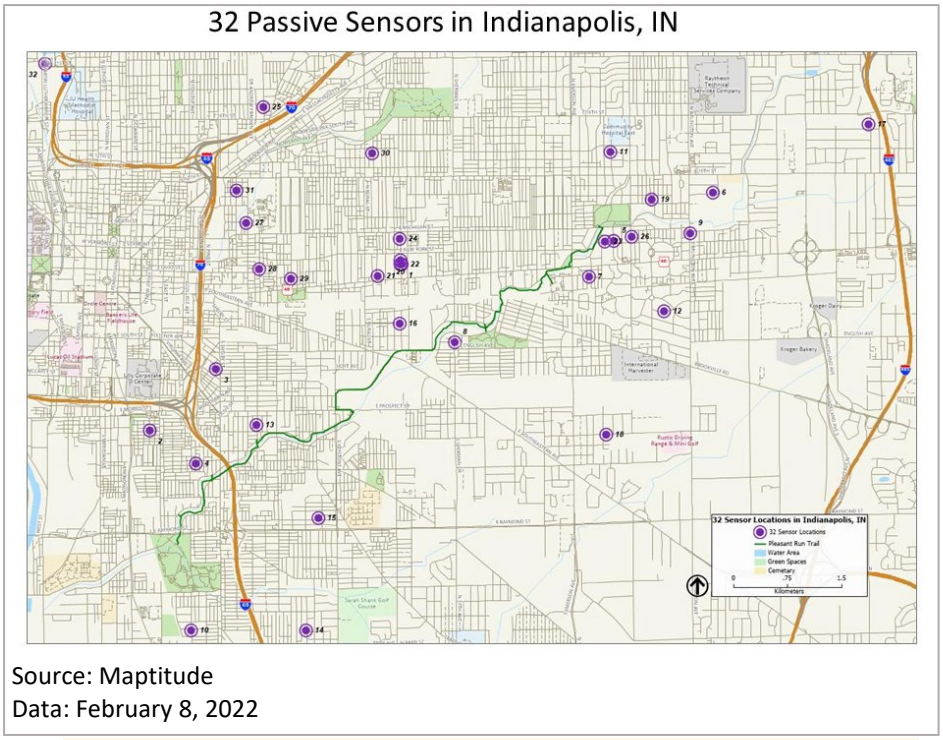

Figure 3.1. The spatial distribution of 32 sensors in the study area.

We recruited 32 citizen scientists in the PR airshed in Indianapolis, Indiana, largely in collaboration with Keep Indianapolis Beautiful (KIB), a local community based nonprofit organization with a focus on improving the environment. As phase 1 we installed PurpleAir PA-II-SD particulate matter sensors, and in phase 2, over several deployment

cycles, we deployed Ogawa passive samplers to capture NO_2 and O_3 concentrations (Figure 3.1). Sensors were installed at approximately 4 feet – 8 feet (1.2 meter – 2.4 meter) above ground with one sensor placed in a 3-story balcony, for one week each seven times between September 2018 and July 2020. Each analysis cycle we also deployed a sensor at one control site in the area (KIB headquarters building). Since data from 3 deployments in 2019 encompassed all 32 sites, the specific time periods used from 2019 in this study covered: January 20-27, March 30- April 6, and June 29- July 6.

Ogawa passive samplers consist of a reusable unit which holds a solid cylindrical tube made up of 6 parts. Each end of the tube has a diffuser end cap followed by a stainless-steel screen, a 14.5 mm collection pad for NO_2 or O_3, a Teflon ring and a Teflon disk. Prior to deployment each unit was rinsed with Milli-Q water and dried before placing the collection pad between the 2 stainless steel screens. After loading the units, they were placed in a small plastic bag securely placed inside a brown vial with a screw top. To streamline deployment and retrieval we designed a contraption shown below that was easily hung at each site (Figure 3.2). At the end of each sampling cycle, we retrieved the exposed devices as well as the unopened control device from KIB back to the lab. At the lab the initial steps were reversed, and the collection pads were placed in separate clear shipping vials before mailing them to RTI International in North Carolina, a lab used by Ogawa for analysis. RTI extracts the NO_2 pads in Deionized (DI) water and analyzes by Ion Chromatography (IC). Ozone pads are extracted the same way and analyzed for nitrate by IC. For IC analysis the lab calibrates their system daily with standard ranges depending on the pollutant. Lastly, to analyze NOx pads they use continuous flow colorimetric analyzer (FIA) (*PROTOCOLS – OGAWA USA*, 2021).

Ogawa passive samplers have been used for different sampling periods (Cowie et al., 2019; Masey et al., 2017a). For example, Cowie et al., 2019 underestimated 7-day exposure concentrations but explained 87% of temporal variation making them a sound NO_2 sampler. Empirical corrections based on wind speed which impacted their sampler's increased accuracy by only 5%. They found the mean of 947 sites in a land use regression model to be between the satellite data mean and a Bayesian model mean. Even without correction this is a more robust measurement process than satellite- land use regression models which have shown to predict 69% variability at urban sites and an overall prediction of 58% at all sites (Knibbs et al., 2016). Even when there are associations and trends between in situ and satellite data measurements, one reason for the in situ measurements being different than satellite data is due to the fact that the former is fine scale concentration versus the latter which is averaged over an area (Kharol et al., 2015).

Figure 3.2. Passive sensor contraption designed for this deployment at 32 sites.

3.2.2 Meteorological data

A correlation exists between NO_2 and O_3 (Pancholi et al., 2018; Paraschiv et al., 2020; Zoran et al., 2020), as well as between NO_2 and meteorological variables such as

wind speed, temperature, and the composition of vehicle fleet (Karner et al., 2010; Masey et al., 2017a; Ngarambe et al., 2021; Voiculescu et al., 2020a). We accessed temperature, and wind-speed (January data was from Interstate I-70 monitor only due to missing data from the Washington Park monitor) data from the Indiana Department of Environmental Management (IDEM) Washington Park continuous flow sensor (WP) and Interstate 70 (I-70) (*Monthly Summary Report*, 2021). Due to large gaps in data from the I-70 monitor, we primarily utilized Washington Park monitor data in this analysis. Even though there can be small yet significant temperature variation with green spaces being cooler and impervious spaces being warmer (Scott et al., 2017), we are assuming here that the predominant temperature variation is temporal rather than spatial.

3.2.3 Tree canopy data

Estimates of tree canopy cover (TC) in the study region were based on 1-meter resolution land cover raster produced by our partner KIB and the University of Vermont Spatial Analysis Laboratory. The land cover data were derived from classification of National Agricultural Imagery Program (NAIP) data acquired in 2013 and LiDAR data acquired in 2009. This dataset was used to quantify tree canopy (TC) in the study region census tracts and within buffers at varying distances from the sensor locations. We ran our analysis in this study of tree canopy coverage in a 1 km buffer to capture the immediate impacts of the sensor locations (Mullen et al., 2022). TC is constituted by layers of branches, stems, and leaves on trees that cover the ground when it is viewed from above. ArcMap 10.8.1 ® was used to access and extract these values at varying length from the sensors. At the census tract level tree canopy coverage ranged between 17-46%, with an average of 29%.

We know that urban Heat Islands (UHI) are a product of the built environment (Speak et al., 2020). Additionally, tree canopies play a role in the thermal energy balance, and canopy traits like Leaf Area Index and crown widths have been found be the most impactful on temperature variations within the UHI (Scott et al., 2017). Urban greening initiatives, as discussed in our $PM_{2.5}$ study in this same study area, have positive impacts on air quality (Heintzelman, 2019). There we found that increases in percent of tree canopy cover at the census tract level were negatively associated with $PM_{2.5}$ concentration. Trees also uptake NO_2 at varying rates, also referred to as dry deposition, based on species, stomatal apertures and light (Chaparro-Suarez et al., 2011), thus impacting the amount of pollutants present. Downward flux of the pollutant has been calculated as a product of the deposition velocity of the pollutant and the pollutant concentration in the atmosphere. The deposition velocity, which can be challenging to calculate, takes into account the boundary layer and the resistances by the canopy (Baldocchi et al., 1987; Nowak et al., 2006). Canopy stomatal resistance can be affected by a magnitude of four which is based on the species, and the plants physiological and environmental conditions (Baldocchi et al., 1987),

3.2.4 Land use data

The distribution of three types of land use within the study region ('Heavy Industrial', 'Heavy Commercial', and 'Light Industrial') were examined, but only Heavy Industry due to its potential emissions was modeled using a vector-based GIS dataset from the City of Indianapolis's data portal (*Open Indy Data Portal*, 2021). This data was further processed using mapping software Maptitude 2020 by Caliper ® and was used to capture local impacts on the census tracts (Harper et al., 2021).

3.2.5 American Community Survey

The most recent American Community Survey (ACS) 5-year estimates (2014 - 2018) was used for socio-economic and demographic variables (*Explore Census Data*, 2021). Statistical analysis incorporating these variables was conducted using open-source software RStudio version 4.0.3. Census tract level variables of race and education were used as a proxy for neighborhood characteristics to examine socio economic bias in air pollution exposures in PR (Li et al., 2022; Mullen et al., 2022).

3.2.6 GIS based measurements and StreetLight data

Proximity to gasoline stations (Huppé et al., 2013) and traffic has also been associated with increased negative health impacts in children and adults (Alemany et al., 2018; Bowatte et al., 2017; Kreis et al., 2022; Wang et al., 2019). Furthermore, proximity to major highways and traffic information has also been used to assess local impacts of air pollution (Filigrana et al., 2020). Therefore, gas stations in a radius of 10 km, distance to highways, and road and highway lengths in the census tracts were utilized in this analysis.

Additionally, we utilized StreetLight (SL) platform, which uses smart phones and navigational units to measure various modes of traffic in the U.S. in this analysis. This platform has several output options; however, we utilized three output measures namely StreetLight Volume and StreetLight Index (for heavy and medium trucks). After setting up 42 pass-through zones at street segments in front of each sensor location, StreetLight volume was used to examine estimated vehicle trips. SL data is based on an algorithm that utilizes real-world data and seasonal factors to calculate an estimated count for each zone. They consider this the best output to compare data across time. Even though this is not estimated on real-world counts, this normalized relative volume considers space and time

when calculating sample size variations and is a good method to compare values in the analysis across time, thus it is used as a traffic proxy in PR (Filigrana et al., 2020). StreetLight Index is based on medium-duty commercial vehicles are those that fall between 14,000 – 26,000 lbs. and heavy-duty commercial vehicles are those that are over 26,000 lbs.

3.2.7 Statistical analysis

Initially correlations between NO_2 and the significant variables from the regression were examined before comparing NO_2 and O_3 averages between the WP monitor and its three closest passive sensors. As the next step, regression analysis was run on the categories of data listed in Table 3.1(APPENDIX A). To address multicollinearity represented by the variance inflation factor (VIF) there were a total of 5 models run (APPENDIX B) to capture the local impacts. Lastly, a stepwise regression model was run which produced our final model.

Table 3.1 - Data.

Data Categories	
StreetLight:	vehicle data
ACS 5-year 2018 estimates:	population-based census bureau data
City of Indianapolis Portal:	land use parcel data
High resolution Imagery:	tree canopy coverage data
Washington Park IDEM monitor:	meteorological data*
GIS data:	spatial measurement data

**For January this measurement was from I-70 monitor*

3.3 Results

Examining the averages of the two pollutants from Ogawa sensors we found that the overall trend of NO_2 decreases as the months progress while as O_3 concentrations increased. There was a substantial increase in the Heavy truck index from January to June in 2019, an increase that is not consistent with the medium truck index across the sensor networks (Table 3.2).

Table 3.2 - Ogawa and StreetLight platform averages in the study area.

	Averages		
	Jan	Mar	Jun
NO_2 Averages(ppb)	9.5	8.8	6.0
O_3 Averages(ppb)	21.5	25.9	33.5
All Vehicle count	2,063	2,215	2,716
Medium Truck Daily Index	431	515	513
Heavy Truck Daily Index	481	620	643

3.3.1 Regression

Significant correlations of the variables used in the regression model was run in R-studio and the results are reported in Table 3.3 (APPENDIX B). NO_2 was found to be negatively correlated with O_3 ($r = -0.75$, Table 3.3), consistent with other studies (Matthes et al., 2007; Palmgren et al., 1996). Additionally, NO_2 was also negatively correlated with tree canopy cover ($r = -0.38$), and as distance to highway from each sensor location increased. While as NO_2 was positively correlated to increase in windspeed, heavy truck index increases, population with less than high school increases, and heavy industry percentage in the census tract increases. The positive correlation between NO_2 concentrations and windspeed as we have here has been examined in a Ogawa sampler

study, and can be attributed to turbulence in the shelter that is induced when wind speed increases (Masey et al., 2017b).

Table 3.3 - Significant Correlation output of variables with NO_2.

Correlations with NO_2	**Type**	**Corr**	**P-value**
Tree canopy-1 km	Pearson	-0.37900	0.000179 **
Windspeed kmh	Pearson	0.69800	0.000000 **
O_3 (ppb)	Spearman	-0.74820	0.000000 **
Heavy Truck Index	Spearman	0.24700	0.016600 *
Pop25+LT high school %	Spearman	0.25200	0.014400 *
Heavy Industry %	Spearman	0.27990	0.006570 **
Distance to hwy	Spearman	-0.23500	0.023080 *

** Correlation coefficient significance at P <0.05;*
***Correlation coefficient significance at P <0.01.*

In total there were 5 regression models run with a stepwise regression model at the end. Output from Model 1, Model 4, and the stepwise regression analysis are listed in Table 3.4. In Model 1 Temp C resulted in high collinearity with a variance inflation factor (VIF) of 67.09. This was removed in Model 2, where Medium Truck Index resulted in high collinearity with a VIF of 20.90. Model 3, where this variable was also removed, resulted in Road Length-10 km reporting a high VIF of 10.95. Once this variable was also removed Model 4, reported all VIF values under 10. Lastly, a stepwise regression model was run on Model 4. Adjusted R-square decreases from Model 1 to Model 4 from 79.1% to 73.84%, however, from Model 4 to the stepwise model it increases and explains 75.29% variation in the data. In Model 1, the negative relationship of temperature, a product of solar radiation, and NO_2 is probably due to its transformation into its secondary pollutants (Korf et al., 2020). Comparing the results of Model 4 and the stepwise model we see that the same 6 variables (O_3, All Vehicle Count, Tree Canopy – 1 km, Windspeed kmh, Distance to Hwy, and Gas Station-10 km) are significant in both models.

Table 3.4. Three regression models including a stepwise regression model output of coefficients and significance for NO_2.

	Model 1 (Adj-R^2 =79.1)	**Model 4 (Adj-$R^=$ =73.84)**	**Stepwise (Adj-R^2 =75.29)**
(Intercept)	17.2700 **	5.6490	5.7370 .
O_3 (ppb)	-0.1434 **	-0.2094 **	-0.2093 **
All Vehicle Count	0.0001	0.0001 *	0.0001 *
Medium Truck Index	-1.5430		
Heavy Truck Index	-2.1350	-2.1710	-2.1150
Hispanic Latino %	-0.0229	-0.0154	
White only %	0.0106	-0.0025	
Pop25+LT high school %	18.0300	5.7100	
Pop25+bachelors %	-15.8800	-5.9020	
Heavy Industry %	0.0173	0.0185	
Tree Canopy-1 km	-1.7470 .	-2.1920 *	-2.4060 **
Windspeed kmh	-1.1450 **	0.1694 *	0.1686 *
Temp C	-0.2678 **		
Hwy Length-10 km	-0.0027	0.0026	
Road Length-10 km	0.0011		
Distance to Hwy	-0.3744	-0.4471 .	-0.4155 *
Gas Station-10 km	0.0185	0.0546 *	0.0562 **

. p-value 0.1
** Significance at P <0.05.*
***Significance at P <0.01.*
All models are significant at p-value < 0.05.

Ozone formation is impacted by complex dynamics in the atmosphere, (Korf et al., 2020), is negatively correlated with NO_2 in the stepwise regression model. Based on the highly significant variables of the stepwise regression model a 1 ppb increase in ozone results in a decrease in NO_2 of 0.21 ppb. Second, a 1 km^2 increase in tree canopy coverage (in a circle with a radius of 1 km from each sensor) results in a decrease in NO_2 of 2.41 ppb which is highly significant. A study between 2009-2014 showed that U.S had a reduction of 175,000 acres per year of tree canopy area in urban/community areas, which

is equivalent to approximately 36 million trees/year, resulting in a loss of benefits estimated at $96 million a year. This decrease in tree cover was accompanied with increase in impervious surface in urban areas by 1 percent in the 5 years (Nowak & Greenfield, 2018b). We also find that gas stations play a very significant role in our study, with one additional gas station within 10 km radius results in increasing NO_2 by 0.06 ppb.

Stepwise model, like Model 4, also shows that only all vehicles count data, from the StreetLight platform, plays a role in increasing NO_2 values, and truck indices do not., A 1,000-count increase in all vehicles increases NO_2 by approximately 0.1 ppb. The reasoning for the medium sized trucks or the heavy trucks not being significant could be a factor of the short time this data was collected.

Land cover, not significant in Model 1-4, is removed in the stepwise model, while as wind speed is significant at p-value < 0.05. As wind speed increases by 1 kmh it increases NO_2 concentrations by 0.17 ppb. The positive relationship between windspeed and NO_2 is once again witnessed here due to internal turbulence created in the shelter resulting in an increased pollutant load on the sensor pads (Masey et al., 2017b). Lastly, distance to highway in the stepwise model is significant at p-value <0.05. As the sensor location moves further away from the highway by 1 km NO_2 decreases by 0.42 ppb.

3.3.2 Three passive sensors and Washington Park (WP) continuous regulatory monitor data

The three passive sensors closest to the WP sensor are sensors 25, 30, and 31 (Figure 3.3). Four days of data were missing from the January 2019 deployment dates, therefore January data from WP was not utilized in comparisons of NO_2. June resulted in the lowest concentrations for NO_2 while January and March had higher concentrations (Table 3.5). In

March, WP concentrations were the lowest, and in June they were the highest when compared to the three sensors. WP and its three closest passive sensors indicate that NO_2 values are higher in March, a cooler month, when compared to June (Table 3.5). Ozone was consistently highest in June when compared to January and March. Due to this temporal variation, also reflected in an analysis of variance test (ANOVA), we cannot rely on the one WP continuous regulatory monitor data to examine and capture fine scale variations which exist in the study area.

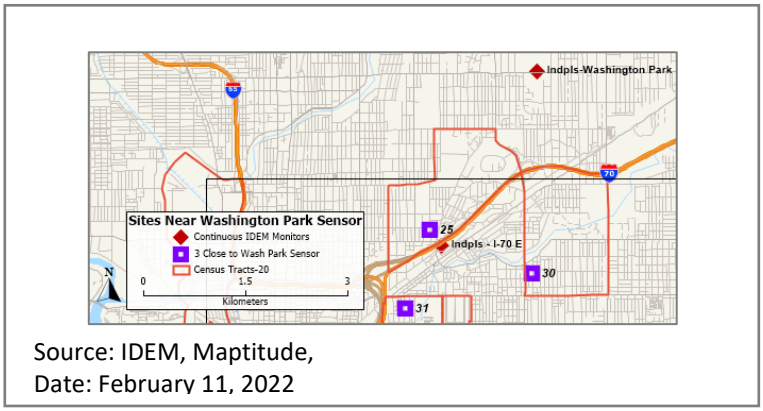

Figure 3.3 - Sensors closest to Indiana Department of Environmental Management monitors.

Table 3.5. 2019 NO_2 and O_3 data from three closest sensors to Washington Park (WP) continuous regulatory monitor data.

		NO_2 (ppb)			**O_3 (ppb)**	
	Jan	Mar	Jun	Jan	Mar	Jun
Sen 30	9.67	9.98	6.58	19.43	24.68	30.27
Sen 25	9.99	10.45	5.21	20.21	25.62	44.17
Sen 31	11.2	10.32	7.00	19.90	25.03	32.56
WP	NA	9.61	8.31	27.63	32.63	32.88

NA (not applicable)

3.3.3 NO_2 and O_3 for all passive sensors and Washington Park (WP) continuous regulatory monitor data

Seasonal median values for NO_2 and O_3 display opposite trends with median NO_2 values in June being relatively low and O_3 being relatively high. In January, this trend is inversed (Table 3.6) with the median NO_2 concentration being relatively high and O_3 concentration being relatively high low (Table 3.6). The inverse trend of O_3, a secondary pollutant from NO_2, with its highest values in June is due to the photochemical reactions that result in its formation in warmer months (Bozkurt et al., 2018).

During March and June, where we have complete data from the WP sensor, there are significant NO_2 differences between the fixed sensor and three proximal passive sensors. In March, there was an 8% difference in NO_2, and June a 28% difference (Table 3.7). For O_3, this difference is 21% in March and 2% in June (Table 3.8).

Table 3.6 - 2019 NO_2 and O_3 descriptive statistics from passive Ogawa samplers.

	NO_2 (ppb)			**O_3 (ppb)**		
	Jan	Mar	Jun	Jan	Mar	Jun
Min	6.95	6.05	3.98	19.43	22.89	25.67
Max	12.26	11.33	9.04	31.31	30.31	44.17
Median	9.53	8.77	5.99	21.00	25.59	33.38
Variance	2.02	1.98	1.12	4.76	3.20	15.87

Table 3.7 - March and June 2019, NO_2 data comparison across all sensors from passive Ogawa samplers and Washington Park (WP) continuous regulatory monitor data.

March-NO_2	Min	Max	Avg	June-NO_2	Min	Max	Avg
Sensors	6.05	11.33	8.84		3.98	9.04	5.96
WP	4.10	12.20	9.61		5.60	10.30	8.31
% diff from WP	47.52%	-7.17%	-8.05%		-28.89%	-12.24%	-28.29%

Table 3.8 - March and June, 2019 NO_2 data comparison across all sensors from passive Ogawa samplers and Washington Park (WP) continuous regulatory monitor data.

March-O_3	Min	Max	Avg	June-O_3	Min	Max	Avg
Sensors	22.89	30.31	25.90		25.67	44.17	33.47
WP	22.00	41.00	32.63		21.00	41.00	32.88
% diff from WP	4.03%	-26.08%	-20.62%		22.25%	7.73%	1.79%

3.3.4 StreetLight data

On examining 2018 and 2019 average annual daily traffic (AADT) near the sensor locations we found data sets from the two years to be almost identical with majority of the estimates displaying less than 5% difference across the locations. Focusing on the three weeks when the passive sensors were deployed. StreetLight data indicates that there was an upward trend in all vehicles count from January to June 2019. Medium trucks index was comparable in March and June while the heavy truck index was highest in June (Figure 3.4).

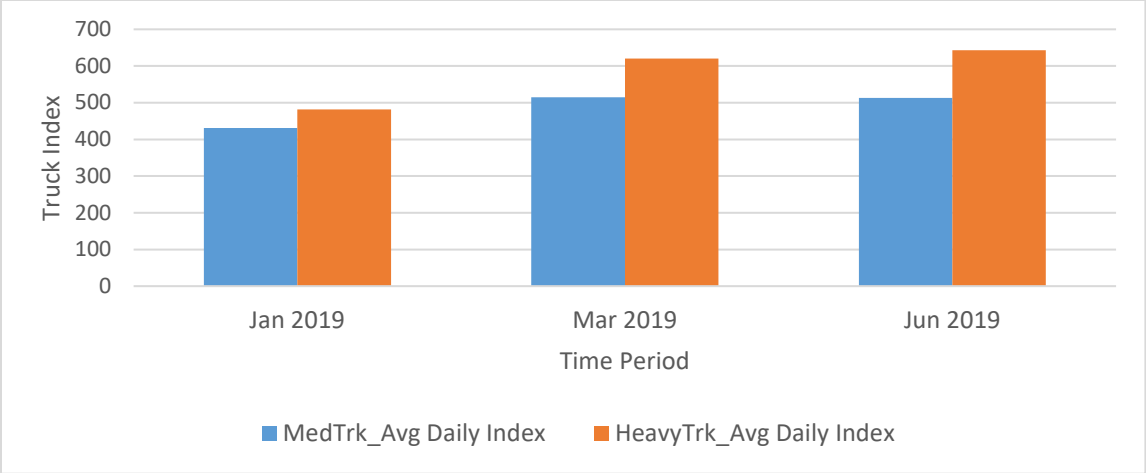

Figure 3.4. StreetLight data from the three deployments for medium truck, and heavy-duty truck index in 2019.

3.4 Discussion

This study examines variations in urban ground-level NO_2, and its relationship to traffic and tree canopy cover. Unlike emissions from power plants and other industries, traffic related emissions can contribute as much as 70% of urban air pollution (Palmgren et al., 1996; Ravina et al., 2021). Traffic related emissions are problematic for human health (Sinharay et al., 2018) especially since they occur at the ground level. Due to the production cycle of O_3 (Equation 1-3), it is not surprising that it is inversely correlated with NO_2 and positively correlated with temperature. While NO_2 and temperature drive O_3 concentrations, NO_2 concentrations are driven by many other environmental and built-environment variables.

3.4.1 Regression output

Our stepwise regression model (Table 3.4) explains ~ 75% of the variability in the study which is comparable to a study in Canada that was designed to estimate NO_2 and other air pollutants at a local scale (Hystad et al., 2011). We find that in the PR airshed, using a reference monitor (WP) is inadequate for characterizing the fine scale variation observed in the network of low-cost sensors (Table 3.7 and 3.8).

3.4.2 Trees

In a stepwise regression model with adjusted R-square of 75%, we find that tree canopy coverage in a 1 Km radius is a significant predictor of increased levels of NO_2. Our final model indicates that as we increase 1 km^2 of tree canopy in the 1 Km radius circle we can help reduce NO_2 by 2.46 ppb, which is consistent with results from previous studies (Nowak et al., 2014; Nowak & Greenfield, 2018b).

Mitigation of pollutants by trees is complex, and is affected by factors such as tree cover, leaf seasons length, plants physiology, and ozone concentration in the air, among others. Therefore, focused tree plantings contribution to the removal of pollution provides a benefit to public health. This can be particularly used as a potential mitigation tool in the favor of climate-related changes in air quality. Trees not only help in reducing urban pollutants, but they also play a role in reducing urban heat (Renaud et al., 2011) which in turn also plays a role in improving human health. It has been found that short term (2-day moving average) and long term (1-year moving average) exposure to NO_2 and O_3 have a causal association with increased risk of mortality with ozone exposure risks being significant even at lower levels (Wei et al., 2020).

A 2006 study encompassing 55 cities in the U.S., using 1994 EPA data and 1990 urban boundaries from the census, concluded that for Indianapolis, canopy cover removed a total of 2,910 metric tons of pollutants within its urban boundary. The greatest air quality improvement from increased canopy coverage were in ozone, particulate matter, and sulfur dioxide (Nowak et al., 2006).

Since vegetation can serve as a sink for atmospheric NO_2 and its by products, it is important to target planting trees, plants, and green infrastructure that are fast growing resilient to the changing climate, and that don't have unintended negative environmental and public health impacts (e.g., heavy pollen producers could exacerbate asthma incidences). Such a planned approach to urban greening can yield both direct UHI reductions and also achieve substantial NO_2 and ozone mitigation in urban settings (Anderson & Gough, 2020; Takahashi et al., 2005; Zhang et al., 2020). A combination of these techniques has been shown to successfully reduced ozone an average of 31% and NO_2 by an average of 65% (Anderson & Gough, 2020). Some of this effect might be that neighborhoods with higher green density also are likely to have lower traffic volume and perhaps lower medium and heavy truck traffic. Thus, it is not just the effects of trees "scrubbing" the air but also local NO_2 emissions avoided by other sources.

3.4.3 Health impacts quantified

As tree species play a direct role in pollen allergenicity in cities (Nowak & Ogren, 2021), care should be taken in researching and encouraging plantings that are beneficial to the residents. Nowak and Ogren (2021) found that in a 53-city study, Indiana has 4.3% leaf area coverage in low allergy trees and shrubs while as 54% are in medium allergy trees and shrubs, and 37.6% in high allergy trees and shrubs. Since it is estimated that 75% of canopy

cover in residential areas is a result of on-property plantings, it was suggested that managing plantings around personal spaces that are low on the allergy spectrum could provide the greatest benefits in terms of pollen exposure to the residents (Nowak, 2012). Urban development tends to reduce tree canopy cover, which poses a challenge both locally and nationally. For example, urban land in Indiana increased from covering 6.1% of the state's land area to 7% from 2000 to 2010, which is a change in acreage by 205 x $10^{3.}$ This is supposed to grow to 17.5% by year 2060. Nationally, urban land in the conterminous U.S is projected to increase by 95.5 million acres to 163.1 million acres from 2010 to 2060. (Nowak & Greenfield, 2018a). Indiana urban forests resulted in pollution removal savings of over 432 million/year based on costs associated with illness, loss of life and productivity. This was broken down into carbon sequestering, removal of air pollution, avoided energy usage, and avoided emissions (Nowak & Greenfield, 2018a). For the conterminous U.S., it was also estimated that trees and forests removed 17.4 million tons (range of 9.0 – 23.2 million tons) of pollution which equated to a human health benefit of $6.8 billion (range of $1.5 -$13.0 billion) with urban removal being significantly less than in rural areas. However, the cost saving in urban areas was far greater at $4.7 billion versus $2.2 billion in rural areas owing to urban population density. NO_2 and O_3 pollution were the highest removed pollutants in that study. These benefits translated nationally to a decrease of 850 cases of human mortality (range of 184-1634 in states). Incidence of acute respiratory symptoms, exacerbated asthma, and school days lost were 670,000 (range of 221,000-1,035,000), 430,000 (range of 198,000 – 688,000), and 200,000 (range of 78,000 – 266,000)(Nowak et al., 2014).

3.4.4 Census data

In Indiana, urban pollution removal was estimated at 12.9 kg ha^{-1} and valued at $96.9 ha^{-1}. Average values for pollution removal in urban areas were $436 t^{-1} for NO_2 (Nowak et al., 2006, 2014). Extrapolating from Indianapolis pollution removal data (Nowak et al., 2006) we find that tree canopy cover in our study area results in an estimated removal of NO_2 of 7 tons for A (ct 18097361400—referred to as "A"), and 0.2273 tons for B (ct 18097355900—referred to as "B"). If the total pollutant removal in Indianapolis for NO_2, O_3, PM_{10}, SO_2, and CO was 2,910 tons with a savings of $15,500(x1000), then the 0.2273 tons for B results in approximately $1211 in savings for B. Thus in the PR area the annual average health savings range from approximately $1,211 in B to $37,338 in A (removal of NO_2 tons based on canopy coverage of ct x $5,326 per ton of all pollutant removal based on Table 1 in Nowak et al., 2006) (Nowak et al., 2022). When these census tracts are normalized by land area, cost savings in A are 1.2 times higher than in B. Population of A is 5.8 times that of B, while as the racial composition of the two are similar. Median age of A is 36.9 years, and median household income is $56,250. Median age in B is 32.1 years, median household income is $43,083. Additionally, A's median year of owner and renter occupied structure is 1988 with a canopy coverage of 28% while B's is 1939 with canopy coverage at 23%. One reason for reduced canopy coverage in B could be due to the age of that neighborhood. In 1934, Dutch Elm Disease appeared in Indianapolis, and may have also been a factor in the reduced percentage of canopy coverage in B versus A (Carter & Illinois., 1967). Another potential driver of this disparity in tree canopy cover is the legacy of historic racist red-lining policies (Nowak et al., 2022) in the 1940s-60s, which resulted in far fewer green resources invested in some communities compared to others. Nowak et

al., 2022 research highlighted that redline-class A census places (best) had lowest impervious cover at 30.6% and highest tree cover at 40.1%, while as Class-D census place (hazardous) was at 53% and 20.8% respectively. Regardless, canopy coverage along with the make-up of the two census tracts in terms of population, age of the neighborhoods could all be playing a role in the difference in health savings. Such calculations could assist in identifying and targeting census tracts for further in-depth health analysis and/or additional green investments.

3.4.5 Vehicle and land use data

While tree canopy cover is associated with net NO_2 reductions, only vehicle counts play a role in NO_2 increases in PR. A 1,000-count increase in the StreetLight all vehicle results in an increase of NO_2 by 0.10 ppb. Medium and heavy-duty truck indices were not significant in this study area as it is largely residential. Perhaps if we analyzed the sensor locations in the StreetLight platform for a longer period, with calibrated truck data, we could enhance our understanding of the impact of trucks (14,000 lbs and over) on these sensors. Such vehicles are primarily fueled by diesel, and have high idle times in neighborhoods, two factors that may impact local NO_2 emissions over time.

As mentioned earlier this is primarily a residential area and even though parcels may be zoned as heavy industrial, there is not a significant visual presence of such industry there at this time. Even though this variable is included in Model 1-4, it is excluded from the stepwise regression model and is not significant in making an impact in the study area.

3.4.6 Meteorology

Wind speed and temperature were both significant in Model 1, but due to multicollinearity temperature was removed from Model 2 and beyond. Wind speed

outcome is like that observed by Masey et al., 2017 with Ogawa sensors. They concluded that the design of the shelter results in increased uptake rate due to increased turbulence and reduced length of the diffusion segment of the pollutants into the shelter (Table 4). Typically, we would expect an inverse effect from wind, which does not happen here (Voiculescu et al., 2020b).

3.4.7 Distance to highway and gas stations

Not only do gas stations result in increased emissions of pollutants which have negative health implications, due to their locations result in roads with heavier traffic (Huppé et al., 2013). We found that gas stations have a positive impact on NO_2 concentrations, a factor of increased emissions from vehicles. Additionally, the inverse relationship of distance to highways and NO_2 concentrations can be explained by the presence of higher emission vehicles on highways versus in residential spaces. Thus, as the sensors' locations move further away from highways, they are impacted less by NO_2 emissions.

3.5 Conclusion

Community engagement, a powerful tool links the public with researchers, and creates a group of engaged citizenry (*About Us*, 2022; *About Us*, 2022; Den Broeder et al., 2018; Rosner, 2013). Such citizen science networks, utilizing air pollution sensors, result in well informed public that is equipped to actively participate in conversations regarding the health of their communities (Snyder et al., 2013). Low-cost Ogawa passive sensors are an inexpensive way for communities to use citizen science to participate in examining air quality at a fine scale (English et al., 2017). These sensors have been used successfully by

other researchers for varying sampling periods over time (Cowie et al., 2019; Masey et al., 2017a). Passive sampling does not require power supply, making it a useful tool that can be easily deployed in multiple sites. Additionally, they can be used repeatedly and thus are a cost effective avenue (Korf et al., 2020) to examine and implement solutions to varying population exposures. It has been found that these sensors underestimated 7-day exposure concentrations but can explain 87% of temporal variation making them a sound NO_2 sensor, while a sampler empirical correction based on wind speed only increases its accuracy by 5% (Masey et al., 2017a). Therefore, even without wind correction based on Masey et al., 2017a, Ogawa samplers can be considered accurate in their reporting.

In our study in Indianapolis, we use this approach to examine O_3 and NO_2 as a function of land use, leaf canopy cover, traffic type and volume, and meteorological factors. Significant O_3 relationships were found in this study, and we could quantify that a 1 % increase in tree canopy results in a significant decrease of 2.46 ppb in NO_2. It is often challenging to establish a connection between urban pollution impacts from NO_2, therefore, adding traffic data from SteetLight's platform gave us a deeper insight into understanding the vehicular emission impacts.

The approach used here can be utilized as a tool to partner communities with government entities to find solutions to create resilient communities. The next steps in this study should include calibrated StreetLight truck data for a longer time to re-examine and estimated truck counts by category. That could establish ground truth to further improve our understanding of the traffic component in this analysis which can be further enhanced by conducting a health assessment of the census tracts to identify and address high impact regions.

3.6 References

About Us. (2022, July 8). Audubon. https://www.audubon.org/about

Alemany, S., Vilor-Tejedor, N., García-Esteban, R., Bustamante, M., Dadvand, P., Esnaola, M., Mortamais, M., Forns, J., van Drooge, B. L., Álvarez-Pedrerol, M., Grimalt, J. O., Rivas, I., Querol, X., Pujol, J., & Sunyer, J. (2018). Traffic-Related Air Pollution, APOEε4 Status, and Neurodevelopmental Outcomes among School Children Enrolled in the BREATHE Project (Catalonia, Spain). *Environmental Health Perspectives*, *126*(8), 087001. https://doi.org/10.1289/EHP2246

Almaraz, M., Bai, E., Wang, C., Trousdell, J., Conley, S., Faloona, I., & Houlton, B. Z. (2018). Agriculture is a major source of NOx pollution in California. *Science Advances*, *4*(1). https://doi.org/10.1126/sciadv.aao3477

Anderson, V., & Gough, W. A. (2020). Evaluating the potential of nature-based solutions to reduce ozone, nitrogen dioxide, and carbon dioxide through a multi-type green infrastructure study in Ontario, Canada. *City and Environment Interactions*, *6*, 100043. https://doi.org/10.1016/j.cacint.2020.100043

Anenberg, S. C., Henze, D. K., Tinney, V., Kinney, P. L., Raich, W., Fann, N., Malley, C. S., Roman, H., Lamsal, L., Duncan, B., Martin, R. V., van, D. A., Brauer, M., Doherty, R., Jonson, J. E., Davila, Y., Sudo, K., & Kuylenstierna, J. C. I. (2018). Estimates of the Global Burden of Ambient PM2.5, Ozone, and NO2 on Asthma Incidence and Emergency Room Visits. *Environmental Health Perspectives*, *126*(10), 107004. https://doi.org/10.1289/EHP3766

Baldocchi, D. D., Hicks, B. B., & Camara, P. (1987). A canopy stomatal resistance model for gaseous deposition to vegetated surfaces. *Atmospheric Environment (1967)*, *21*(1), 91–101. https://doi.org/10.1016/0004-6981(87)90274-5

Bowatte, G., Erbas, B., Lodge, C. J., Knibbs, L. D., Gurrin, L. C., Marks, G. B., Thomas, P. S., Johns, D. P., Giles, G. G., Hui, J., Dennekamp, M., Perret, J. L., Abramson, M. J., Walters, E. H., Matheson, M. C., & Dharmage, S. C. (2017). Traffic-related air pollution exposure over a 5-year period is associated with increased risk of asthma and poor lung function in middle age. *The European Respiratory Journal*, *50*(4), 1602357. https://doi.org/10.1183/13993003.02357-2016

Bozkurt, Z., Üzmez, Ö. Ö., Döğeroğlu, T., Artun, G., & Gaga, E. O. (2018). Atmospheric concentrations of SO2, NO2, ozone and VOCs in Düzce, Turkey using passive air samplers: Sources, spatial and seasonal variations and health risk estimation. *Atmospheric Pollution Research*, *9*(6), 1146–1156. https://doi.org/10.1016/j.apr.2018.05.001

Carter, J. C. & Illinois. (1967). *Dutch elm disease in Illinois*. [s.n.]. https://doi.org/10.5962/bhl.title.46163

Çel, M. B. (2007). *The Relation Between Meteorological Factors and Pollutants Concentrations in Karabük City*. 9.

Chaparro-Suarez, I. G., Meixner, F., & Kesselmeier, J. (2011). Nitrogen dioxide (NO2) uptake by vegetation controlled by atmospheric concentrations and plant stomatal aperture. *Atmospheric Environment - ATMOS ENVIRON*, *45*, 5742–5750. https://doi.org/10.1016/j.atmosenv.2011.07.021

Cichowicz, R., Wielgosiński, G., & Fetter, W. (2017). Dispersion of atmospheric air pollution in summer and winter season. *Environmental Monitoring and Assessment*, *189*(12), 605. https://doi.org/10.1007/s10661-017-6319-2

Cowie, C. T., Garden, F., Jegasothy, E., Knibbs, L. D., Hanigan, I., Morley, D., Hansell, A., Hoek, G., & Marks, G. B. (2019). Comparison of model estimates from an intra-city land use regression model with a national satellite-LUR and a regional Bayesian Maximum Entropy model, in estimating NO2 for a birth cohort in Sydney, Australia. *Environmental Research*, *174*, 24–34. https://doi.org/10.1016/j.envres.2019.03.068

Den Broeder, L., Devilee, J., Van Oers, H., Schuit, A. J., & Wagemakers, A. (2018). Citizen Science for public health. *Health Promotion International*, *33*(3), 505–514. https://doi.org/10.1093/heapro/daw086

Díaz-Álvarez, E. A., Lindig-Cisneros, R., & de la Barrera, E. (2018). Biomonitors of atmospheric nitrogen deposition: Potential uses and limitations. *Conservation Physiology*, *6*(1). https://doi.org/10.1093/conphys/coy011

Elliott, E. M., Kendall, C., Wankel, S. D., Burns, D. A., Boyer, E. W., Harlin, K., Bain, D. J., & Butler, T. J. (2007). Nitrogen isotopes as indicators of NO x source contributions to atmospheric nitrate deposition across the midwestern and northeastern United States. *Environmental Science & Technology*, *41*(22), 7661–7667.

English, P. B., Olmedo, L., Bejarano, E., Lugo, H., Murillo, E., Seto, E., Wong, M., King, G., Wilkie, A., Meltzer, D., Carvlin, G., Jerrett, M., & Northcross, A. (2017). The Imperial County Community Air Monitoring Network: A Model for Community-

based Environmental Monitoring for Public Health Action. *Environmental Health Perspectives*, *125*(7), 074501. https://doi.org/10.1289/EHP1772

Explore Census Data. (2021, July 8). https://data.census.gov/cedsci/

Fann, N., Lamson, A. D., Anenberg, S. C., Wesson, K., Risley, D., & Hubbell, B. J. (2011). Estimating the National Public Health Burden Associated with Exposure to Ambient PM2.5 and Ozone. *Risk Analysis*, *32*(1), 81–95. https://doi.org/10.1111/j.1539-6924.2011.01630.x

Filigrana, P., Milando, C., Batterman, S., Levy, J. I., Mukherjee, B., & Adar, S. D. (2020). Spatiotemporal variations in traffic activity and their influence on air pollution levels in communities near highways. *Atmospheric Environment*, *242*, 117758. https://doi.org/10.1016/j.atmosenv.2020.117758

Gackière, F., Saliba, L., Baude, A., Bosler, O., & Strube, C. (2011). Ozone inhalation activates stress-responsive regions of the CNS. *Journal of Neurochemistry*, *117*(6), 961–972. https://doi.org/10.1111/j.1471-4159.2011.07267.x

Galloway, J. N., Aber, J. D., Erisman, J. W., Seitzinger, S. P., Howarth, R. W., Cowling, E. B., & Cosby, B. J. (2003). The Nitrogen Cascade. *BioScience*, *53*(4), 341–356. https://doi.org/10.1641/0006-3568(2003)053[0341:TNC]2.0.CO;2

Galloway, J. N., Bleeker, A., & Erisman, J. W. (2021). The Human Creation and Use of Reactive Nitrogen: A Global and Regional Perspective. *Annual Review of Environment and Resources*, *46*(1), 255–288. https://doi.org/10.1146/annurev-environ-012420-045120

Galloway, J. N., Dentener, F. J., Capone, D. G., Boyer, E. W., Howarth, R. W., Seitzinger, S. P., Asner, G. P., Cleveland, C. C., Green, P. A., Holland, E. A., Karl, D. M.,

Michaels, A. F., Porter, J. H., Townsend, A. R., & Vosmarty, C. J. (2004). Nitrogen Cycles: Past, Present, and Future. *Biogeochemistry*, *70*(2), 153–226. https://doi.org/10.1007/s10533-004-0370-0

Harper, A., Baker, P. N., Xia, Y., Kuang, T., Zhang, H., Chen, Y., Han, T.-L., & Gulliver, J. (2021). Development of spatiotemporal land use regression models for PM2.5 and NO2 in Chongqing, China, and exposure assessment for the CLIMB study. *Atmospheric Pollution Research*, *12*(7), 101096. https://doi.org/10.1016/j.apr.2021.101096

Hazlehurst, M., Nurius, P., & Hajat, A. (2018). Individual and Neighborhood Stressors, Air Pollution and Cardiovascular Disease. *International Journal of Environmental Research and Public Health*, *15*(3), 472. https://doi.org/10.3390/ijerph15030472

He, C., Hong, S., Zhang, L., Mu, H., Xin, A., Zhou, Y., Liu, J., Liu, N., Su, Y., Tian, Y., Ke, B., Wang, Y., & Yang, L. (2021). Global, continental, and national variation in PM2.5, O3, and NO2 concentrations during the early 2020 COVID-19 lockdown. *Atmospheric Pollution Research*, *12*(3), 136–145. https://doi.org/10.1016/j.apr.2021.02.002

Heaton, T. H. E. (1990). 15N/14N ratios of NOx from vehicle engines and coal-fired power stations. *Tellus B*, *42*(3), 304–307. https://doi.org/10.1034/j.1600-0889.1990.00007.x-i1

Heintzelman, A. (2019, December 11). *Results from a dense urban air quality monitoring system: Volatile and particulate matter analysis in Indianapolis, USA.* AGU Conference 2019, AGU Conference 2019. https://agu.confex.com/agu/fm19/meetingapp.cgi/Paper/487825

Heintzelman, A., Filippelli, G., & Lulla, V. (2021). Substantial Decreases in U.S. Cities' Ground-Based NO2 Concentrations during COVID-19 from Reduced Transportation. *Sustainability*, *13*(16), 9030. https://doi.org/10.3390/su13169030

Huppé, V., Kestens, Y., Auger, N., Daniel, M., & Smargiassi, A. (2013). Residential proximity to gasoline service stations and preterm birth. *Environmental Science and Pollution Research International*, *20*(10), 7186–7193. https://doi-org.proxy.ulib.uits.iu.edu/10.1007/s11356-013-1677-y

Hwang, M.-J., Cheong, H.-K., & Kim, J.-H. (2019). Ambient Air Pollution and Sudden Infant Death Syndrome in Korea: A Time-Stratified Case-Crossover Study. *International Journal of Environmental Research and Public Health*, *16*(18), 3273. https://doi.org/10.3390/ijerph16183273

Hystad, P., Setton, E., Cervantes, A., Poplawski, K., Deschenes, S., Brauer, M., van, D. A., Lamsal, L., Martin, R., Jerrett, M., & Demers, P. (2011). Creating National Air Pollution Models for Population Exposure Assessment in Canada. *Environmental Health Perspectives*, *119*(8), 1123–1129. https://doi.org/10.1289/ehp.1002976

Jaeglé, L., Steinberger, L., Martin, R. V., & Chance, K. (2005). Global partitioning of NOx sources using satellite observations: Relative roles of fossil fuel combustion, biomass burning and soil emissions. *Faraday Discussions*, *130*(0), 407–423. https://doi.org/10.1039/B502128F

Karner, A. A., Eisinger, D. S., & Niemeier, D. A. (2010). Near-Roadway Air Quality: Synthesizing the Findings from Real-World Data. *Environmental Science & Technology*, *44*(14), 5334–5344. https://doi.org/10.1021/es100008x

Kendrick, C. M., Koonce, P., & George, L. A. (2015). Diurnal and seasonal variations of NO, NO 2 and PM 2.5 mass as a function of traffic volumes alongside an urban arterial. *Atmospheric Environment*, *122*, 133–141. https://doi.org/10.1016/j.atmosenv.2015.09.019

Kharol, S. K., Martin, R. V., Philip, S., Boys, B., Lamsal, L. N., Jerrett, M., Brauer, M., Crouse, D. L., McLinden, C., & Burnett, R. T. (2015). Assessment of the magnitude and recent trends in satellite-derived ground-level nitrogen dioxide over North America. *Atmospheric Environment*, *118*, 236–245. https://doi.org/10.1016/j.atmosenv.2015.08.011

Knibbs, L. D., Coorey, C. P., Bechle, M. J., Cowie, C. T., Dirgawati, M., Heyworth, J. S., Marks, G. B., Marshall, J. D., Morawska, L., Pereira, G., & Hewson, M. G. (2016). Independent Validation of National Satellite-Based Land-Use Regression Models for Nitrogen Dioxide Using Passive Samplers. *Environmental Science & Technology*, *50*(22), 12331–12338. https://doi.org/10.1021/acs.est.6b03428

Korf, E. P., Muscope, F. P., Bragagnolo, L., Treméa, R., & Grzybowski, J. M. V. (2020). Application of Passive Samplers for Monitoring O3 and No2 and Correlation of Concentration Levels with Meteorological Data. *Environmental Engineering & Management Journal (EEMJ)*, *19*(11), 2077–2088.

Kreis, C., Héritier, H., Scheinemann, K., Hengartner, H., de Hoogh, K., Röösli, M., & Spycher, B. D. (2022). Childhood cancer and traffic-related air pollution in Switzerland: A nationwide census-based cohort study. *Environment International*, 107380. https://doi.org/10.1016/j.envint.2022.107380

Lamsal, L. N., Martin, R. V., Parrish, D. D., & Krotkov, N. A. (2013). Scaling Relationship for NO2 Pollution and Urban Population Size: A Satellite Perspective. *Environmental Science & Technology*, *47*(14), 7855–7861. https://doi.org/10.1021/es400744g

Li, Z., Christensen, G. M., Lah, J. J., Marcus, M., Russell, A. G., Ebelt, S., Waller, L. A., & Hüls, A. (2022). Neighborhood characteristics as confounders and effect modifiers for the association between air pollution exposure and subjective cognitive functioning. *Environmental Research*, *212*, 113221. https://doi.org/10.1016/j.envres.2022.113221

Masey, N., Gillespie, J., Heal, M. R., Hamilton, S., & Beverland, I. J. (2017a). Influence of wind-speed on short-duration NO2 measurements using Palmes and Ogawa passive diffusion samplers. *Atmospheric Environment*, *160*, 70–76. https://doi.org/10.1016/j.atmosenv.2017.04.008

Masey, N., Gillespie, J., Heal, M. R., Hamilton, S., & Beverland, I. J. (2017b). Influence of wind-speed on short-duration NO2 measurements using Palmes and Ogawa passive diffusion samplers. *Atmospheric Environment*, *160*, 70–76. https://doi.org/10.1016/j.atmosenv.2017.04.008

Matthes, S., Grewe, V., & Sausen, R. (2007). Global impact of road traffic emissions on tropospheric ozone. *Atmos. Chem. Phys.*, *30*, 13.

Mavko, M. E., Tang, B., & George, L. A. (2008). A sub-neighborhood scale land use regression model for predicting NO2. *Science of The Total Environment*, *398*(1), 68–75. https://doi.org/10.1016/j.scitotenv.2008.02.017

Meng, X., Liu, C., Chen, R., Sera, F., Vicedo-Cabrera, A. M., Milojevic, A., Guo, Y., Tong, S., Coelho, M. de S. Z. S., Saldiva, P. H. N., Lavigne, E., Correa, P. M., Ortega, N. V., Osorio, S., Garcia, null, Kyselý, J., Urban, A., Orru, H., Maasikmets, M., … Kan, H. (2021). Short term associations of ambient nitrogen dioxide with daily total, cardiovascular, and respiratory mortality: Multilocation analysis in 398 cities. *BMJ (Clinical Research Ed.)*, *372*, n534. https://doi.org/10.1136/bmj.n534

Meo, S. A., Ahmed Alqahtani, S., Saad binmeather, F., Abdulrhman AlRasheed, R., Mohammed Aljedaie, G., & Mohammed Albarrak, R. (2022). Effect of environmental pollutants PM2.5, CO, O3 and NO2, on the incidence and mortality of SARS-COV-2 in largest metropolitan cities, Delhi, Mumbai and Kolkata, India. *Journal of King Saud University - Science*, *34*(1), 101687. https://doi.org/10.1016/j.jksus.2021.101687

Monthly Summary Report. (2021, July 8). https://idem.meteostar.com//cgi-bin/monthly_summary.pl

Mukerjee, S., Smith, L. A., Norris, G. A., Morandi, M. T., Gonzales, M., Noble, C. A., Neas, L. M., & Özkaynak, A. H. (2004). Field Method Comparison between Passive Air Samplers and Continuous Monitors for VOCs and NO2 in El Paso, Texas. *Journal of the Air & Waste Management Association*, *54*(3), 307–319. https://doi.org/10.1080/10473289.2004.10470903

Mullen, C., Flores, A., Grineski, S., & Collins, T. (2022). Exploring the distributional environmental justice implications of an air quality monitoring network in Los Angeles County. *Environmental Research*, *206*, 112612. https://doi.org/10.1016/j.envres.2021.112612

Ngarambe, J., Joen, S. J., Han, C.-H., & Yun, G. Y. (2021). Exploring the relationship between particulate matter, CO, SO2, NO2, O3 and urban heat island in Seoul, Korea. *Journal of Hazardous Materials*, *403*, 123615. https://doi.org/10.1016/j.jhazmat.2020.123615

Nowak, D. J. (2012). Contrasting natural regeneration and tree planting in fourteen North American cities. *Urban Forestry & Urban Greening*, *11*(4), 374–382. https://doi.org/10.1016/j.ufug.2012.02.005

Nowak, D. J., Crane, D. E., & Stevens, J. C. (2006). Air pollution removal by urban trees and shrubs in the United States. *Urban Forestry & Urban Greening*, *4*(3–4), 115–123. https://doi.org/10.1016/j.ufug.2006.01.007

Nowak, D. J., Ellis, A., & Greenfield, E. J. (2022). The disparity in tree cover and ecosystem service values among redlining classes in the United States. *Landscape and Urban Planning*, *221*, 104370. https://doi.org/10.1016/j.landurbplan.2022.104370

Nowak, D. J., & Greenfield, E. J. (2018a). US Urban Forest Statistics, Values, and Projections. *Journal of Forestry*, *116*(2), 164–177. https://doi.org/10.1093/jofore/fvx004

Nowak, D. J., & Greenfield, E. J. (2018b). Declining urban and community tree cover in the United States. *Urban Forestry & Urban Greening*, *32*, 32–55. https://doi.org/10.1016/j.ufug.2018.03.006

Nowak, D. J., Hirabayashi, S., Bodine, A., & Greenfield, E. (2014). Tree and forest effects on air quality and human health in the United States. *Environmental Pollution*, *193*, 119–129. https://doi.org/10.1016/j.envpol.2014.05.028

Nowak, D. J., & Ogren, T. L. (2021). Variations in urban forest allergy potential among cities and land uses. *Urban Forestry & Urban Greening*, *63*, 127224. https://doi.org/10.1016/j.ufug.2021.127224

Olaniyan, T., Jeebhay, M., Röösli, M., Naidoo, R. N., Künzli, N., de Hoogh, K., Saucy, A., Badpa, M., Baatjies, R., Parker, B., Leaner, J., & Dalvie, M. A. (2020). The association between ambient NO2 and PM2.5 with the respiratory health of school children residing in informal settlements: A prospective cohort study. *Environmental Research*, *186*, 109606. https://doi.org/10.1016/j.envres.2020.109606

Open Indy Data Portal. (2021, July 8). https://data.indy.gov/

Padula, A. M., Yang, W., Schultz, K., Lee, C., Lurmann, F., Hammond, S. K., & Shaw, G. M. (2021). Gene–environment interactions between air pollution and biotransformation enzymes and risk of birth defects. *Birth Defects Research*, *113*(9), 676–686. https://doi.org/10.1002/bdr2.1880

Palmgren, F., Berkowicz, R., Hertel, O., & Vignati, E. (1996). Effects of reduction of NOx on the NO2 levels in urban streets. *Science of The Total Environment*, *189–190*, 409–415. https://doi.org/10.1016/0048-9697(96)05238-2

Pancholi, P., Kumar, A., Bikundia, D. S., & Chourasiya, S. (2018). An observation of seasonal and diurnal behavior of O3–NOx relationships and local/regional oxidant (OX = O3 + NO2) levels at a semi-arid urban site of western India. *Sustainable Environment Research*, *28*(2), 79–89. https://doi.org/10.1016/j.serj.2017.11.001

Paraschiv, S., Barbuta-Misu, N., & Paraschiv, S. L. (2020). Influence of NO2, NO and meteorological conditions on the tropospheric O3 concentration at an industrial station. *Energy Reports*, *6*, 231–236. https://doi.org/10.1016/j.egyr.2020.11.263

Pope, F. D., Gatari, M., Ng'ang'a, D., Poynter, A., & Blake, R. (2018). Airborne particulate matter monitoring in Kenya using calibrated low-cost sensors. *Atmospheric Chemistry and Physics*, *18*(20), 15403–15418. https://doi.org/10.5194/acp-18-15403-2018

PROTOCOLS – OGAWA USA. (2021, August 25). https://ogawausa.com/protocols/

Rao, M., George, L. A., Rosenstiel, T. N., Shandas, V., & Dinno, A. (2014). Assessing the relationship among urban trees, nitrogen dioxide, and respiratory health. *Environmental Pollution*, *194*, 96–104. https://doi.org/10.1016/j.envpol.2014.07.011

Ravina, M., Esfandabadi, Z. S., Panepinto, D., & Zanetti, M. (2021). Traffic-induced atmospheric pollution during the COVID-19 lockdown: Dispersion modeling based on traffic flow monitoring in Turin, Italy. *Journal of Cleaner Production*, *317*, 128425. https://doi.org/10.1016/j.jclepro.2021.128425

Renaud, V., Innes, J. L., Dobbertin, M., & Rebetez, M. (2011). Comparison between open-site and below-canopy climatic conditions in Switzerland for different types of forests over 10 years (1998−2007). *Theoretical and Applied Climatology*, *105*(1–2), 119–127. https://doi.org/10.1007/s00704-010-0361-0

Roberts, S., Arseneault, L., Barratt, B., Beevers, S., Danese, A., Odgers, C. L., Moffitt, T. E., Reuben, A., Kelly, F. J., & Fisher, H. L. (2019). Exploration of NO2 and PM2.5 air pollution and mental health problems using high-resolution data in London-

based children from a UK longitudinal cohort study. *Psychiatry Research*, *272*, 8–17. https://doi.org/10.1016/j.psychres.2018.12.050

Rosner, H. (2013). Data on Wings. *Scientific American*, *308*(2), 68–73.

Sather, M. E., Slonecker, E. T., Kronmiller, K. G., Williams, D. D., Daughtrey, H., & Mathew, J. (2006). Evaluation of short-term Ogawa passive, photolytic, and federal reference method sampling devices for nitrogen oxides in El Paso and Houston, Texas. *Journal of Environmental Monitoring*, *8*(5), 558–563. https://doi.org/10.1039/B601113F

Sather, M. E., Slonecker, E. T., Mathew, J., Daughtrey, H., & Williams, D. D. (2007). Evaluation of ogawa passive sampling devices as an alternative measurement method for the nitrogen dioxide annual standard in El Paso, Texas. *Environmental Monitoring and Assessment*, *124*(1), 211–221. https://doi.org/10.1007/s10661-006-9219-4

Sather, M. E., Varns, J. L., Mulik, J. D., Glen, G., Smith, L., & Stallings, C. (2001). Passive Ozone Network of Dallas: A Modeling Opportunity with Community Involvement. 2. *Environmental Science & Technology*, *35*(22), 4426–4435. https://doi.org/10.1021/es010889z

Scott, A. A., Zaitchik, B., Waugh, D. W., & O'Meara, K. (2017). Intraurban Temperature Variability in Baltimore. *Journal of Applied Meteorology and Climatology*, *56*(1), 159–171. https://doi.org/10.1175/JAMC-D-16-0232.1

Sinharay, R., Gong, J., Barratt, B., Ohman-Strickland, P., Ernst, S., Kelly, F. J., Zhang, J. J., Collins, P., Cullinan, P., & Chung, K. F. (2018). Respiratory and cardiovascular responses to walking down a traffic-polluted road compared with walking in a

traffic-free area in participants aged 60 years and older with chronic lung or heart disease and age-matched healthy controls: A randomised, crossover study. *Lancet (London, England)*, *391*(10118), 339–349. https://doi.org/10.1016/S0140-6736(17)32643-0

Snyder, E. G., Watkins, T. H., Solomon, P. A., Thoma, E. D., Williams, R. W., Hagler, G. S. W., Shelow, D., Hindin, D. A., Kilaru, V. J., & Preuss, P. W. (2013). The Changing Paradigm of Air Pollution Monitoring. *Environmental Science & Technology*, *47*(20), 11369–11377. https://doi.org/10.1021/es4022602

Speak, A., Montagnani, L., Wellstein, C., & Zerbe, S. (2020). The influence of tree traits on urban ground surface shade cooling. *Landscape and Urban Planning*, *197*, 103748. https://doi.org/10.1016/j.landurbplan.2020.103748

Takahashi, M., Higaki, A., Nohno, M., Kamada, M., Okamura, Y., Matsui, K., Kitani, S., & Morikawa, H. (2005). Differential assimilation of nitrogen dioxide by 70 taxa of roadside trees at an urban pollution level. *Chemosphere*, *61*(5), 633–639. https://doi.org/10.1016/j.chemosphere.2005.03.033

Tanzer-Gruener, R., Li, J., Eilenberg, S. R., Robinson, A. L., & Presto, A. A. (2020). Impacts of Modifiable Factors on Ambient Air Pollution: A Case Study of COVID-19 Shutdowns. *Environmental Science & Technology Letters*, *7*(8), 554–559. https://doi.org/10.1021/acs.estlett.0c00365

US EPA, O. (2014a, April 10). *NAAQS Table* [Other Policies and Guidance]. https://www.epa.gov/criteria-air-pollutants/naaqs-table

US EPA, O. (2014b, July 16). *Research on Near Roadway and Other Near Source Air Pollution* [Overviews and Factsheets]. https://www.epa.gov/air-research/research-near-roadway-and-other-near-source-air-pollution

Voiculescu, M., Constantin, D.-E., Condurache-Bota, S., Călmuc, V., Roșu, A., & Dragomir Bălănică, C. M. (2020a). Role of Meteorological Parameters in the Diurnal and Seasonal Variation of NO2 in a Romanian Urban Environment. *International Journal of Environmental Research and Public Health*, *17*(17), 6228. https://doi.org/10.3390/ijerph17176228

Voiculescu, M., Constantin, D.-E., Condurache-Bota, S., Călmuc, V., Roșu, A., & Dragomir Bălănică, C. M. (2020b). Role of Meteorological Parameters in the Diurnal and Seasonal Variation of NO2 in a Romanian Urban Environment. *International Journal of Environmental Research and Public Health*, *17*(17), 6228. https://doi.org/10.3390/ijerph17176228

Wallace, J., & Hobbs, P. (2006). *Atmospheric Science—2nd Edition*. https://www.elsevier.com/books/atmospheric-science/wallace/978-0-12-732951-2

Wang, M., Hou, Z.-H., Xu, H., Liu, Y., Budoff, M. J., Szpiro, A. A., Kaufman, J. D., Vedal, S., & Lu, B. (2019). Association of Estimated Long-term Exposure to Air Pollution and Traffic Proximity With a Marker for Coronary Atherosclerosis in a Nationwide Study in China. *JAMA Network Open*, *2*(6), e196553. https://doi.org/10.1001/jamanetworkopen.2019.6553

Wei, Y., Wang, Y., Wu, X., Di, Q., Shi, L., Koutrakis, P., Zanobetti, A., Dominici, F., & Schwartz, J. D. (2020). Causal Effects of Air Pollution on Mortality Rate in

Massachusetts. *American Journal of Epidemiology*, *189*(11), 1316–1323. https://doi.org/10.1093/aje/kwaa098

Zhang, J., Ghirardo, A., Gori, A., Albert, A., Buegger, F., Pace, R., Georgii, E., Grote, R., Schnitzler, J.-P., Durner, J., & Lindermayr, C. (2020). Improving Air Quality by Nitric Oxide Consumption of Climate-Resilient Trees Suitable for Urban Greening. *Frontiers in Plant Science*, *0*. https://doi.org/10.3389/fpls.2020.549913

Zoran, M. A., Savastru, R. S., Savastru, D. M., & Tautan, M. N. (2020). Assessing the relationship between ground levels of ozone (O3) and nitrogen dioxide (NO2) with coronavirus (COVID-19) in Milan, Italy. *Science of The Total Environment*, *740*, 140005. https://doi.org/10.1016/j.scitotenv.2020.140005

CHAPTER 4: EFFICACY OF LOW-COST SENSOR NETWORKS AT DETECTING FINE-SCALE VARIATIONS IN PARTICULATE MATTER IN URBAN ENVIRONMENTS

4.1 Introduction

Particulate Matter 2.5 ($PM_{2.5}$), defined as particle mass with aerodynamic diameter that is less than 2.5 μm, is regulated by the United States Clean Air Act and reported as micrograms per meter cubed ($\mu g\ m^{-3}$) which is a mass based concentration (Zimmerman, 2021). $PM_{2.5}$ is typically found in higher concentrations in densely populated regions (Ji et al., 2018), and in combination with other criteria air pollutants such as nitrogen dioxide (NO_2), and O_3 (Ozone) has been associated with serious health effects and increased risk of mortality (Cohen et al., 2017; Kasdagli et al., 2021). A global integrated satellite and ground-based measurement of $PM_{2.5}$ in 2015 attributed 4.2 million deaths to this factor, which was a rise from 3.5 million deaths in 1990 and calculated 13.1 million disability-adjusted life-years (DALY). $PM_{2.5}$ was ranked #1 as a risk factor for deaths in China and #6 as a risk factor for deaths in the U.S. (Cohen et al., 2017). By combining the years lost due to premature mortality and years lost as a result of living with a disease, DALY is a holistic method to measure the impact of disease (Indicator Metadata Registry Details, 2021). In 2011, a World Health Organization (WHO) Global Burden of Disease (GBD) study estimated that $PM_{2.5}$ resulted in 28,000 premature mortalities in United States, Canada, and Cuba alone. Using an atmospheric chemical transport model, Anenberg et al. (2010) estimated that global anthropogenic $PM_{2.5}$ was associated with 3.5 +/- 0.9 million cases of cardiopulmonary mortality and 220,000 +/- 80,000 lung cancer mortalities, but

when reduced to a lower concentration of 5.8 μg m^{-3} mortality estimates were reduced approximately by 30% (Anenberg et al., 2010). In a study utilizing monitor data and a photochemical Community Multiscale Air Quality (CMAQ) model across USA, Fann et al. (2011) estimated that 130,000 deaths and 1.1 million life years were lost due to $PM_{2.5}$ exposure during 2005 (Fann et al., 2011). Between 2010-2012, roadway air pollution alone in 42 neighborhoods in New York City resulted in 320 deaths and 870 hospitalization and emergency room visits due to $PM_{2.5}$ (Kheirbek et al., 2016). An overlap of high particulate matter, high population and poor health quality in the Midwestern region of the U.S results in a high incident of premature mortality (Fann et al., 2011).

Due to serious human health impacts of $PM_{2.5}$ exposure, the U.S. Environmental Protection Agency (EPA) requires states to monitor $PM_{2.5}$ and other gases. They have set exposure limits of $PM_{2.5}$ at 35 μg/m^3 in a 24-hour cycle that is averaged over three years, and a 12 μg/m^3 annual standard limit. Many studies, however, indicate that chronic human exposure to levels of air pollution below the EPA standards show a positive association with adverse health effects including shaping DNA methylation through epigenetic mechanisms that can have multi-generational effects. It is reported that during pregnancy, childhood and the elderly stages of life, humans are most susceptible to DNA methylation alteration (Christidis et al., 2019; Chu et al., 2015; Ferrari et al., 2019; Shi Liuhua et al., 2016; Tan et al., 2020; You et al., 2020). Even though anthropogenic pollution from vehicles and industry result in increased $PM_{2.5}$, there is also a correlation between $PM_{2.5}$ and meteorological variables, which can explain up to 50% of the daily variations in some regions. For instance, on stagnant days average $PM_{2.5}$ concentrations tend to be 2.6 μg/m^3 higher (Tai et al., 2010; Wang et al., 2019). Independent of geography, age, or gender, long

term exposure for every 10 μg/$m^3$of $PM_{2.5}$ increases non-accidental mortality by 6% (Chen et al., 2008). One serious limitation of studies that use $PM_{2.5}$ in relation to human health outcomes is that due to cost and maintenance limitations, most U.S. cities only have a handful of monitors to gauge air quality and health burdens, sometimes for millions of people. Enhanced spatial and temporal granularity in monitoring is critical as a host of studies show the important role local sources play in driving air pollution (Tai et al., 2010; Li et al., 2017; Heintzelman et al., 2021).

Scarcity of regulatory monitors has led to the use of satellite data to extend coverage (Bi et al., 2019; Xiao et al., 2017). Deployment of low cost sensors in air quality studies has also increased with the development of more accurate monitoring devices, which has contributed to monitoring and examining fine-scale variations (English et al., 2017; Pope et al., 2018; Tanzer-Gruener et al., 2020). Although lower cost monitors have their analytical drawbacks, they have been used effectively in research (Bi et al., 2020; Snyder et al., 2013). Due to low cost and good performance with respect to EPA regulatory monitors, PurpleAir (PA) sensors in particular have been used in several air quality studies (Mousavi & Wu, 2021) as a cheaper alternative to regulatory monitors to examine indoor and outdoor $PM_{2.5}$ in various regions (Bi et al., 2020; Gupta et al., 2018). Interest in low cost sensors grew as the need to assess and evaluate personal exposures to airborne pollutants and their impacts on humans and communities became clearer (Koehler & Peters, 2015; Liang, 2021; Zimmerman, 2021). PA sensors have been found to have high self-consistency, and can be used to fill in the gaps from sparse data coverage of regulatory grade data (Malings et al., 2020)

The goal of this study was to measure and model spatio-temporal variability of outdoor air quality using 25 PA units that record and report real time $PM_{2.5}$, temperature, and humidity. Sensors were deployed from August 2018 through November 2019 and the resulting data was used to analyze relationships between $PM_{2.5}$ and various meteorological, land-use and census variables in the Pleasant Run airshed in Indianapolis, Indiana. We examined: (1) the driving factors that result in daily averages of $PM_{2.5}$ values of the sensors exceed World Health Organization (WHO) guidelines of 25 $\mu g/m^3$ (in 2021 this was changed to 15 $\mu g/m^3$) (Krzyzanowski & Cohen, 2008), (2) those locations with the highest odds ratio in exceeding the daily average of 25 $\mu g/m^3$, and (3) the impact of tree canopy percentage on $PM_{2.5}$ averages at the census tract level.

4.2 Methodology

4.2.1 Sensor Network

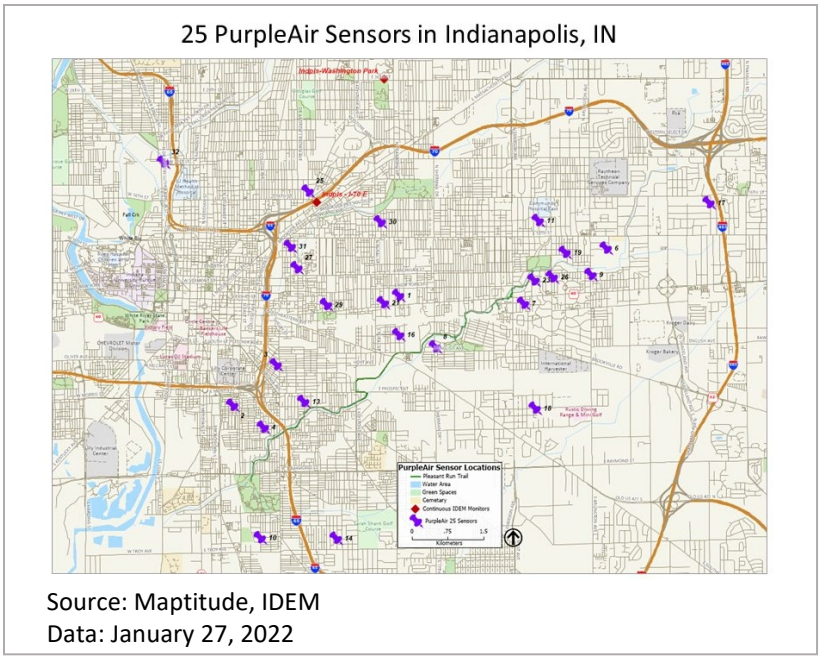

Figure 4.1 - Locations of 25 PurpleAir sensors in the study area.

In collaboration with Keep Indianapolis Beautiful (KIB), a local community based nonprofit organization with a focus on improving the environment, we identified a list of individual households to contact, and recruited 32 citizen scientists within the study area. We installed 32 PurpleAir PA-II-SD sensors, with Wi-Fi capabilities, over a roughly 96 (12x8) km^2 in the eastern part of Indianapolis to collect $PM_{2.5}$ data (Figure 4.1). Since several SD cards in the PA units were corrupted for this study, $PM_{2.5}$ data was downloaded directly from the PA server. One of the sensors was installed in a 3-story balcony. We are assuming that at such a height there may only be a small monotonic gradient difference between the ground and that level for $PM_{2.5}$ (Zauli Sajani et al., 2018). All the sensors, per the recommendation of the manufacturer, were installed under at least an overhang to provide some protection against the weather. Installation height of all but one sensor ranged from approximately 4–8 feet (1.2-2.4 meters) above ground, based on the availability of power outlets and overhead coverage at each location.

PurpleAir sensors are designed with a fan that draws a sample of air past its two independent laser counters labeled 'Channel A' and 'Channel B'. Light from a particle is reflected to a detection plate where it is measured by a pulse. Particle size is determined by the length of each pulse, and particle count is determined by the number of pulses. Airborne particulate matter can include organic particles, inorganic particles, smoke, or dust. Particle sizes of 0.3, 0.5, 1, 2.5, 5, and 10μm are counted which are used to calculate mass concentrations ($\mu g/m^3$) of $PM_{1.0}$, $PM_{2.5}$, and PM_{10} using an algorithm that was developed by Plantower for the PMS5003 sensor, a factory-calibrated instrument that estimates the number of suspended air particles based on the method outlined above. This compensates for the varying densities of various sources of $PM_{2.5}$. $PM_{2.5}$ readings are averaged and

reported every 120 seconds on an interactive website. These readings are also stored on the PA website and can be downloaded as needed. This technology, which uses a 5v USB power source, offers a cheaper option than federal reference monitors to report $PM_{2.5}$. (Map - PurpleAir, 2021; PurpleAir | Real Time Air Quality Monitoring, 2021).

4.2.2 Processing $PM_{2.5}$ data

PurpleAir sensor were deployed from August 2018 through November 2019. However, due to gaps in data, 25 of the total 32 sensors, covering 20 census tracts and spanning 11 months from November 2018 to October 2019, were used in this study (a recall of power cords by the company in February 2019 resulted in about one lost data month as the sensors were disconnected and new cords were delivered and installed in all units). Once the hourly data was downloaded from the PA website, we utilized Base-R in R-Studio version 4.0.3, an open-sourced statistical computing software, for data processing and analysis.

PurpleAir Sensors have been evaluated by South Coast AQMD, who found that laser b (Channel B) reported 11-37% higher $PM_{2.5}$ mass concentration, however, the two independent laser counters had a coefficient of determination of 0.99 (R-square) tested over a range from 0-250 $\mu g/m^3$. Due to a much higher number of rows of data missing (9,197) we used output from Channel B instead of Channel A in this study (*PurpleAir PA-II*, 2021).

PurpleAir units do not adjust for humidity which impacts hygroscopic growth of particles and particle count (Crilley et al., 2018; Malings et al., 2020). To reduce this humidity effect and account for the hygroscopic growth, $PM_{2.5}$ data was corrected using the formula in Equation 1 (Tryner et al., 2020):

$$\text{C-PM}_{2.5} = \frac{PM_{2.5}}{1+\frac{0.25RH^2}{(1-RH)}} \qquad \textbf{(}\textbf{\textit{Equation 1)}}$$

In Equation 1, C-$PM_{2.5}$ is the corrected $PM_{2.5}$ that is reported by PA in $\mu g/m^3$, $PM_{2.5}$ is the raw $PM_{2.5}$ value reported by PA ($\mu g/m^3$), and RH is relative humidity retrieved from Indiana Department of Environmental Management's (IDEM) regulatory air quality monitor at Washington Park in Indianapolis. After this adjustment, correlation between the data of the three closest sensors (Sensor 25, Sensor 30, and Sensor 31) to the two IDEM monitors (Washington Park monitor and I-70 monitor) was also examined. The Washington Park (WP) location is the only location that has a Photochemical Assessment Monitoring Station (PAMS), providing hourly samples of data which is available via the IDEM website from 1999 to present day (Monitoring, 2021).

4.2.3 Meteorological data

Some abnormal fluctuations in temperature and humidity data were detected in the PA sensors in our study area. A study in Pittsburg (USA) concluded that due to the shape of the PA units, they can trap heat and increase the inside temperature by an average of 2.7º C (36.86º F), and lower the humidity by an average of 9.7% versus outside the unit (Malings et al., 2020). This necessitated downloading meteorological data (temperature, relative humidity, wind-speed) from the IDEM air quality monitor at WP. Meteorological factors such as relative humidity, windspeed and drought conditions play a role in $PM_{2.5}$ concentrations (Chaloulakou et al., 2003; Hart et al., 2020; Tai et al., 2010; Zhang et al., 2017).

4.2.4 Land use and land cover

Estimates of tree canopy cover (TC) in the study region was based on 1-meter resolution land cover raster produced by our partner KIB and the University of Vermont Spatial Analysis Laboratory. The land cover data were derived from classification of

National Agricultural Imagery Program (NAIP) data acquired in 2013 and LiDAR data acquired in 2009. This dataset was used to quantify tree canopy (TC) in the study region census tracts and within buffers at varying distances from the PA sensor locations.

Additionally, the distribution of "Heavy Industrial" land use was modeled using a vector-based GIS dataset from the City of Indianapolis's data portal (*Open Indy Data Portal*, 2021) and processed using mapping software Maptitude 2020 by Caliper ®. This variable was incorporated in the analysis to capture its impact on this study area (Harper et al., 2021).

4.2.5 American Community Survey

The most recent American Community Survey (ACS) 5-year estimates (2014 - 2018), at the census tract level, were used for socio-economic and demographic variables (*Explore Census Data*, 2021). Census tract data has been used in the past in conjunction with PurpleAir to examine environmental justice implications (Mullen et al., 2022). Statistical analysis incorporating all these variables (Appendix C) was conducted using open-source software RStudio version 4.0.3.

4.3 Results

Sparse networks of regulatory monitors established by states are inadequate in providing us local information, limiting the use of this data to make informed decisions on zoning and infrastructure required to build robust communities. A dense network of sensors, as established in this study, enables us to quantify local impacts which can then be utilized to make future informed decisions. The temporal array for each sensor spans thousands of data points, but the spatial array is limited. Two analyses were conducted to

assess spatial patterns in the $PM_{2.5}$ data (kriging and Inverse Distance Weighting (IDW)) - both are included in Appendix C, but neither approach the sample size to be considered statistically valid (C1-C2).

One clear example of local monitoring to assess event-based air quality variations involves smoke emissions from U.S. Independence Day celebrations during the late evening of July 4, 2021 (Figure 4.2). During that celebration several sensors (Sensor 16 and Sensor 22) revealed higher daily $PM_{2.5}$ averages due to local fireworks than values reported later that month that resulted from massive forest fires in the Pacific Northwest and southern Canada (Jaipuriar, 2021; *Smoke Across North America*, 2021; "Wildfire Smoke Pouring into Mid-Atlantic Prompts Air-Quality Alert for D.C. and Baltimore," 2021).

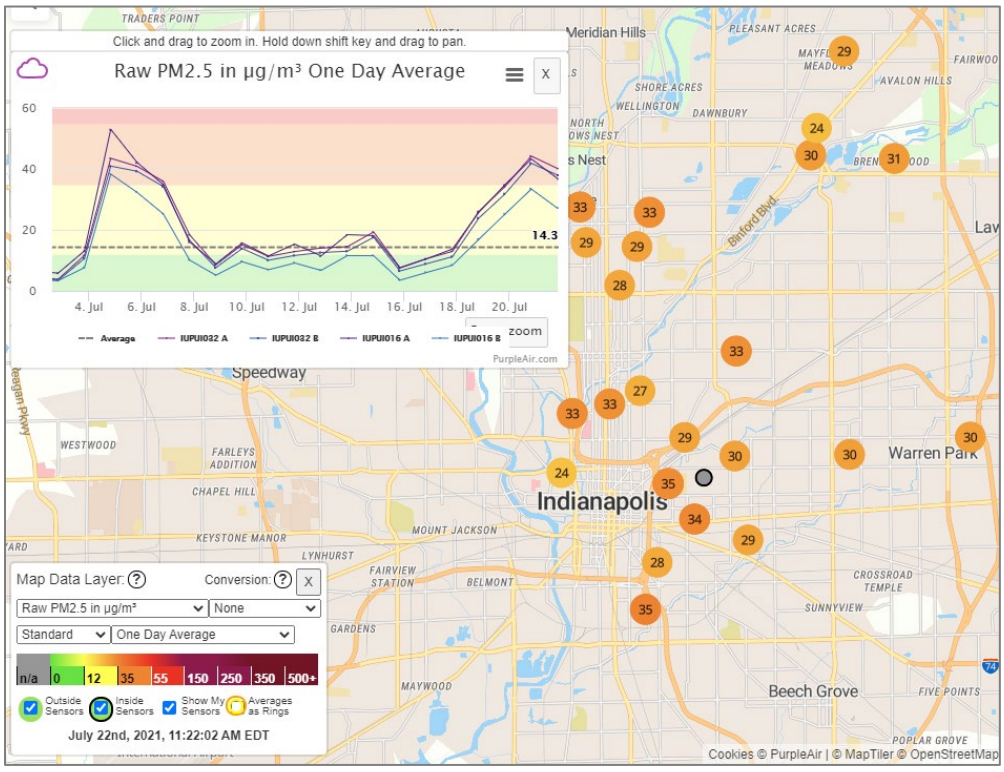

Figure 4.2 - PurpleAir map from the website with daily averages for Sensor 16 and 22, highlighting July 4 and 21, 2021.

4.3.1 PurpleAir data and portable EPA grade sensor

To validate the output from PA, at deployment we compared raw PA online readings with an EPA-grade portable sensor (Thermo Scientific MIE pDR-1500). On average, the values for 21 of the 25 sensors deployed were 13.56% higher than the EPA grade sensor, which is within a relative accuracy of +/-20% (Malings et al., 2020). It is important to note that PA sensors factory calibration is based on specific ambient aerosol, which may not be identical to our study region and could have contributed to the observed differences. Calibration of raw data has shown to reduce errors as much as 25% for extreme cases and by 10% for typical cases. Additionally, there is a systematic bias between instruments which can be compounded with the variation of particle composition and the sensors performance in the field, which can be balanced by longer term (one year) averaging thus significantly reducing the error (Malings et al., 2020). Our field validation was limited with the EPA grade portable sensor, typically lasting just ~1 hour at the beginning of deployment.

4.3.2 Correlation of PurpleAir data against IDEM monitor data

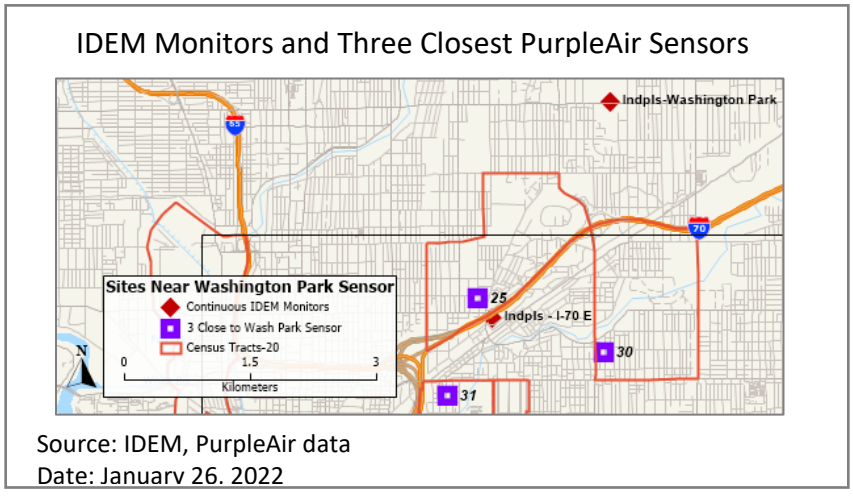

Figure 4.3 - Sensors nearest to Indiana Department of Environmental Management (IDEM) regulatory monitors.

Spearman correlation was used to examine the relationship between $PM_{2.5}$ measurements collected at the two IDEM monitoring sites and the adjusted $PM_{2.5}$ data collected at the three closest PA sensors (labeled 25, 30 and 31; Figure 4.3). This calculation was based on data spanning 11 months with over 300 observations each for the three sensors (Table 4.1).

Table 4.1 - Correlation of sensor 25, 30, and 31 with IDEM monitors and $PM_{2.5}$ data.

Sensor number	IDEM site	Correlation (Spearman)	P-value
25	WP	0.7469891	< 2.2e-16
30	WP	0.7443245	< 2.2e-16
31	WP	0.7208154	< 2.2e-16
25	I-70	0.7219634	< 2.2e-16
30	I-70	0.7129242	< 2.2e-16
31	I-70	0.7020652	< 2.2e-16

The association between $PM_{2.5}$ readings at the three PA sensors was strongest with the IDEM Washington Park sensor. The range of raw $PM_{2.5}$ was 0.36 -103.80 µg m^{-3} with RH ranging from 44-99%, and the average temperature was between -2.7–85.2 F (-19-30 C), based on the WP sensor data. After applying the relative humidity correction this range adjusted to 0.08 – 80.14 µg m^{-3}, the mean values to 16.22-9.03 µg m^{-3}, and the median to 14.64 - 8.10 µg m^{-3}. This RH correction underestimation may be more pronounced due to higher humidity in Indianapolis most of the year versus a less humid environment like that examined in Colorado where median bias was reduced by -15% after the correction (Tryner et al., 2020). In a separate study, Malings et al. (2020) found that PA sensors in the short term had a mean absolute error of approximately 4 µg m^{-3} and in the long run (year-long) that error went down to under 1 µg m^{-3}.

Based on the methodology outlined by Malings et al. (2020), we examined the overlap of WP and Sensor 30 data where WP $PM_{2.5}$ data <=20 µg m^{-3}, with humidity < 77%. The subset of data <=20 µg m^{-3} (range 1.82 -19.66 µg m^{-3}) with 146 observations, was used to calculate the regression coefficients to correct the raw Sensor 30 observations by PA. Initially, we used equation 2 to determine the coefficients of the independent variables. In Equation 2-3, T is temperature, DP is dewpoint and RH is relative humidity from the WP sensor. Since Equation 2 resulted in high collinearity with DP we removed it and used Equation 3 instead to correct Sensor 30 concentrations. In Equation 2 and 3 'PA' represents PurpleAir.

$[\text{Corrected } PM_{2.5}]_{PA} = \beta_0 + \beta_1[PM_{2.5}]_{PA} + \beta_2 T + \beta_3 RH + \beta_4 DP(T, RH)$

if WP $PM_{2.5}$ <= 20 ***Equation 2***

$[\text{Corrected } PM_{2.5}]_{PA} = 3.865673 + 0.318848\,[PM_{2.5}]_{PA} + 0.041092*T + -0.022493*RH$ ***Equation 3***

Table 4.2 - Results from applying Equation 3 to PurpleAir data.

Var	Median (µg m^{-3})	% Diff from WP $PM_{2.5}$	unit diff from WP $PM_{2.5}$
Raw $PM_{2.5}$	12.874	36.45%	3.439
WP adjusted $PM_{2.5}$ (Eq 1)	9.616	1.92%	0.181
WP $PM_{2.5}$	9.435	0.00%	0.000
Sensor30 (predicted-Eq 3)	9.064	-3.93%	-0.371

Table 4.2 shows that WP adjusted $PM_{2.5}$ which is based on Equation 1 correction is under 2% different from WP data and the predicted values based on Equation 3 is about 4% different. This indicates that based on the chemical composition of the pollutants in

this region, a RH-based correction (Equation 1) is adequate for calibration and further analysis. Mean value of $PM_{2.5}$ is lower in this network of 25 locations than reported in a prior study in Indianapolis (Sullivan & Pryor, 2014).

4.3.3 Driving factors impacting daily averages of $PM_{2.5}$ exceeding WHO limits

A total of 8,124 counts of cumulative data by month were used in the regression analysis (Table 4.3). To identify potential factors impacting the days that $PM_{2.5}$ values exceed the WHO threshold of 25 $\mu g/m^3$, independent variables listed in Table 4.4 (APPENDIX C -D) were used in setting up a logistic regression equation. The dependent binary variable is represented by 1 when the adjusted $PM_{2.5}$ values are greater than or equal to the WHO limit of 25 $\mu g/m^3$, and 0 when the adjusted $PM_{2.5}$ values are less than the WHO limit of 25 $\mu g/m^3$.

Table 4.3 - Logistic regression observation breakdown by month for 25 deployed sensors.

Month	Month Group	Observations
2018		
November	1	728
December	2	769
2019		
January	2	739
March	3	753
April	3	726
May	3	773
June	4	702
July	4	752
August	4	751
September	5	733
October	5	698
Total		8,124

Five significant variables arose from the regression modeling (Table 4.4). The logistic regression output is further extrapolated in Table 4.5 into odds ratios which represents the strength of the significant variables resulting in a day exceeding WHO guidelines for $PM_{2.5}$. Any ratio under 1 is represented by reduced odds, and over 1 by increased odds, of resulting in a high $PM_{2.5}$ concentration exceeding WHO guidelines per day. Increased precipitation, increased windspeed, and Month group 5 (September and October) have reduced odds of exceeding WHO guidelines per day (Table 4.5). On Saturday the odds of exceeding the WHO limit are sixfold compared to the other days of the week, and on Tuesday the odds decrease to threefold.

Table 4.4 - Logistic regression output. Negative values indicate a decrease, and positive values an increase, in the number of days with $PM_{2.5}$ averages above WHO guidelines.

Variable	**Estimate**	**Pr(>|z|)**
(Intercept)	-2.05301	0.0014 **
Precip cm	-34.137	0.0060 **
Windspeed kmh	-0.27462	0.0000 **
Temp C	-0.02154	0.2569
Month group 2	-0.58128	0.1487
Month group 3	0.10966	0.7550
Month group 4	-1.08057	0.0518 .
Month group 5	-1.1233	0.0214 *
Day (Mon)	0.5873	0.2822
Day (Sat)	1.84268	0.0002 **
Day (Sun)	1.01762	0.0509 .
Day (Thur)	0.09561	0.8816
Day (Tue)	1.17912	0.0184 *

“.” signifies p-value < 0.1
“*” signifies p-value < 0.05
“**” signifies p-value < 0.01

Table 4.5 - Odds of the significant coefficients from the regression output.

Variable	Odds Ratio
Precip cm	0.0000
Windspeed_kmh	0.7599
Month group 5	0.3252
Day (Sat)	6.3134
Day (Sun)	2.7666
Day (Tue)	3.2515

4.3.4 Identify sensors with highest odds ratio of exceeding the WHO daily limit

Odds ratio calculations were run to identify locations within the study area that are likeliest to exceed the WHO daily limit for $PM_{2.5}$. There were only two sensors out of a total of 25 that had significant odds ratios for days that exceed the WHO daily limit of 25 $\mu g/m^3$. Odds for sensor 16 is 3.04 times that of other locations to meet or exceed 25 $\mu g/m^3$, and for sensor 13 it is 2.37 (Table 4.6). Interestingly, the two sites proximal to major interstate freeways in the area (Sensors 32 and 25) had low odds ratios for exceeding air quality parameters, perhaps owing to freeway turbulence, lack of idling, and modern emission controls for most vehicles.

Table 4.6 - Odds ratios output from significant sensors.

Sensor#	chi_sq (p-val)	Significant Status	OR
13	0.0243	Signif Relationship	2.37
16	0.0008	Signif Relationship	3.04

4.3.5 Analysis at the census tract level

Correlations at the census tract level of $PM_{2.5}$ data revealed that four variables are significant (p-value 0.05) with one being almost significant at that level (Table 4.7). The two negative relationships with Tree Canopy % and White Only % indicate that they have an inverse relationship with $PM_{2.5}$ concentrations. The two positive correlations were found with 'Heavy Ind %' and 'Hwy Length km' with $PM_{2.5}$ concentrations.

Table 4.7 - Correlations of average $PM_{2.5}$ at the census tract level.

Correlations with $PM_{2.5}$ Census Tract Level	***Method***	***Value***
Tree Canopy %	Spearman	-0.6677 *
Heavy Ind %	Spearman	0.6338 *
Hwy Length km	Spearman	0.4964 *
Road Length km	Spearman	0.2887
Pop25+LT high school %	Spearman	0.4376 [a]
Pop25+Some College_Assoc %	Pearson	-0.0955
Pop25+ Graduate_Prof Degree %	Spearman	-0.2023
Hispanic Latino %	Spearman	0.2369
Black One Race %	Spearman	0.2977
White Only %	Spearman	-0.4739 *
Median HH Inc	Spearman	-0.4060
Median Rent	Pearson	0.1012

*' * ' represents p-value < 0.05*
' [a] ' represents almost significant at p-value 0.05

Regression models were run with all the variables (Table 4.8). Model 1 resulted in adjusted r-square of 66.47% with 4 significant variables at p-value < 0.05. However, this model resulted in a high variance inflation factor (VIF) of 176.17 for 'Black One Race %', which led to running Model 2 without this variable. The second model with an adjusted r-square of 57.94% resulted in a high VIF value of 12.57 for 'Road Length km'. Model 3 was run without 'Road Length km' which resulted in adjusted r-square of 59.92%, higher that Model 2 but lower than Model 1, with all VIF values < 10. Output of Model 3 is detailed in Table 4.8, which shows 4 significant variables at p-value < 0.05, and population with some college and associates degree at p-value 0.1. As an additional step, stepwise regression model was run on Model 3 which resulted in an adjusted r-square of 62.79% with 2 significant variables at p-value < 0.01 and 3 variables significant at p-value < 0.05. All VIF values for the variables in the final model (Stepwise model) are under 10,

indicating that multi-collinearity is not an issue in this model. We can make the following observations from the final model for our data points at the census tract level:

- A 1% increase in canopy coverage deceases average $PM_{2.5}$ at the census tract level by 0.12 +/- 0.03 $\mu g/m^3$ (at the 95% confidence interval).
- A 1% increase of Heavy Industrial area increases $PM_{2.5}$ by 0.07 $\mu g/m^3$ +/- 0.02 $\mu g/m^3$
- As the percentage of population over 25 with some college and associates degree increases it results in a proportional increase of $PM_{2.5}$ by 0.08 $\mu g/m^3$ +/- 0.03
- Hispanic Latino % has a proportional increase indicating that as this population increases by one percent it results in an increase of $PM_{2.5}$ by 0.06 $\mu g/m^3$ +/- 0.02
- Median Rent has an inverse relationship. An increase of $100 in median rent results in a decrease of $PM_{2.5}$ by 0.9 $\mu g/m^3$ +/- 0.03

Table 4.8 - stepwise regression output.

	Model 1 (Adj-R^2 =66.47)	***Model 3 (Adj-$R^=$ =59.92)***	***Stepwise (Adj-R^2 =62.79)***
(Intercept)	32.1600*	16.0000 **	16.66913 **
Tree Canopy %	-0.1840 *	-0.1165 *	-0.1243 **
Heavy Ind %	0.0796 *	0.0724 *	0.069337 *
Hwy Length km	-0.1284	0.0225	
Road Length km	0.0097		
Pop25+LT high school %	-0.4331	-0.4173	-0.48426 .
Pop25+Some College_Assoc %	0.1603 *	0.0790 .	0.080368 *
Pop25+ Grad Prof Degree %	-0.0131	0.0634	0.044515
Hispanic Latino %	-0.0831	0.0590 *	0.060178 *
Black One Race %	-0.1201		
White Only %	-0.0860	0.0167	0.01149

Median HH Inc	0.0000	0.0000	
Median Rent	-0.0153 *	-0.0083 *	-0.00873 **

"*" signifies p-value < 0.05
"**" signifies p-value < 0.01

4.4 Discussion

Community engagement may have its earliest examples dating back to 1840's in meteorology (Rosner, 2013). At any level citizen science poses many challenges as well as opportunities (Den Broeder et al., 2018; Hayhow et al., 2021). By creating a link between researchers and the public such engagement not only benefits the researchers but it also creates a group of engaged citizenry (Rosner, 2013). Low-cost sensors like PA are an inexpensive way for communities to use citizen science to participate in examining air quality at a fine scale (English et al., 2017).

The South Coast AQMD has tested PurpleAir sensors to evaluate their performance and found high field accuracy. Our findings generally corroborate this instrumental fidelity, with correlation between the three sensors tested against the Washington Park sensor of > 0.7. Over time, sensor fidelity does degrade (Masson et al., 2015), along with the added confounding effects of temperature and humidity. Thus, low-cost monitor data needs to be carefully examined over time to ensure that the calibration equation is adequately addressing data deviations. To suppress sensor from humidity (Bi et al., 2020), we calibrated the PA sensor output with humidity values (Equation 1) from the Washington Park IDEM monitor (Jiao et al., 2016). We also transformed data using Equation 3 for assessing reliability but found that in the PR dataset a relative humidity correction alone was adequate (Table 4.2).

In our study area, weekend days are in the top three days for exceeding WHO $PM_{2.5}$ standards. This may be due to a higher volume of vehicle trips during these days on local roadways, with an increase in idling time as well as stop and go traffic. This enhanced local time that vehicles stay proximal to the sensors would be captured by the hyper-local sensor locations, as opposed to standard work commute days when the traffic would be more limited to travelling to and from work. A previous study in Indianapolis (Sullivan & Pryor, 2014) found higher $PM_{2.5}$ during weekdays, in contrast to our results, but this is likely driven by the fact that this study used stationary sites from IDEM monitoring sites that are intentionally placed distant from local air pollution sources and transects that largely were proximal to freeways and major arterials as opposed to our neighborhood-based sites.

We expected sensor 32 or sensor 25, both near a major interstate with high traffic volumes, to have high odds of exceeding WHO limits, but we find instead that sensors 13 and 16 are the sensors with significant odds of exceeding those daily limits. We expect that the exhaust from traffic on highways creates a temperature gradient between it and the ambient air which due to thermal buoyancy results in the plume to rise which is then impacted by wind speed and direction. Lower wind speeds versus high wind speed on highways result in traffic exhaust plumes to disperse more slowly, thus resulting in higher measurements that are detected for longer periods of time (He & Dhaniyala, 2012). However, since Sensor 32 is upwind from I-65, it is impacted by local versus highway traffic. Sensor 16 on the other hand along with vehicles is also impacted by the frequent use of a wood burning stove by its neighbor, thus having a unique local impact resulting in consistently higher values at that sensor location.

Urban greening initiatives in canopy-deprived census tracts can positively impact air quality and reduce related health disparities. This will be extremely critical, as urban land is projected to increase to 8.1% in 2050 versus 3.1% in 2000. Indiana is projected to increase its urban landscape to 16.7% by 2050 from 8.8% in 2000, ranking 14 in the lower 48 states in the USA. In 1990, 2.6% of Indiana's forestland was in urban areas. This percentage increased to 3.6% in 2000 and is expected to increase to a staggering 12.1% by 2050. By 2050, 8.8% of Indiana's forestland outside of urban areas in 2000 will be subsumed by urban growth. This projection equates to 1,500 km^2 of farmland being subsumed by urbanization in Indiana from 2000 to 2050. Since forests and trees are critical in enhancing human and environmental health, urban canopy cover should be prioritized (Nowak & Walton, 2005). Not only does reduced $PM_{2.5}$ improve air quality it also results in reduction in expenses. A 10-city study in the USA found mortality related to $PM_{2.5}$ to range between 1-7.6 people/year, and the average value per mortality incidence to be $7.8 million. Additionally, average health benefits were $1,600 per hectare of tree cover, with an average of $1.6 billion in health benefits per 1$\mu g/m^3$ reduction (Nowak et al., 2013). According to this study, the health savings in our 20 census tracts range approximately between $36,300 (census tract 18097355900) – $1,121,585 (census tract 18097361400). This was calculated by multiplying the canopy coverage in each census tract by cost savings of $1,600 as reported by Nowak et al. (2013). When this calculation is normalized by area, health savings in census tract 18097361400 is 1.2 times that of the former.

Planting trees in the census tract with lower canopy coverage in conjunction with dividing the study area into Low Emission Zones (LEZs), where there are restrictions placed on high polluting vehicles from entering against non-LEZ could give us direct

control over minimizing the impacts from vehicle pollution (Morfeld et al., 2014) and combatting it through nature simultaneously.

4.5 Conclusion

This air quality study in Indianapolis is a community-based attempt in examining local impacts of $PM_{2.5}$ over a dense network of 25 sensors. This network was established by collaborating with local partners through community engagement and enhancing the examination of the impacts of canopy coverage along with land use data and other variables on $PM_{2.5}$ in the city.

We found that the relative humidity correction, as captured in Equation 1, is adequate for calibrating raw $PM_{2.5}$ data which is used in all the analysis. Our most significant finding captured at the census tract level was that increased percentage of tree canopy coverage at the census tract level produced positive externalities which should then be encouraged through collective efforts, especially in regions of higher health issues related to $PM_{2.5}$. A 1 % increase in canopy coverage at the census tract level resulted in decreasing $PM_{2.5}$ by approximately 0.12 $\mu g/m^3$. Based on research by Nowak et al. (2013), we extrapolate further that the canopy coverage in our study region provides between \$36,000 - \$1,121,585 in health savings in the census tracts. Additionally, a 1% increase of Heavy Industrial area classification in the census tract resulted in increasing $PM_{2.5}$ by a modest 0.07 $\mu g/m^3$.

In our logistic regression analysis, we found that increase in wind speed and precipitation result in lowering $PM_{2.5}$ concentrations. We also found that local impacts, as witnessed by the wood burning stove of Sensor 16's neighbor, trumped location near

highways, resulting in higher accumulation of $PM_{2.5.}$ Lastly, being predominantly a residential area possibly played a large role on Saturdays resulting in highest accumulations of these particles due to potentially robust internal traffic on the weekends.

Air pollutants like $PM_{2.5}$ can vary vastly spatially and temporally based on the sources its exposed to, atmospheric transformations as well as its built environment features (Zimmerman et al., 2020). Such networks as established in our study along with enhanced health data can enable us to understand micro impacts from spatial variability of air quality and should be utilized as a tool to examine and understand regions and to facilitate partnership between the community and government entities to find solutions to quantify and then improve their health thus creating resilient communities.

4.6 References

Anenberg, S. C., Horowitz, L. W., Tong, D. Q., & West, J. J. (2010). An Estimate of the Global Burden of Anthropogenic Ozone and Fine Particulate Matter on Premature Human Mortality Using Atmospheric Modeling. *Environmental Health Perspectives*, *118*(9), 1189–1195. https://doi.org/10.1289/ehp.0901220

Bi, J., Belle, J. H., Wang, Y., Lyapustin, A. I., Wildani, A., & Liu, Y. (2019). Impacts of snow and cloud covers on satellite-derived PM2.5 levels. *Remote Sensing of Environment*, *221*, 665–674. https://doi.org/10.1016/j.rse.2018.12.002

Bi, J., Wildani, A., Chang, H. H., & Liu, Y. (2020). Incorporating Low-Cost Sensor Measurements into High-Resolution PM $_{2.5}$ Modeling at a Large Spatial Scale. *Environmental Science & Technology*, *54*(4), 2152–2162. https://doi.org/10.1021/acs.est.9b06046

Chaloulakou, A., Kassomenos, P., Spyrellis, N., Demokritou, P., & Koutrakis, P. (2003). Measurements of PM10 and PM2.5 particle concentrations in Athens, Greece. *Atmospheric Environment*, *37*(5), 649–660. https://doi.org/10.1016/S1352-2310(02)00898-1

Chen, H., Goldberg, M. S., & Viileneuve, P. J. (2008). A systematic review of the relation between long-term exposure to ambient air pollution and chronic diseases. *Reviews on Environmental Health*, *23*(4), 243–297. Scopus.

Christidis, T., Erickson, A. C., Pappin, A. J., Crouse, D. L., Pinault, L. L., Weichenthal, S. A., Brook, J. R., van Donkelaar, A., Hystad, P., Martin, R. V., Tjepkema, M., Burnett, R. T., & Brauer, M. (2019). Low concentrations of fine particle air pollution and mortality in the Canadian Community Health Survey cohort. *Environmental Health*, *18*(1), 84. https://doi.org/10.1186/s12940-019-0518-y

Chu, M., Sun, C., Chen, W., Jin, G., Gong, J., Zhu, M., Yuan, J., Dai, J., Wang, M., Pan, Y., Song, Y., Ding, X., Guo, X., Du, M., Xia, Y., Kan, H., Zhang, Z., Hu, Z., Wu, T., & Shen, H. (2015). Personal exposure to PM2.5, genetic variants and DNA damage: A multi-center population-based study in Chinese. *Toxicology Letters*, *235*(3), 172–178. https://doi.org/10.1016/j.toxlet.2015.04.007

Cohen, A. J., Brauer, M., Burnett, R., Anderson, H. R., Frostad, J., Estep, K., Balakrishnan, K., Brunekreef, B., Dandona, L., Dandona, R., Feigin, V., Freedman, G., Hubbell, B., Jobling, A., Kan, H., Knibbs, L., Liu, Y., Martin, R., Morawska, L., … Forouzanfar, M. H. (2017). Estimates and 25-year trends of the global burden of disease attributable to ambient air pollution: An analysis of data from the Global

Burden of Diseases Study 2015. *The Lancet*, *389*(10082), 1907–1918. https://doi.org/10.1016/S0140-6736(17)30505-6

Crilley, L. R., Shaw, M., Pound, R., Kramer, L. J., Price, R., Young, S., Lewis, A. C., & Pope, F. D. (2018). Evaluation of a low-cost optical particle counter (Alphasense OPC-N2) for ambient air monitoring. *Atmospheric Measurement Techniques*, *11*(2), 709–720. https://doi.org/10.5194/amt-11-709-2018

Den Broeder, L., Devilee, J., Van Oers, H., Schuit, A. J., & Wagemakers, A. (2018). Citizen Science for public health. *Health Promotion International*, *33*(3), 505–514. https://doi.org/10.1093/heapro/daw086

English, P. B., Olmedo, L., Bejarano, E., Lugo, H., Murillo, E., Seto, E., Wong, M., King, G., Wilkie, A., Meltzer, D., Carvlin, G., Jerrett, M., & Northcross, A. (2017). The Imperial County Community Air Monitoring Network: A Model for Community-based Environmental Monitoring for Public Health Action. *Environmental Health Perspectives*, *125*(7), 074501. https://doi.org/10.1289/EHP1772

Explore Census Data. (2021, July 8). https://data.census.gov/cedsci/

Fann, N., Lamson, A. D., Anenberg, S. C., Wesson, K., Risley, D., & Hubbell, B. J. (2011). Estimating the National Public Health Burden Associated with Exposure to Ambient PM2.5 and Ozone. *Risk Analysis*, *32*(1), 81–95. https://doi.org/10.1111/j.1539-6924.2011.01630.x

Ferrari, L., Carugno, M., & Bollati, V. (2019). Particulate matter exposure shapes DNA methylation through the lifespan. *Clinical Epigenetics*, *11*(1), 129. https://doi.org/10.1186/s13148-019-0726-x

Gupta, P., Doraiswamy, P., Levy, R., Pikelnaya, O., Maibach, J., Feenstra, B., Polidori, A., Kiros, F., & Mills, K. C. (2018). Impact of California Fires on Local and Regional Air Quality: The Role of a Low-Cost Sensor Network and Satellite Observations. *GeoHealth*, *2*(6), 172–181. https://doi.org/10.1029/2018GH000136

Harper, A., Baker, P. N., Xia, Y., Kuang, T., Zhang, H., Chen, Y., Han, T.-L., & Gulliver, J. (2021). Development of spatiotemporal land use regression models for PM2.5 and NO2 in Chongqing, China, and exposure assessment for the CLIMB study. *Atmospheric Pollution Research*, *12*(7), 101096. https://doi.org/10.1016/j.apr.2021.101096

Hart, R., Liang, L., & Dong, P. (2020). Monitoring, Mapping, and Modeling Spatial–Temporal Patterns of PM2.5 for Improved Understanding of Air Pollution Dynamics Using Portable Sensing Technologies. *International Journal of Environmental Research and Public Health*, *17*(14), 4914. https://doi.org/10.3390/ijerph17144914

Hayhow, C., Brabander, D., Jim, R., Lively, M., and Filippelli, G.M., 2021. Addressing the need for just GeoHealth engagement: Evolving models for actionable research that transform communities. *GeoHealth*. https://doi.org/10.1029/2021GH000496

He, M., & Dhaniyala, S. (2012). Vertical and horizontal concentration distributions of ultrafine particles near a highway. *Atmospheric Environment*, *46*, 225–236. https://doi.org/10.1016/j.atmosenv.2011.09.076

Indicator Metadata Registry Details. (2021, October 15). https://www.who.int/data/gho/indicator-metadata-registry/imr-details/158

Jaipuriar, R. (2021, July 22). Residents told to stay indoors as wildfire smoke crosses state. *Indianapolis Star*, A.3.

Ji, X., Yao, Y., & Long, X. (2018). What causes PM2.5 pollution? Cross-economy empirical analysis from socioeconomic perspective. *Energy Policy*, *119*, 458–472. https://doi.org/10.1016/j.enpol.2018.04.040

Jiao, W., Hagler, G., Williams, R., Sharpe, R., Brown, R., Garver, D., Judge, R., Caudill, M., Rickard, J., Davis, M., Weinstock, L., Zimmer-Dauphinee, S., & Buckley, K. (2016). Community Air Sensor Network (CAIRSENSE) project: Evaluation of low-cost sensor performance in a suburban environment in the southeastern United States. *Atmospheric Measurement Techniques*, *9*(11), 5281–5292. https://doi.org/10.5194/amt-9-5281-2016

Kasdagli, M.-I., Katsouyanni, K., de Hoogh, K., Lagiou, P., & Samoli, E. (2021). Associations of air pollution and greenness with mortality in Greece: An ecological study. *Environmental Research*, *196*, 110348. https://doi.org/10.1016/j.envres.2020.110348

Kheirbek, I., Haney, J., Douglas, S., Ito, K., & Matte, T. (2016). The contribution of motor vehicle emissions to ambient fine particulate matter public health impacts in New York City: A health burden assessment. *Environmental Health: A Global Access Science Source*, *15*, 1–14. aph.

Koehler, K. A., & Peters, T. M. (2015). New Methods for Personal Exposure Monitoring for Airborne Particles. *Current Environmental Health Reports*, *2*(4), 399–411. https://doi.org/10.1007/s40572-015-0070-z

Krzyzanowski, M., & Cohen, A. (2008). Update of WHO air quality guidelines. *Air Quality, Atmosphere & Health*, *1*(1), 7–13. https://doi.org/10.1007/s11869-008-0008-9

Liang, L. (2021). Calibrating low-cost sensors for ambient air monitoring: Techniques, trends, and challenges. *Environmental Research*, *197*, 111163. https://doi.org/10.1016/j.envres.2021.111163

Malings, C., Tanzer, R., Hauryliuk, A., Saha, P. K., Robinson, A. L., Presto, A. A., & Subramanian, R. (2020). Fine particle mass monitoring with low-cost sensors: Corrections and long-term performance evaluation. *Aerosol Science and Technology*, *54*(2), 160–174. https://doi.org/10.1080/02786826.2019.1623863

Map—PurpleAir. (2021, July 8). https://www.purpleair.com/gmap?&zoom=3&lat=39.51596757727815&lng=-99.35539180755613&clustersize=45&sensorsActive2=10080&orderby=L&nwlat=74.04797179959134&selat=-25.54831832561498&nwlng=178.9063269424439&selng=-17.617110557556135

Masson, N., Piedrahita, R., & Hannigan, M. (2015). Quantification Method for Electrolytic Sensors in Long-Term Monitoring of Ambient Air Quality. *Sensors*, *15*(10), 27283–27302. https://doi.org/10.3390/s151027283

Monitoring, A. (2021, March 4). *Air Toxics Data Map*. Air Monitoring. https://www.in.gov/idem/airmonitoring/air-quality-data/air-toxics-data-map

Morfeld, P., Groneberg, D. A., & Spallek, M. F. (2014). Effectiveness of Low Emission Zones: Large Scale Analysis of Changes in Environmental NO2, NO and NOx

Concentrations in 17 German Cities. *PLoS ONE*, *9*(8), 1–18. https://doi.org/10.1371/journal.pone.0102999

Mousavi, A., & Wu, J. (2021). Indoor-Generated PM2.5 During COVID-19 Shutdowns Across California: Application of the PurpleAir Indoor–Outdoor Low-Cost Sensor Network. *Environmental Science & Technology*, *55*(9), 5648–5656. https://doi.org/10.1021/acs.est.0c06937

Mullen, C., Flores, A., Grineski, S., & Collins, T. (2022). Exploring the distributional environmental justice implications of an air quality monitoring network in Los Angeles County. *Environmental Research*, *206*, 112612. https://doi.org/10.1016/j.envres.2021.112612

Nowak, D. J., Hirabayashi, S., Bodine, A., & Hoehn, R. (2013). Modeled PM2.5 removal by trees in ten U.S. cities and associated health effects. *Environmental Pollution*, *178*, 395–402. https://doi.org/10.1016/j.envpol.2013.03.050

Nowak, D. J., & Walton, J. T. (2005). Projected Urban Growth (2000 – 2050) and Its Estimated Impact on the US Forest Resource. *Journal of Forestry*, 7.

Open Indy Data Portal. (2021, July 8). https://data.indy.gov/

Pope, F. D., Gatari, M., Ng'ang'a, D., Poynter, A., & Blake, R. (2018). Airborne particulate matter monitoring in Kenya using calibrated low-cost sensors. *Atmospheric Chemistry and Physics*, *18*(20), 15403–15418. https://doi.org/10.5194/acp-18-15403-2018

PurpleAir | Real Time Air Quality Monitoring. (2021, June 30). PurpleAir. https://www2.purpleair.com/

PurpleAir PA-II. (2021, July 8). https://www.aqmd.gov/aq-spec/product/purpleair-pa-ii

Rosner, H. (2013). Data on Wings. *Scientific American*, *308*(2), 68–73.

Shi Liuhua, Zanobetti Antonella, Kloog Itai, Coull Brent A., Koutrakis Petros, Melly Steven J., & Schwartz Joel D. (2016). Low-Concentration PM2.5 and Mortality: Estimating Acute and Chronic Effects in a Population-Based Study. *Environmental Health Perspectives*, *124*(1), 46–52. https://doi.org/10.1289/ehp.1409111

Smoke Across North America. (2021, July 21). [Text.Article]. NASA Earth Observatory. https://earthobservatory.nasa.gov/images/148610/smoke-across-north-america

Snyder, E. G., Watkins, T. H., Solomon, P. A., Thoma, E. D., Williams, R. W., Hagler, G. S. W., Shelow, D., Hindin, D. A., Kilaru, V. J., & Preuss, P. W. (2013). The Changing Paradigm of Air Pollution Monitoring. *Environmental Science & Technology*, *47*(20), 11369–11377. https://doi.org/10.1021/es4022602

Sullivan, R. C., & Pryor, S. C. (2014). Quantifying spatiotemporal variability of fine particles in an urban environment using combined fixed and mobile measurements. *Atmospheric Environment*, *89*, 664–671. https://doi.org/10.1016/j.atmosenv.2014.03.007

Tai, A. P. K., Mickley, L. J., & Jacob, D. J. (2010). Correlations between fine particulate matter (PM2.5) and meteorological variables in the United States: Implications for the sensitivity of PM2.5 to climate change. *Atmospheric Environment*, *44*(32), 3976–3984. https://doi.org/10.1016/j.atmosenv.2010.06.060

Tan, Y., Wang, Y., Zou, Y., Zhou, C., Yi, Y., Ling, Y., Liao, F., Jiang, Y., & Peng, X. (2020). LncRNA LOC101927514 regulates PM2.5-driven inflammation in human bronchial epithelial cells through binding p-STAT3 protein. *Toxicology Letters*, *319*, 119–128. https://doi.org/10.1016/j.toxlet.2019.10.009

Tanzer-Gruener, R., Li, J., Eilenberg, S. R., Robinson, A. L., & Presto, A. A. (2020). Impacts of Modifiable Factors on Ambient Air Pollution: A Case Study of COVID-19 Shutdowns. *Environmental Science & Technology Letters*, *7*(8), 554–559. https://doi.org/10.1021/acs.estlett.0c00365

Tryner, J., L'Orange, C., Mehaffy, J., Miller-Lionberg, D., Hofstetter, J. C., Wilson, A., & Volckens, J. (2020). Laboratory evaluation of low-cost PurpleAir PM monitors and in-field correction using co-located portable filter samplers. *Atmospheric Environment*, *220*, 117067. https://doi.org/10.1016/j.atmosenv.2019.117067

Wang, P., Guo, H., Hu, J., Kota, S. H., Ying, Q., & Zhang, H. (2019). Responses of PM2.5 and O3 concentrations to changes of meteorology and emissions in China. *Science of The Total Environment*, *662*, 297–306. https://doi.org/10.1016/j.scitotenv.2019.01.227

Wildfire smoke pouring into Mid-Atlantic prompts air-quality alert for D.C. and Baltimore. (2021, December 1). *Washington Post*. https://www.washingtonpost.com/weather/2021/07/20/wildfire-smoke-air-quality-dc/

Xiao, Q., Wang, Y., Chang, H. H., Meng, X., Geng, G., Lyapustin, A., & Liu, Y. (2017). Full-coverage high-resolution daily PM2.5 estimation using MAIAC AOD in the Yangtze River Delta of China. *Remote Sensing of Environment*, *199*, 437–446. https://doi.org/10.1016/j.rse.2017.07.023

You, D., Qin, N., Zhang, M., Dai, J., Du, M., Wei, Y., Zhang, R., Hu, Z., Christiani, D. C., Zhao, Y., & Chen, F. (2020). Identification of genetic features associated with fine

particulate matter (PM2.5) modulated DNA damage using improved random forest analysis. *Gene*, *740*, 144570. https://doi.org/10.1016/j.gene.2020.144570

Zauli Sajani, S., Marchesi, S., Trentini, A., Bacco, D., Zigola, C., Rovelli, S., Ricciardelli, I., Maccone, C., Lauriola, P., Cavallo, D., Poluzzi, V., Cattaneo, A., & Harrison, R. (2018). Vertical variation of PM 2.5 mass and chemical composition, particle size distribution, NO 2 , and BTEX at a high rise building *. *Environmental Pollution*, *235*, 339–349. https://doi.org/10.1016/j.envpol.2017.12.090

Zhang, H., Wang, Y., Park, T.-W., & Deng, Y. (2017). Quantifying the relationship between extreme air pollution events and extreme weather events. *Atmospheric Research*, *188*, 64–79. https://doi.org/10.1016/j.atmosres.2016.11.010

Zimmerman, N. (2021). Tutorial: Guidelines for implementing low-cost sensor networks for aerosol monitoring. *Journal of Aerosol Science*, 105872. https://doi.org/10.1016/j.jaerosci.2021.105872

Zimmerman, N., Li, H. Z., Ellis, A., Hauryliuk, A., Robinson, E. S., Gu, P., Shah, R. U., Ye, Q., Snell, L., Subramanian, R., Robinson, A. L., Apte, J. S., & Presto, A. A. (2020). Improving Correlations between Land Use and Air Pollutant Concentrations Using Wavelet Analysis: Insights from a Low-cost Sensor Network. *Aerosol and Air Quality Research*, *20*(2), 314–328. https://doi.org/10.4209/aaqr.2019.03.0124

CHAPTER 5: DISSERTATION CONCLUSION

5.1 Air pollution

There have been multiple studies examining air pollution (Beelen et al., 2013; Gupta et al., 2018; Heintzelman et al., 2021) and tying them to health impacts (Cohen et al., 2017; Lamsal et al., 2013; Meng et al., 2021; Rao et al., 2014). Studies have ranged in utilizing satellite data to low-cost ground level sensor (Bi, Stowell, et al., 2020; Bi, Wildani, et al., 2020; Lamsal et al., 2013). Stationary and mobile monitoring (Miller et al., 2020; Padilla et al., 2022) technology used independently and in conjunction with other methods present limitations but are also an avenue to promoting awareness of the environment to not just researchers but community members as well.

Recent research is highlighting the interaction between our environment and our genes, referred to as Epigenetics. It is found that environmental stresses like social stresses can alter our gene expression, which can span three generations. Several DNA variations that resulted from single nucleotide (DNA building block) variants (SNV) have been identified that play a role in regulating epigenetics and should be targeted for treatments and future research (Chu et al., 2015; Ferrari et al., 2019; Tan et al., 2020; You et al., 2020). In fact during pregnancy, in childhood and the elderly are the highest susceptible to negative impacts from air pollution (Ferrari et al., 2019). This presents a need for frequent and consistent air pollution measurements which can be successfully achieved by low-cost sensor studies assessing from local and regional impacts to personal and community based impacts from air pollution (Jiao et al., 2016; Kortoçi et al., 2022; Malings et al., 2020).

5.2 Contributions of this dissertation

As highlighted in Chapter 2, sparsely placed sensors are not adequate in examining finer scale geographies. We must accept that there are limitations not just in low-cost sensor studies, as highlighted in the next section, but also satellite data studies. However, as highlighted in this body of work, there is a way to address and mitigate the shortcomings of low-cost sensor technology as improvements are made to this technology. COVID-19 gave us a glimpse into a natural experiment, which was taken advantage of in Chapter 2, to assess and quantify the impacts of reduced air pollution.

Next, to achieve fine scale analysis, a dense network of citizen scientist with low-cost sensors was established to quantify air pollution impacts while incorporating other variables. Passive Ogawa sensors, used in Chapter 3, have historically tracked well with EPA grade monitors, therefore that data was not modified. No research study was found that not only utilized a citizen scientist network, but also incorporated Ogawa passive sensors in conjunction with accurate traffic data, and high-resolution imagery in analyzing a region. Incorporating StreetLight platform as done in Chapter 3, provides an opportunity to highlight how we can use the two together in evaluating urban spaces.

Lastly, in Chapter 4, in the Pleasant Run airshed study area, PurpleAir active sensors were utilized with an equation-based correction for calibration. It was found that this data correction is adequate in Pleasant Run, thus providing a low-cost alternative for air quality examination.

5.3 Study limitations

One of the main limitations of Chapter 2 is the short-time period as well as the number of usable data points from cities and sensors. Air pollution data could be accessed from only some of the top populated cities in the U.S. Therefore, Chapter 2 analysis is limited to 11 cities in the country.

Chapter 3 utilized low-cost Ogawa, passive sensors, in a fine scale citizen science approach to examine pollution in the Pleasant Run airshed in Indianapolis; however, data from only 3 deployment cycles could be utilized that spanned over 32 sensors. A larger number of sensors and deployment cycles would have enriched the data for analysis. Another limitation in Chapter 3 related to the time frame used for traffic data extraction from StreetLight. StreetLight data platform is set up to provide greater accuracy when examining a longer time frame. To overcome this limitation, future work should extend traffic data analysis over several months rather than a week at a time.

Chapter 4 utilized low-cost active PurpleAir sensors, that have internal limitations and have been scrutinized in research. However, a relative humidity correction was utilized, which was demonstrated to be adequate in the Pleasant Run airshed. Higher quality data and precise instrumentation is always preferred, but we must be careful to not paralyze our investigations in the interest of EPA grade results. We need to access the needs of the study and proceed with reasonable accommodations. Validating data from low-cost ground-based sensors is an ongoing debate, with several methods proposed. A study, based on its needs, may not require FRM accuracy and could utilize a unique correction to get reasonable accuracy.

There was an assumption made in both Chapters 3-4 since meteorological data was based on one IDEM monitor near the sensor network. This assumption means that there is no variation in these variables in our space, even though we know that built environment and tree cover, amongst other factors, do influence their measurements. Future work will also benefit from the usage of more recent high resolution tree canopy data.

Lastly, we know that humans are not stationary and not incorporating mobility, especially of those individuals with long commutes has been shown to underestimate human exposure by an average of 13% (Lu, 2021). This study bases its analysis on the sensor locations and does not incorporate participants mobility, which should be consider in the future.

5.4 Future suggestions

There are many areas of research as they pertain to air pollution and health that have not yet been explored fully, which poses an unknown threat that we cannot quantify (Szyszkowicz et al., 2022). Clean Air Act in 1970 initiated legislation being passed to protect the public and the nation (US EPA, 2015), which has helped the U.S. at a macro level; however we need to examine the current state and incorporate research and new methods for combating air pollution and its fallout. Investment needs to be made to address and act upon the pollution we suffer, and the very serious ramifications from it. COVID-19, a natural experiment, gave us insight into quantifying health impacts of our restricted movements on us. For instance, New York Times reported a reduction in heart attacks in early pandemic days (Appelbaum, 2022).

We have also come to realize that communities of color have suffered disproportionately, and working on improving them directly also benefits the less diverse places (Demetillo et al., 2021). Satellite data has its place in research, but to examine air pollution burden, in particular that of NO_2 and thus its secondary products has to be monitored at a much finer resolution than what is readily available (Rao et al., 2014). That being the case we need to turn towards low-cost air pollution sensor options not the few EPA monitors to keep our eye on pollution to accurately assess its impacts on the humans and the environment. Thus, we need to work on modifying and making the validation process of low-cost sensors user friendly and not prohibitive in ease of use by researchers, keeping the attainable accuracy within a reasonable range.

Epigenetics research is highlighting the serious impacts from air pollution; therefore, the urgency presents opportunities to first examine widely at a finer scale and work with the public to make our air cleaner for us and the future generations. Low-cost sensors have huge promise especially in regions of low coverage (Gupta et al., 2018), and have to be made more acceptable for future research.

5.5 References

Appelbaum, B. (2022, April 19). Opinion | Enough About Climate Change. Air Pollution Is Killing Us Now. *The New York Times*. https://www.nytimes.com/2022/04/19/opinion/air-pollution-fossil-fuels.html

Beelen, R., Hoek, G., Vienneau, D., Eeftens, M., Dimakopoulou, K., Pedeli, X., Tsai, M.-Y., Künzli, N., Schikowski, T., Marcon, A., Eriksen, K. T., Raaschou-Nielsen, O., Stephanou, E., Patelarou, E., Lanki, T., Yli-Tuomi, T., Declercq, C., Falq, G.,

Stempfelet, M., … de Hoogh, K. (2013). Development of NO2 and NOx land use regression models for estimating air pollution exposure in 36 study areas in Europe – The ESCAPE project. *Atmospheric Environment*, *72*, 10–23. https://doi.org/10.1016/j.atmosenv.2013.02.037

Bi, J., Stowell, J., Seto, E. Y. W., English, P. B., Al-Hamdan, M. Z., Kinney, P. L., Freedman, F. R., & Liu, Y. (2020). Contribution of low-cost sensor measurements to the prediction of PM2.5 levels: A case study in Imperial County, California, USA. *Environmental Research*, *180*, 108810. https://doi.org/10.1016/j.envres.2019.108810

Bi, J., Wildani, A., Chang, H. H., & Liu, Y. (2020). Incorporating Low-Cost Sensor Measurements into High-Resolution PM $_{2.5}$ Modeling at a Large Spatial Scale. *Environmental Science & Technology*, *54*(4), 2152–2162. https://doi.org/10.1021/acs.est.9b06046

Chu, M., Sun, C., Chen, W., Jin, G., Gong, J., Zhu, M., Yuan, J., Dai, J., Wang, M., Pan, Y., Song, Y., Ding, X., Guo, X., Du, M., Xia, Y., Kan, H., Zhang, Z., Hu, Z., Wu, T., & Shen, H. (2015). Personal exposure to PM2.5, genetic variants and DNA damage: A multi-center population-based study in Chinese. *Toxicology Letters*, *235*(3), 172–178. https://doi.org/10.1016/j.toxlet.2015.04.007

Cohen, A. J., Brauer, M., Burnett, R., Anderson, H. R., Frostad, J., Estep, K., Balakrishnan, K., Brunekreef, B., Dandona, L., Dandona, R., Feigin, V., Freedman, G., Hubbell, B., Jobling, A., Kan, H., Knibbs, L., Liu, Y., Martin, R., Morawska, L., … Forouzanfar, M. H. (2017). Estimates and 25-year trends of the global burden of disease attributable to ambient air pollution: An analysis of data from the Global

Burden of Diseases Study 2015. *The Lancet*, *389*(10082), 1907–1918. https://doi.org/10.1016/S0140-6736(17)30505-6

Demetillo, M. A. G., Harkins, C., McDonald, B. C., Chodrow, P. S., Sun, K., & Pusede, S. E. (2021). Space-Based Observational Constraints on NO2 Air Pollution Inequality From Diesel Traffic in Major US Cities. *Geophysical Research Letters*, *48*(17), e2021GL094333. https://doi.org/10.1029/2021GL094333

Ferrari, L., Carugno, M., & Bollati, V. (2019). Particulate matter exposure shapes DNA methylation through the lifespan. *Clinical Epigenetics*, *11*(1), 129. https://doi.org/10.1186/s13148-019-0726-x

Gupta, P., Doraiswamy, P., Levy, R., Pikelnaya, O., Maibach, J., Feenstra, B., Polidori, A., Kiros, F., & Mills, K. C. (2018). Impact of California Fires on Local and Regional Air Quality: The Role of a Low-Cost Sensor Network and Satellite Observations. *GeoHealth*, *2*(6), 172–181. https://doi.org/10.1029/2018GH000136

Heintzelman, A., Filippelli, G., & Lulla, V. (2021). Substantial Decreases in U.S. Cities' Ground-Based NO2 Concentrations during COVID-19 from Reduced Transportation. *Sustainability*, *13*(16), 9030. https://doi.org/10.3390/su13169030

Jiao, W., Hagler, G., Williams, R., Sharpe, R., Brown, R., Garver, D., Judge, R., Caudill, M., Rickard, J., Davis, M., Weinstock, L., Zimmer-Dauphinee, S., & Buckley, K. (2016). Community Air Sensor Network (CAIRSENSE) project: Evaluation of low-cost sensor performance in a suburban environment in the southeastern United States. *Atmospheric Measurement Techniques*, *9*(11), 5281–5292. https://doi.org/10.5194/amt-9-5281-2016

Kortoçi, P., Motlagh, N. H., Zaidan, M. A., Fung, P. L., Varjonen, S., Rebeiro-Hargrave, A., Niemi, J. V., Nurmi, P., Hussein, T., Petäjä, T., Kulmala, M., & Tarkoma, S. (2022). Air pollution exposure monitoring using portable low-cost air quality sensors. *Smart Health*, *23*, 100241. https://doi.org/10.1016/j.smhl.2021.100241

Lamsal, L. N., Martin, R. V., Parrish, D. D., & Krotkov, N. A. (2013). Scaling Relationship for NO2 Pollution and Urban Population Size: A Satellite Perspective. *Environmental Science & Technology*, *47*(14), 7855–7861. https://doi.org/10.1021/es400744g

Lu, Y. (2021). Beyond air pollution at home: Assessment of personal exposure to PM2.5 using activity-based travel demand model and low-cost air sensor network data. *Environmental Research*, *201*, 111549. https://doi.org/10.1016/j.envres.2021.111549

Malings, C., Tanzer, R., Hauryliuk, A., Saha, P. K., Robinson, A. L., Presto, A. A., & Subramanian, R. (2020). Fine particle mass monitoring with low-cost sensors: Corrections and long-term performance evaluation. *Aerosol Science and Technology*, *54*(2), 160–174. https://doi.org/10.1080/02786826.2019.1623863

Meng, X., Liu, C., Chen, R., Sera, F., Vicedo-Cabrera, A. M., Milojevic, A., Guo, Y., Tong, S., Coelho, M. de S. Z. S., Saldiva, P. H. N., Lavigne, E., Correa, P. M., Ortega, N. V., Osorio, S., Garcia, null, Kyselý, J., Urban, A., Orru, H., Maasikmets, M., … Kan, H. (2021). Short term associations of ambient nitrogen dioxide with daily total, cardiovascular, and respiratory mortality: Multilocation analysis in 398 cities. *BMJ (Clinical Research Ed.)*, *372*, n534. https://doi.org/10.1136/bmj.n534

Miller, D. J., Actkinson, B., Padilla, L., Griffin, R. J., Moore, K., Lewis, P. G. T., Gardner-Frolick, R., Craft, E., Portier, C. J., Hamburg, S. P., & Alvarez, R. A. (2020). Characterizing Elevated Urban Air Pollutant Spatial Patterns with Mobile Monitoring in Houston, Texas. *Environmental Science & Technology*, *54*(4), 2133–2142. https://doi.org/10.1021/acs.est.9b05523

Padilla, L. E., Ma, G. Q., Peters, D., Dupuy-Todd, M., Forsyth, E., Stidworthy, A., Mills, J., Bell, S., Hayward, I., Coppin, G., Moore, K., Fonseca, E., Popoola, O. A. M., Douglas, F., Slater, G., Tuxen-Bettman, K., Carruthers, D., Martin, N. A., Jones, R. L., & Alvarez, R. A. (2022). New methods to derive street-scale spatial patterns of air pollution from mobile monitoring. *Atmospheric Environment*, *270*, 118851. https://doi.org/10.1016/j.atmosenv.2021.118851

Rao, M., George, L. A., Rosenstiel, T. N., Shandas, V., & Dinno, A. (2014). Assessing the relationship among urban trees, nitrogen dioxide, and respiratory health. *Environmental Pollution*, *194*, 96–104. https://doi.org/10.1016/j.envpol.2014.07.011

Szyszkowicz, M., Link to external site, this link will open in a new window, Lukina, A., & Dinu, T. (2022). Urban Air Pollution and Emergency Department Visits for Neoplasms and Outcomes of Blood Forming and Metabolic Systems. *International Journal of Environmental Research and Public Health*, *19*(9), 5603. https://doi.org/10.3390/ijerph19095603

Tan, Y., Wang, Y., Zou, Y., Zhou, C., Yi, Y., Ling, Y., Liao, F., Jiang, Y., & Peng, X. (2020). LncRNA LOC101927514 regulates PM2.5-driven inflammation in human

bronchial epithelial cells through binding p-STAT3 protein. *Toxicology Letters*, *319*, 119–128. https://doi.org/10.1016/j.toxlet.2019.10.009

US EPA, O. (2015, May 27). *Clean Air Act Requirements and History* [Overviews and Factsheets]. https://www.epa.gov/clean-air-act-overview/clean-air-act-requirements-and-history

You, D., Qin, N., Zhang, M., Dai, J., Du, M., Wei, Y., Zhang, R., Hu, Z., Christiani, D. C., Zhao, Y., & Chen, F. (2020). Identification of genetic features associated with fine particulate matter (PM2.5) modulated DNA damage using improved random forest analysis. *Gene*, *740*, 144570. https://doi.org/10.1016/j.gene.2020.144570

APPENDICES

APPENDIX A

This appendix contains variable explanations used in the Ogawa data and the writing.

Ogawa sensor data in parts per billion (ppb):

NO_2 (ppb) = NO2_ppb_blankcorrected = NO_2 concentration (ppb)

O_3 (ppb) = O3_ppb_blankcorrected = O3 concentration (ppb)

StreetLight (SL) platform data excluding the control site:

All Vehicle Count = AllVehiclesAvgDailyCount = avg daily vehicle count data

Medium Truck Index = MedTrk_AvgDaily_pct_exclkib = avg daily medium truck index

Heavy Truck Index = HvyTrk_AvgDaily_pct_exclkib = avg daily heavy truck index

Washington Park (WP) IDEM monitor data:

Temp C = Avg_Temp_C = average temperature in Celsius

Solar Energy = WP_avgsolar_rad = avg solar energy in watts per square meter

Windspeed kmh = Avg_wndspd_kmh = avg wind speed in kilometer per hour

American Community Survey 5-year 2018, at census tract level:

Hispanic Latino % = pop_pct_hispanic_latino = percent of Hispanic and Latino population

White only % = pop_pct_whitealone = % white only population

Pop25+LT high school % = plus25LTHS_ovr25pop = % 25+ population with less than high school

Pop25+bachelors % = plus25Bachelors_ovr25pop = % 25+ population with bachelor's degree

Indianapolis land use data from open data portal by census tract:

Heavy Industry % = HeavyInd_pct = percentage of heavy industrial parcels

Measurements (GIS software):

Hwy Length-10 km = hwy_length_10km_inKm = highway length in a 10-kilometer radius from each sensor in kilometers

Road Length-10 km =rd_length_10km_inKm = road length in a 10-kilometer radius from each sensor in kilometers

Distance to Hwy =dist_to_hwy_inKm = distance from each sensor to nearest highway in kilometers

Gas Station-10 km = gas_st_10km = gas stations in a 10-kilometer radius

Tree Canopy-1 km = tree_canopy_in1km_sqKm = tree canopy coverage in a 1-kilometer radius circle from each sensor

APPENDIX B

This appendix contains R code with some explanation for the regression models run for this study.

Model 1

Explanation: Model 1 included all the variables extracted for this study. However, this resulted in high collinearity indicated by a high variance inflation factor (VIF) of 67.09 for 'Avg_Temp_C'.

Code for Model 1 below:

```
md_1 <- lm(NO2_ppb_blankcorrected ~ O3_ppb_blankcorrected +
        AllVehiclesAvgDailyCount + MedTrk_AvgDaily_pct_exclkib +
        HvyTrk_AvgDaily_pct_exclkib  + pop_pct_hispanic_latino +
        pop_pct_whitealone + plus25LTHS_ovr25pop + plus25Bachelors_ovr25pop +
        HeavyInd_pct + tree_canopy_in1km_sqKm +
        Avg_wndspd_kmh + Avg_Temp_C+
        hwy_length_10km_inKm + rd_length_10km_inKm +
        dist_to_hwy_inKm + gas_st_10km, data = c4)

summary(md_1)
```

Model 2

Explanation: Due to high collinearity of 'Avg_Temp_C ' in Model 1, Model 2 was run without it. *However, this model resulted in high VIF of 20.90 for* 'MedTrk_AvgDaily_pct_exclkib'.

Code for Model 2 below:

```
md_2 <- lm(NO2_ppb_blankcorrected ~ O3_ppb_blankcorrected +
        AllVehiclesAvgDailyCount + MedTrk_AvgDaily_pct_exclkib +
```

```
        HvyTrk_AvgDaily_pct_exclkib  + pop_pct_hispanic_latino +
        pop_pct_whitealone + plus25LTHS_ovr25pop + plus25Bachelors_ovr25pop +
        HeavyInd_pct + tree_canopy_in1km_sqKm +
        Avg_wndspd_kmh + hwy_length_10km_inKm + rd_length_10km_inKm +
        dist_to_hwy_inKm + gas_st_10km, data = c4)
summary(md_2)
vif(md_2)
```

Model 3

Explanation: Due to high collinearity of 'MedTrk_AvgDaily_pct_exclkib'' in Model 2, Model 3 was run without it. *However, this model resulted in high VIF of 10.95 for* 'rd_length_10km_inKm'.

Code for Model 3 below:

```
md_3 <- lm(NO2_ppb_blankcorrected ~ O3_ppb_blankcorrected +
        AllVehiclesAvgDailyCount  +
        HvyTrk_AvgDaily_pct_exclkib  + pop_pct_hispanic_latino +
        pop_pct_whitealone + plus25LTHS_ovr25pop + plus25Bachelors_ovr25pop +
        HeavyInd_pct + tree_canopy_in1km_sqKm +
        Avg_wndspd_kmh + hwy_length_10km_inKm + rd_length_10km_inKm +
        dist_to_hwy_inKm + gas_st_10km, data = c4)
summary(md_3)
vif(md_3)
```

Model 4

Explanation: Due to high collinearity of 'rd_length_10km_inKm' in Model 3, Model 4 was run without it.

Code for Model 4 below:

```
md_4 <- lm(NO2_ppb_blankcorrected ~ O3_ppb_blankcorrected +
        AllVehiclesAvgDailyCount  +
        HvyTrk_AvgDaily_pct_exclkib  + pop_pct_hispanic_latino +
        pop_pct_whitealone + plus25LTHS_ovr25pop + plus25Bachelors_ovr25pop +
        HeavyInd_pct + tree_canopy_in1km_sqKm +
        Avg_wndspd_kmh + hwy_length_10km_inKm  +
        dist_to_hwy_inKm + gas_st_10km, data = c4)

summary(md_4)
vif(md_4)
```

Model 5- Stepwise Regression

Explanation: Since Model 4 resulted in no multicollinearity in the variables an additional step was taken to run a final stepwise regression model.

Code for Model 5 below:

```
stepwise.5 <- step(md_4, direction = "both", trace = FALSE)
summary(stepwise.5)
vif(stepwise.5)
```

APPENDIX C

This appendix contains spatial patterns and variable explanations used in the $PM_{2.5}$ data and the writing.

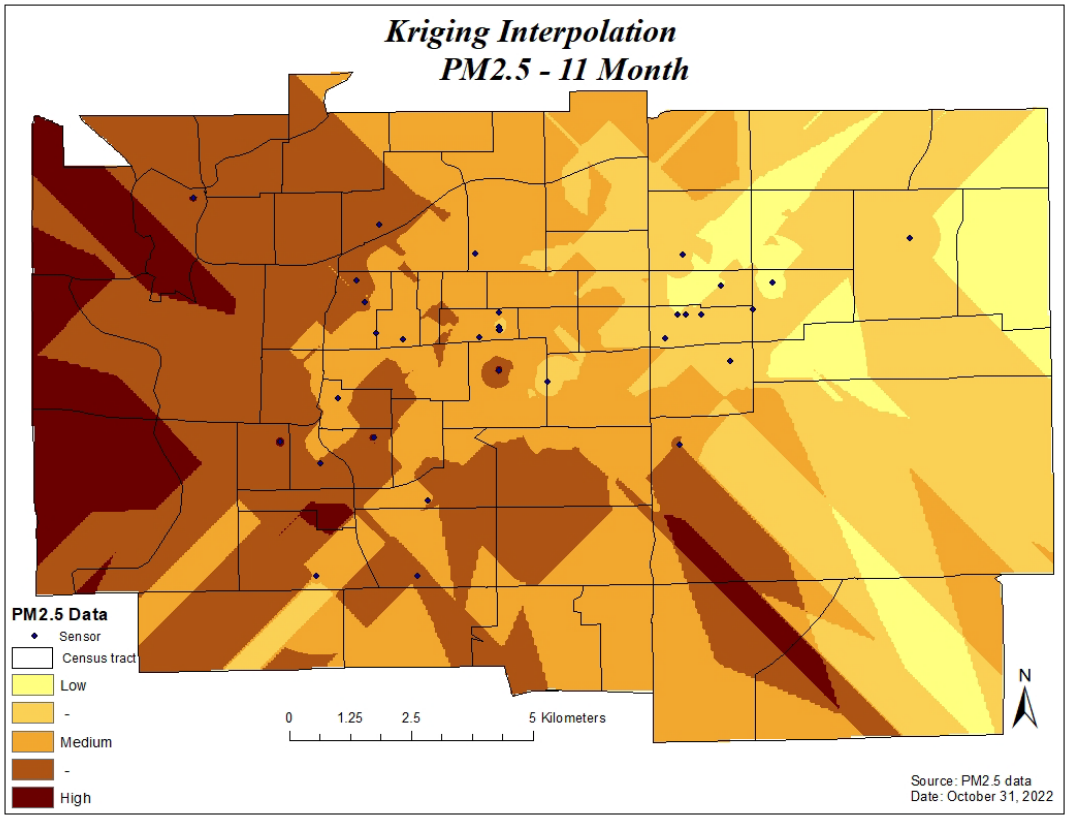

Figure C.1 - Kriging interpolation in ArcMap for $PM_{2.5}$ data

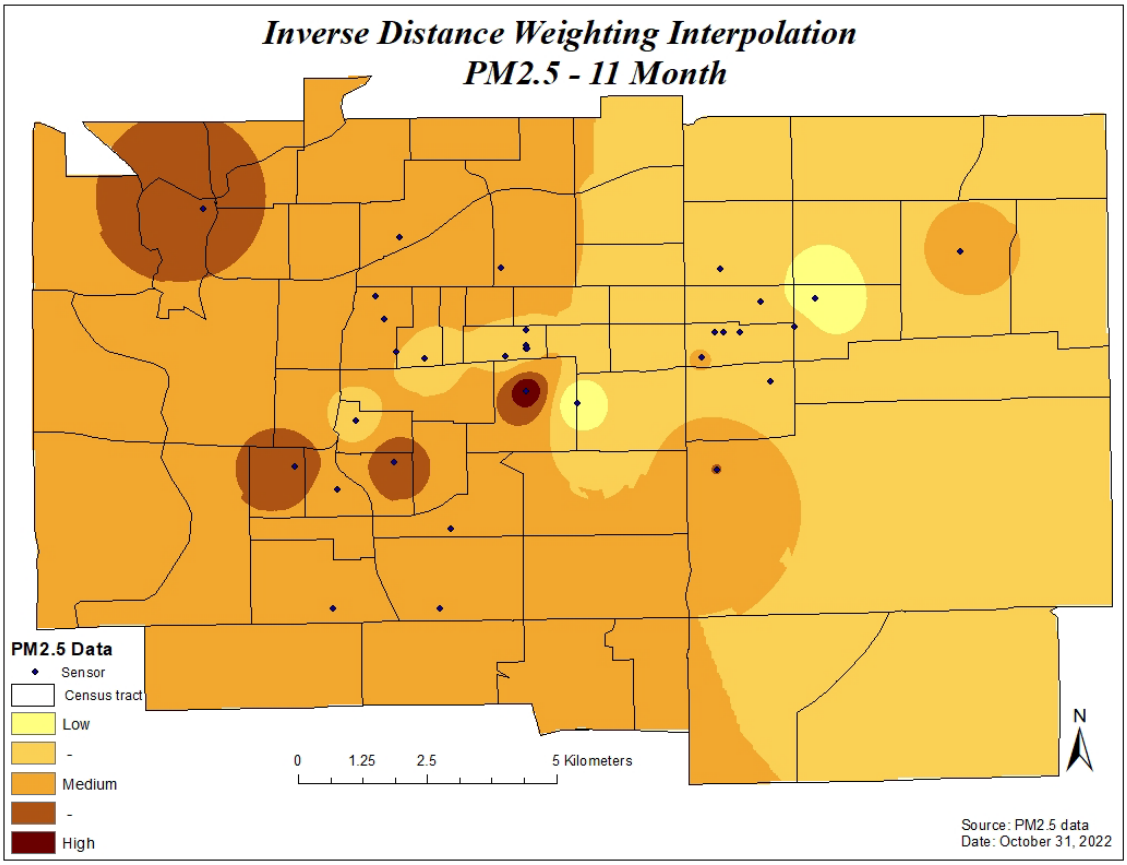

Figure C.2 - Inverse Distance Weighting interpolation in ArcMap for $PM_{2.5}$ data

PurpleAir sensor data in micrograms per cubic meter air ($\mu g/m^3$):

$PM_{2.5}$ ($\mu g/m^3$) = pm25_adj_wp = Relative humidity corrected $PM_{2.5}$

Washington Park (WP) IDEM monitor data and other data:

Temp C = wp_avg_Temp_C = Temperature in Celsius

Precip cm = WP_avg_precip_cum_cm = Precipitation in centimeters

Windspeed kmh = wp_avg_wndspd_kmh_new = Wind speed in kilometer per hour

Day = day = consists of 7 categories for the days of the week

Month group = paper_mth_grp_rank *

* This variable consists of the following groups:

- Month group 1= Fall 1(Nov2018): paper_mth_grp_rank = "1"
- Month group 2 =Winter (Dec2018-Jan2019): paper_mth_grp_rank := "2"
- Month group 3 = Spring (Mar2019-May2019): paper_mth_grp_rank := "3"
- Month group 4 = Summer (June2019-August 2019): paper_mth_grp_rank := "4"
- Month group 5 = Fall 2 (September 2019-October 2019): paper_mth_grp_rank := "5"

American Community Survey 5-year 2018, at census tract level:

Hispanic Latino % = pop_pct_hispanic_latino = percent of Hispanic and Latino population

Black One Race % = pop_pct_onerace_black = percent of black one race population

White only % = pop_pct_whitealone = percent white only population

Median HH Inc = med_hh_inc = median household income

Median Rent = median_rent = median rent

Pop25+LT high school % = plus25LTHS_ovr25pop = % 25+ population with less than high school

Pop25+Some College_Assoc % = plus25_somecollege_assoc= % 25+ population with some college and an associate's degree

Pop25+ Grad_Prof Degree % = plus25_graduate_prof_deg = % 25+ population with a graduate or a professional degree

Indianapolis land use data from open data portal by census tract:

Heavy Industry % = HeavyInd_pct = percentage of heavy industrial parcels

Measurements (GIS software) in the census tract:

Hwy Length km = hwy_length_km = highway length in kilometers

Road Length km = rd_length_km = road length in a kilometers

Tree Canopy % = canopy_pct_ct_km = tree canopy percentage

APPENDIX D

This appendix contains R code with some explanation for the analysis run for this study in R-Studio.

Meteorology Conversions

```
d3 <- d1[, `:=` (wp_avg_wndspd_kmh_new=WP_wind_spd*1.6090,
        WP_avg_precip_cum_cm=WP_precip_cum*2.54,wp_avg_Temp_C=((wp_avg_te
        mp-32)*5/9))]
```

Logistic regression Model

```
summary (mod20 <- glm(who1_pm25_adj_wp_ge25 ~
        WP_avg_precip_cum_cm+wp_avg_wndspd_kmh_new
       +wp_avg_Temp_C+paper_mth_grp_rank+day,
        family=binomial(link="logit"),
        na.action=na.omit, data=d2)) # in paper 9/22/22
        exp(mod20$coefficients[-1])
```

Table 4.6

Following is an example of what was run in R-Studio for each of the 25 sensors in the study:

```
d1[, sen_13 := as.factor(ifelse(Sensor == '13','1', '2'))]
t_sen13 <- d1[,table(sen_13,who_adj_GE25)]
colnames(t_sen13)<- c("GE25","Other")
rownames(t_sen13)<- c("Sen13", "Other")
chi_13 <- chisq.test(t_sen13)
```

```
fisher.test(t_sen13, conf.int = T, conf.level = 0.95)
```

Section 4.3.5

Code for Correlation:

```
cor.test(acs4$pm_adj_25Sen_11mt,acs4$canopy_pct_ct_km,              method=c("spearman"))
cor.test(acs4$pm_adj_25Sen_11mt,acs4$HeavyInd_pct,                  method=c("spearman"))
cor.test(acs4$pm_adj_25Sen_11mt,acs4$hwy_length_km,                 method=c("spearman"))
cor.test(acs4$pm_adj_25Sen_11mt,acs4$rd_length_km,                  method=c("spearman"))
cor.test(acs4$pm_adj_25Sen_11mt,acs4$plus25LTHS_ovr25pop,           method=c("spearman"))
cor.test(acs4$pm_adj_25Sen_11mt,acs4$plus25_somecollege_assoc,      method=c("pearson"))
cor.test(acs4$pm_adj_25Sen_11mt,acs4$plus25_graduate_prof_deg,      method=c("spearman"))
cor.test(acs4$pm_adj_25Sen_11mt,acs4$pop_pct_hispanic_latino,       method=c("spearman"))
cor.test(acs4$pm_adj_25Sen_11mt,acs4$pop_pct_whitealone,            method=c("spearman"))
cor.test(acs4$pm_adj_25Sen_11mt,acs4$med_hh_inc,                    method=c("spearman"))
cor.test(acs4$pm_adj_25Sen_11mt,acs4$median_rent,                   method=c("pearson"))
```

CURRICULUM VITAE

ASRAH HEINTZELMAN

Education

2022 **Ph.D.**, Indiana University – Purdue University, Indianapolis (IUPUI)
Major in Applied Earth Sciences (Advisor: Dr. Gabriel Filippelli)
Minor in Individualized-Public Health Analytics (Advisor: Dr. Max J. Moreno-Madriñan)

2010 **MS.**, IUPUI
Major in Geographic Information Science (Advisor: Dr. Aniruddha Banerjee)

1990 **BS.**, Purdue University
Major in Economics

Research Experience

2018 – 2020: Research Assistant for the Department of Earth Sciences at IUPUI
Initiated and established the first fine-scale air quality study in Indianapolis for the department; assisted in water quality research project; assisted in lead analysis studies in Indianapolis and across the nation; assisted in producing maps for paper submissions to journals
(Spring 2018; Summer 2018; Fall 2018; Spring 2019; Summer 2019; Fall 2019; Spring 2020; Summer 2020)

2008 – 2010: Graduate Assistant for the Department of Geography at IUPUI
Worked with medical professionals on a project to identify hot spots of childhood obesity in Indianapolis; incorporated socio-economic and demographic variables in the statistical analysis
(Fall 2008; Spring 2009; Summer 2009; Fall 2009; Spring 2010)

2008: Research Internship at The Polis Center at IUPUI
Computed neighborhood deprivation index; linked student health knowledge and Body Mass Index ("BMI") with contextual data on the communities; performed spatial and network analysis to identify clusters; evaluated and analyzed the impact of student health knowledge, behaviors, and weight status on the census tracts from the adjacent neighbors

Professional Experience

2010 – Present: GIS Analyst with Milestone Ventures Inc, Indianapolis
Analyzed data in Low/Moderate-Income geographies using Housing and Urban Development published data; worked on a project with a not-for-profit in identifying its service area and providing a breakdown of available census data; assisted in preparing revitalization plans for six communities in Indiana. This project consisted of identifying geographic boundaries and manipulating Census 2010 and Census 2000 data; compiled Census 2010 and Census 2000 data, performed statistical analysis, and prepared neighborhood maps for specific

communities in Indiana; identified and mapped Neighborhood Stabilization Program target areas based on Housing and Urban Development published data; prepared network distance-based travel boundaries for consultants to oversee projects in Indiana; generated maps for project proposals and submissions

Conference and Workshops

2020: National Center for Atmospheric Research (NCAR), Boulder, CO
Weather Research and Forecasting Model (WRF) workshop
2020: American Geophysical Union (AGU) annual conference (virtual)
2020: AGU poster presentation (virtual)
"Substantial decreases in NO2 emissions from reduced transportation volumes in US cities during COVID-19 shutdowns reveal health vulnerabilities of urban populations"
2019: University of Sao Paulo, Brazil (International)
Sao Paulo School of Advanced Science on Atmospheric Aerosols (SPSAS); 82 hours of extensive theoretical classes, practical experiments, activities with state-of-the art scientific knowledge
2019: SPSAS poster presentation, Sao Paulo, Brazil
"Air Quality Study in the Pleasant Run Region, Indianapolis, IN, U.S.A."
2019: NCAR workshop on air quality
2019: AGU annual conference, San Francisco, CA
2019: AGU poster presentation, San Francisco, CA
"Results from a dense urban air quality monitoring system: Volatiles and particulate matter analysis in Indianapolis, USA"
2018: Environmental Resilience Institute (ERI) Symposium in Bloomington, IN
2018: ERI Symposium – Bloomington, IN (poster presentation)
"Air Quality Study in the Pleasant Run Region, Indianapolis, IN, U.S.A."
2018: U.S. Environmental Protection Agency (US EPA) - National Air Quality Conference in Austin, TX

Publications

1. Heintzelman, Asrah, Gabriel Filippelli, and Vijay Lulla. "Substantial Decreases in US Cities' Ground-Based NO2 Concentrations during COVID-19 from Reduced Transportation." Sustainability 13.16 (2021): 9030 (published online)
2. Asrah Heintzelman, Gabriel M. Filippelli, Max J. Moreno-Madriñan, Jeffrey S. Wilson, Lixin Wang, and Gregory K. Druschel. "The Role of Local Vehicular Type and Canopy Coverage in Controlling Ground-Level NO_2 in the Urban Environment." (in progress)
3. Asrah Heintzelman, Gabriel M. Filippelli, Max J. Moreno-Madriñan, Jeffrey S. Wilson, Lixin Wang, Gregory K. Druschel, and Vijay O. Lulla. Efficacy of Low-Cost Sensor Networks at Detecting Fine-Scale Variations in Particulate Matter in Urban Environments (in progress)